VITA

MICHAEL E. DEVORE

EDUCATION

PhD. Indiana State University, Terre Haute, Indiana. May 2011.
Major: Technology Management, Manufacturing Systems specialization.

MBA University of North Carolina at Greensboro, Greensboro, North Carolina.
December, 1988. Master of Business Administration.

B.S. University of Cincinnati College of Applied Science, Cincinnati, Ohio.
June 1982. Major: Mechanical Engineering Technology.

TEACHING/INDUSTRIAL EXPERIENCE

1990 – 2011 Cincinnati State Technical & Community College, Cincinnati, Ohio. Program Chair and Instructor. Manage operation of Mechanical Engineering Technology Department. Teach a variety of courses including strength of materials, machine design, thermodynamics, computer aided drafting, and MET capstone courses.

1989 – 1990 Ford Motor Company, Sharonville, Ohio. Process engineer in the manufacturing engineering department. Responsible for all aspects of developing and managing projects to improve the manufacturing processes for a large transmission plant.

1982 – 1989 Eveready Battery Company, Asheboro, North Carolina. Project engineer in the plant engineering department. Responsible for designing and installing new machinery to increase efficiency and productivity.

PUBLICATIONS

DeVore, M. (2000). *Statics – an interactive tutorial*. Prentice-Hall. Upper Saddle River, New Jersey

PROFESSIONAL MEMBERSHIPS

Licensed Professional Engineer, Ohio
Member, American Society of Mechanical Engineers
Member, Association of Technology, Management, and Applied Engineering

AN EXPERIMENTAL STUDY ON REDUCING THE FORMATION OF DROSS WHEN CUTTING 1018 HR STEEL USING A CNC PLASMA CUTTER

A Dissertation

Presented to

The College of Graduate and Professional Studies

Ph.D. Consortium Program

Indiana State University

Terre Haute, Indiana

In Partial Fulfillment

of the Requirements for the Degree

Doctor of Philosophy

---

by

Michael E. DeVore

May 2011

Keywords: plasma arc cutting, CNC, dross, technology management, manufacturing

COMMITTEE MEMBERS

Committee Chair: Dr. Sudershan Jetley, PhD

Associate Professor, Department of Engineering Technology

Bowling Green State University

Committee Member: Gordon Minty, PhD

Professor, Department of Technology Management

Indiana State University

Committee Member: Dr. Marion Schafer, PhD

Associate Professor, Department of Technology Management

Indiana State University

Committee Member: Dr. James Smallwood, PhD

Professor and Chair, Department of Technology Management

Indiana State University

Committee Member: Dr. Todd Waggoner, PhD

Professor, Department of Engineering Technology

Bowling Green State University

ABSTRACT

Many manufacturers who cut metal use plasma arc cutting as part of their manufacturing process. Plasma cutters use electricity and pressurized gas to produce a temperature of up to 50,000 ºF at the cutting tip. These plasma cutters can rapidly cut through metals as much as 12 inches thick. The use of computer numerical controlled (CNC) plasma cutters allow manufacturers to rapidly cut even very intricate and detailed flat parts. This process is a tremendous improvement over traditional torch cutting, saw cutting, or other machining processes for producing near net shapes. It is faster and less expensive than most of the alternative processes available.

There are several processing and quality factors that must be addressed when using a plasma cutter. The most common problem with plasma cutting is the formation of dross (re-solidified metal) on the cut edge. The formation of dross on plasma-cut parts creates several problems in the manufacturing process. By carefully controlling the operating parameters, the formation of dross on the work piece can be minimized, which greatly increases the quality of the part and the efficiency of the production process. Efficient operation of a CNC plasma cutter to minimize the formation of dross requires controlling several variables in the process. These variables include: material type and thickness, arc current (amperage), cutting speed, cutting-gas pressure, cutting tip size, and the gap between the cutting tip and the work piece.

Experience with plasma arc cutting and research on the subject reveals that the variables that most affect the formation of dross are arc current, cutting speed, material thickness, and

nozzle size. A study involving these four variables will be performed to determine the optimum setup for the CNC plasma cutter to minimize the formation of dross.

ACKNOWLEDGEMENTS

I am very thankful to many people for their support in the pursuit of my doctorate. My ability to complete this difficult process was in part due to an amazing group of people in my life. I am very fortunate to be surrounded by a loving family, dedicated professors, and supportive coworkers.

My family has been an invaluable asset as they have allowed me to pursue my dream of obtaining a PhD. My wife Nancy, my daughter Sara, and my son Thomas have been my biggest supporters and most important allies throughout this venture. Their love, support, and understanding have been extraordinary during the last eight years. I also want to thank my parents Don and Dr. Carolyn DeVore for imparting in me a love of learning and the work ethic to never give up. This dissertation is dedicated to my sister Judy DeVore Winzurk, who passed away this year while she was working on her doctorate degree. I'm sorry we can't share this victory.

I would like to thank my committee members who supported me throughout this endeavor; thank you Dr. Todd Waggoner, Dr. James Smallwood, Dr. Marion Schafer, and Dr. Gordon Minty for your time and assistance through this process. I would especially like to thank my committee chair, Dr. Sudershan Jetley, for his encouragement, motivation, and dedication. Completing this dissertation without your guidance would have been impossible.

TABLE OF CONTENTS

LIST OF TABLES

LIST OF FIGURES

CHAPTER 1

INTRODUCTION

Plasma arc cutting (PAC) is a process of cutting metal by melting and burning it using a plasma jet. It has become very popular because of its high productivity and the ability to cut practically all metals (Nemchinsky, 1998). Plasma cutting systems have the ability to quickly and inexpensively cut parts with good cut quality. By understanding and optimizing the performance of the PAC process, companies can quickly and consistently produce high-quality products at a relatively low operating cost (Whiting, 2007). According to Gane, Rogozinski, Polivka, Doolette, and Ramakrishnan, (1994), "The cutting of metallic plate and sheet is one of the most important manufacturing operations in metal fabrication industries" (p. 2). Computer Numerical Control (CNC) PAC is a process that supports just-in-time manufacturing, flexible manufacturing, and lean manufacturing initiatives that most modern organizations are using to maximize the efficiency of their operations (Güllü & Atici, 2006; Lucas, 2005). The flexibility, accuracy, speed, and economy of operation of the PAC process make it an ideal tool for many different industries (Renault & Hussary, 2007; Sommer, 2000). Technical advancements over the last 50 years have made plasma cutting an economically competitive choice for manufacturing companies around the world (Nemchinsky & Severance, 2006; Renault & Hussary, 2007). Walsh (2005, ¶ 19) wrote:

> Plasma cutting systems can cut thicker materials faster than lasers and produce quality parts at the same time. Based on operating costs and periodic machine maintenance, it is

safe to say that plasma cutting is one of the most affordable contour-cutting machine choices to purchase and to operate.

PAC systems can use different cutting gases depending on the application. The four major types of gases used in PAC are oxygen, nitrogen, air, and an argon–nitrogen mixture. While each gas type has its advantages, air PAC has become one of the most popular processes in the last few years (Ramakrishnan, Shrinet, Polivka, Kearney, & Koltun, 2000). An air PAC system uses compressed air as the plasma gas instead of more expensive bottled gas, making the process more economical (Venkatramani, 2002). Some other advantages of air PAC include versatility, good speed, low dross levels, and long consumable life, especially when cutting mild steel (Cook, 2000). Ramakrishnan et al., (2000) compared the air, oxygen, and nitrogen PAC processes and found that air-plasma resulted in the narrowest kerf (width of cut) at low cutting speeds and the highest maximum cutting speed.

Of particular interest to manufacturers using any type of cutting process is maximizing productivity while maintaining the quality of the parts produced. Meeting these requirements with PAC requires the selection of appropriate operating parameters, which can vary greatly for each material and thickness. It can be very time consuming and expensive to determine the appropriate parameters for the quality of cut desired and this procedure must be repeated for each type of material and material thickness to be cut. Companies face this difficulty when using any manufacturing process, but the number of variables involved in the PAC process makes it especially challenging (Renault & Hussary, 2007).

Hussary and Renault (2006) wrote that the demands of the manufacturing industry require companies to maximize the efficiency of their equipment and operations. They stated, “The industry’s strive for a short product-to-market time necessitates a move away from trial and

error style of development work due to its high financial and time cost. This is particularly true of plasma cutting systems" (p. 382). This study is designed to experimentally determine the optimum process parameters to maximize the quality of cut obtained with an air PAC system while cutting a variety of thicknesses of 1018 Hot Rolled (HR) steel.

Technology management includes planning, designing, controlling, and optimizing the technological processes of an organization. Effective technology management in a manufacturing organization includes optimizing the equipment and processes to produce the highest quality products in the least amount of time with the lowest possible costs. Most manufacturing processes today involve machinery whose numerous variables control the performance. PAC is an example of just such a process. The objective of the PhD in Technology Management degree is to create professionals in technology management with the expertise to oversee applied technical research (Indiana State University, 2009). In this context, this study is appropriate to demonstrate the knowledge and skills required of a technology management professional. This study demonstrates the ability to thoroughly research a process, identify critical variables, design a robust and repeatable study, properly collect data, use statistical analysis to analyze the data, and present conclusions from the study.

History of Plasma Arc Cutting

PAC was invented in 1955 by the Linde Division of Union Carbide (Linde Group, 1955). The principal method of thermal cutting for fabrication at that time was oxyacetylene cutting (Walsh, 2005). The scientists at Linde discovered how to modify a tungsten-arc (TIG) welding torch to emit a very hot and very powerful jet of ionized gas. Instead of welding material together, metal could be cut by the plasma jet (Hypertherm, 2008). The arc could reach temperatures of 50,000 ºF, which could rapidly melt almost any metal. Because the gas within

the arc was in a superheated state called plasma, the process became known as plasma cutting (Fernicola, 1998). PAC became a popular method for cutting aluminum and stainless steel, but due to quality problems, oxy–fuel cutting was still the most practical method for cutting steel (Walsh, 2005).

In the early 1960s air PAC was developed which permitted steels to be cut cleanly, economically, and at speeds significantly faster than oxy–fuel cutting (Harris & Lowery, 1996). Besides a different torch design, air PAC used compressed air, instead of nitrogen or an argon–nitrogen gas mix, as the cutting gas (Nemchinsky & Severance, 2006). Air PAC drastically improved PAC performance and reduced the cost of cutting mild steel (Goodwin, 1989). Air PAC was rapidly accepted by industry and the technology spread to manufacturers around the world. "Plasma arc cutting was finally accepted as the new method for metal cutting and considered a valuable tool in all segments of the modern metalworking industry" (Hypertherm, 2008, p. 9).

There has been constant growth in the use and applications for PAC since its introduction in the 1950s, in part due to continuous improvements in equipment. PAC improvements include faster cutting and improved quality that have allowed it to become as useful on mild steel as it was on stainless steel and aluminum (Renault & Hussary, 2007). When used properly, PAC is now able to rapidly produce high-quality cuts on many types and sizes of materials (Fernicola, 1998; Matsuyama, 1997).

PAC combined with the accuracy of a CNC machine has created a very powerful manufacturing tool. The use of CNC, as well as technological advancements, has improved cut quality, accuracy, and flexibility, as well as the popularity of PAC. Widespread use of personal computers and computer aided drafting software allows easy programming of PAC machines,

which has also helped with the popularity of these machines (Walsh, 2005). PAC machine manufacturers in the U.S. expect continued high growth in the demand for their products in the foreseeable future (Hypertherm, 2008).

Plasma Arc Cutting Applications

Many organizations are harnessing the power and flexibility of the PAC process to replace traditional machining processes such as sawing, drilling, and punching. With cutting speeds as fast as 500 inches per minute, the PAC process can be used to rapidly produce multiple identical parts as well as for producing individually customized parts in small numbers. The cost and performance of a PAC system lie between that of oxy–fuel cutting and laser cutting, making it ideal for many applications (Venkatramani, 2002). A properly set up PAC machine can efficiently produce near net shapes that can drastically improve the manufacturing of flat parts. The plasma cutter used in this study is capable of producing flat parts with a tolerance of +/- 0.010 inch with proper settings (Hypertherm, 2008). PAC has become a very popular process in many different industries and is now used by companies producing components for automobiles, agricultural equipment, heavy machinery, aircraft, military equipment, ships, pressure vessels, and air-handling equipment. Specific applications include

- Forming the body panels for buses, tractor trailers, and agricultural equipment
- Cutting complex ductwork for the heating, ventilation, and air-conditioning industry
- Cutting large plates of steel at steel supply companies
- Producing components for large construction, mining, and material-handling equipment
- Producing steel framework for railroad cars, trucks, and other heavy equipment
- Cutting metal panels for shipbuilding

- Manufacturing pressure vessels
- Contour cutting using robotic arms (Hypertherm, 2008)

How Plasma Arc Cutting Works

When a gas is superheated, it breaks down into positively charged ions. This ionized gas is called plasma. High voltage is used to create an arc of electricity that travels from the negatively charged electrode (cathode) inside the torch to the positively charged work piece (anode) through the plasma jet. Injecting the plasma gas at high pressure through a very small diameter nozzle inside the torch creates a high-velocity plasma jet (Kelly, Mancinelli, Prevosto, Minotti, & Marquez, 2004). Constricting the electrically charged gas through the nozzle creates a large voltage drop in the plasma as well as an increase in velocity. These actions create an intense heating of the plasma-gas particles and accelerates the plasma to high velocities (Fernicola, 1998). The gas flow created in modern PAC systems moves at near-supersonic speeds at temperatures up to 50,000 ºF (Sommer, 2000). The high temperature achieved by the plasma melts and vaporizes the work piece, producing the cut, and the high velocity of the plasma displaces the material along the plasma jet's path (Kelly et al., 2004). A schematic diagram of the PAC process is shown in Figure 1.

A PAC system consists of a cutting torch, a power supply, a gas supply, and a torch control system as shown in Figure 2. The plasma torch is the most important part of the PAC system (Whiting, 2007). It is composed of an electrode, a nozzle, a nozzle shield, and a swirl ring as shown in Figure 3. The electrode carries the negative charge to the work piece through the arc. The nozzle constricts and focuses the plasma jet onto the work piece. The nozzle shield protects the nozzle from damage during cutting. The swirl ring spins the plasma gas into a

vortex, which helps to stabilize the plasma jet and improves the cut quality (Gonzalez-Aguilar, Pardo, Rodriquez-Yunta, & Calderon, 1999).

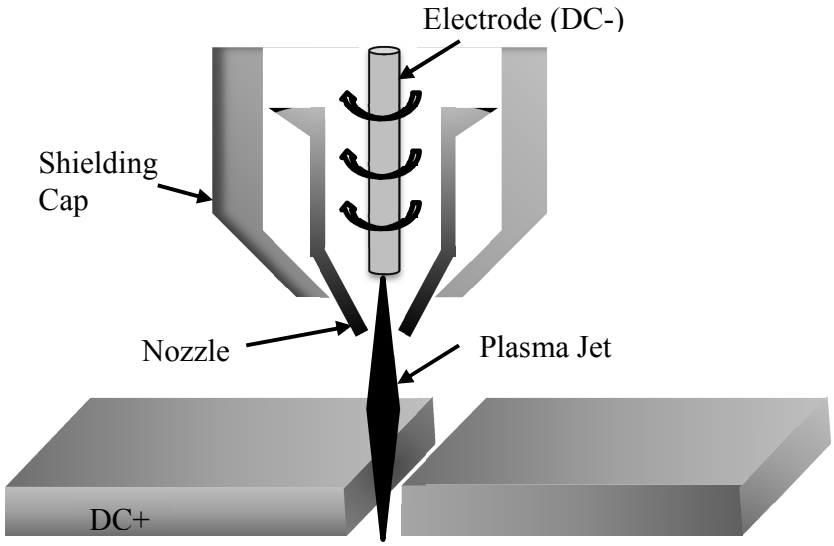

Figure 1. Plasma cutting schematic.

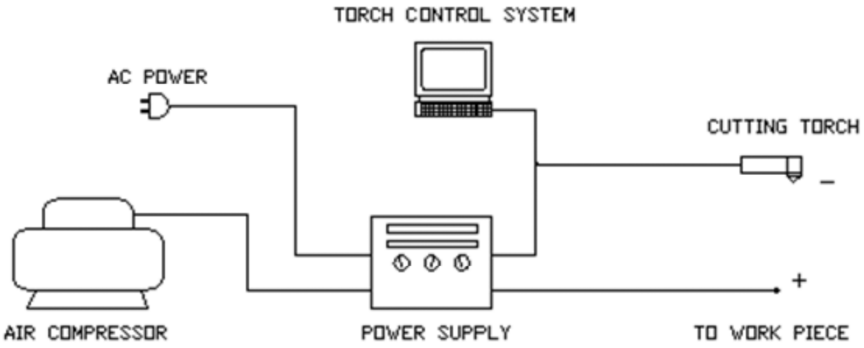

Figure 2. Plasma arc cutting system.

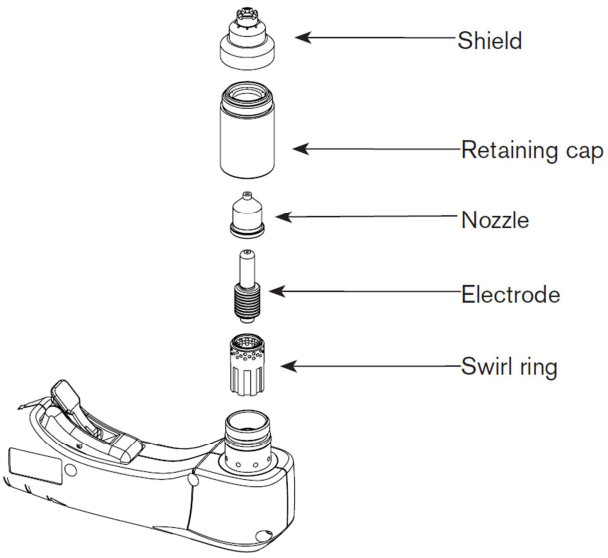

Figure 3. Plasma arc cutting torch.
From Hypertherm Stays Hot on Metalcutting Technology, by R. Lucas, 2005, *Gases and Welding distributor*, retrieved from http://gwd.wedlingmag.com/mag/gwd_11350

The CNC Plasma Cutting Process

An automated CNC plasma system includes a gantry, a torch holder, and a computer system to monitor and control the whole process. The typical CNC PAC machine uses a two-axis gantry with a moving carriage in one axis and a moving torch in the other axis as shown in Figure 4 (Pellecchia, 1995). The material being cut remains stationary while a CNC program controls the movement of the torch above the work piece. A servomotor controls the movement of the plasma torch in the z direction (up and down) (Gane et al., 1994). Most PAC systems today are equipped with torch height control to automatically adjust the distance between the plasma torch and the work piece (Whiting, 2007).

When a job is started, the machine moves to the first cut position and the torch descends until a sensor makes contact with the surface of the material. The torch then rises above the material to a predetermined pierce height. The pierce height raises the torch away from the work piece to prevent hot metal from splattering directly back into the torch nozzle while piercing the work piece (Thompson & Hanchette, 2003). The actual cutting process starts with arc ignition.

First a high-voltage spark creates a pilot arc between the electrode (cathode) and the nozzle, which acts as a temporary anode. With the pilot arc started, a boost in gas flow forces the pilot arc outside the nozzle and creates an arc loop protruding from the nozzle (Nemchinsky & Severance, 2006). The pilot arc forms a conduit to the metal work piece. Since the torch is very close to the work piece at this point, ranging from 1/8" to 1/2", the arc transfers from the electrode, through the nozzle, to the work piece which now acts as the anode in the electrical circuit until cutting is completed (Landry, 1997). The current flow now travels across the gap between the electrode and the work piece (Nemchinsky & Severance, 2006), which initiates piercing of the work piece. Once the work piece is pierced, the torch moves closer to the metal to the cut height and continues with the cut as it moves horizontally.

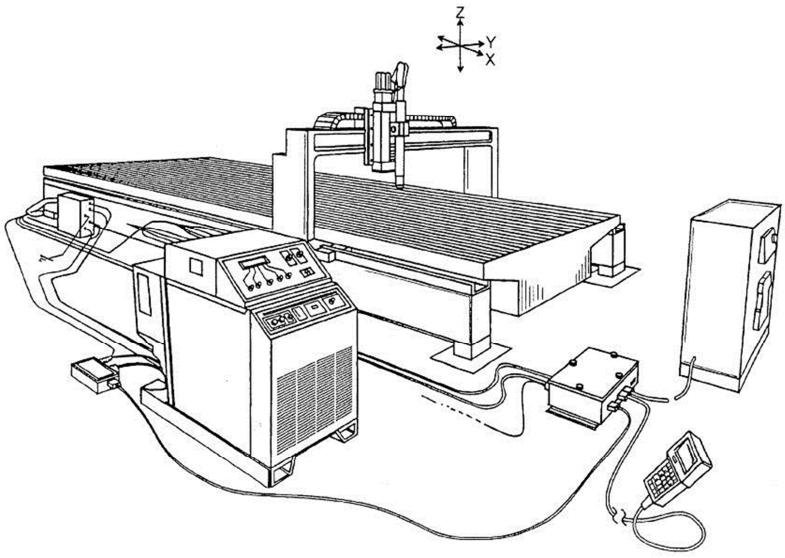

Figure 4. CNC plasma arc cutting system.
From *Centralized Control Architecture for a Plasma Arc System*, 2008, retrieved from http:www.freepatentsonline.com/672040.html

Once cutting begins, the distance between the torch and the work piece is controlled by the machine's automatic torch height control using the voltage readings from the plasma arc. This is especially useful when cutting thin-gage material that may not lie flat while cutting. It is

important to maintain a constant distance between the torch and the work piece to reduce arc variation and to ensure a high-quality cut (Thompson & Hanchette, 2003). The plasma jet from the nozzle concentrates the arc on a small area of the work piece, rapidly heating it to its melting point and simultaneously forcing the molten material out of the cut area (Landry, 1997). After the work piece has been pierced, the cutting torch moves as required until the programmed shape has been cut out.

Statement of Problem

The ability to adjust the operating parameters of the PAC process makes it very useful for many different cutting situations. In order to maximize the quality of parts produced with the PAC process, the proper combination of machine settings is necessary for each different type and thickness of material being cut. The problem is that the optimum settings of cutting speed, arc current, and nozzle size for achieving the best quality cuts with various materials and thicknesses are not well known.

Statement of Purpose

The purpose of this study was to determine the optimum operating parameters on a CNC PAC machine to minimize the creation of dross when cutting a range of thicknesses of 1018 HR steel. Therefore, experiments were conducted to determine the machine settings that minimize dross formation when cutting 1018 HR steel sheets. The results of this study should enable PAC machine operators to readily determine the proper settings for each material thickness they process. This will greatly improve the efficiency of the PAC process.

Need for the Study

A review of the current literature demonstrates that there is a need for additional studies on plasma arc cutting. The complexity of the process and the number of parameters involved

make it difficult for users of PAC machines to find the proper machine settings to produce the best quality parts. While this study concentrates on minimizing dross formation, there are various other quality concerns to be considered when producing parts using the PAC process. Kerf width, edge inclination, cutting tolerance, and the heat affected zone (HAZ) are other quality parameters that need to be addressed depending on the requirements of the finished product. Hypertherm (2008) predicts continued growth in the market for PAC machines that can produce high-quality, close-tolerance parts. PAC machines can produce parts with minimal amounts of dross, narrow kerfs, square edges, and tolerances of +/- 0.010 inch when properly set up. The challenge for the companies that use these machines is to control all of the variables to maximize the quality of parts produced in the least amount of time. A review of available literature on the PAC process reveals a lack of understanding of how to use a PAC machine to produce the best quality parts. The following authors discuss the lack of published studies dealing with plasma cutting and provide evidence that supports the need for the proposed study.

Numerous studies have been performed to advance scientific knowledge of the PAC process. In their experimental study of an oxygen plasma torch, Girard et al. (2006) examined plasma-jet behavior. They wrote, “Although plasma cutting devices are widespread in the industry sector, there are only a few detailed experimental studies on the matter” (p. 1543). In their paper, “Correlations Between System Parameters and Process Responses in Plasma Cutting,” Hussary and Renault (2006) stated, “Despite the wealth of work that has been done in the last decade on thermal plasmas, both industrial and academic, there still seems to be a consensus regarding the lack of basic phenomena understanding” (p. 382). In an article titled “What We Know and What We Do Not Know About Plasma Arc Cutting,” Nemchinsky and

Severance (2006) wrote, “There is very little experimental data available on plasma cutting parameters” (p. R423), and

> “At the present time, our understanding is far from this ideal situation. Many basic phenomena do not have even a qualitative explanation. Unfortunately, these are the phenomena that determine the limitations of the method: cathode erosion, double arcing and cut quality” (p. R426)

They also stated, “The ultimate goal of the PAC process is heating, melting, and removing of the metal from the cut. It is, therefore, surprising there are only a few papers dedicated to these issues” (p. R433). In their study of an oxygen plasma cutting torch, Freton et al. (2001) wrote, “In spite of its industrial development, not many scientific publications exist on the plasma cutting process” (p. 115). In his dissertation on plasma-torch design and operating conditions, Peters (2006) noted, “Despite its widespread use, the plasma cutting arc has not been as intensively studied as other plasma sources” (p. 2). In their examination of the operating parameters of a PAC torch, Kelly et al. (2004) asserted, “In spite of the widespread application in industry of the plasma arc cutting process, a comprehensive description of this phenomenon has received relatively little research attention” (p. 1518). In their study of the plasma-arc –material interaction, Teulet et al. (2006) wrote, “In spite of this industrial development, there are only a few scientific publications concerning plasma cutting process.” (p. 1557). Venkatramani (2002) also discussed the lack of studies on PAC systems in his examination of industrial plasma torches. He stated, “The need of the hour [for PAC] is the creation of basic database, improvements in instrumentation, formulation of control strategy, process modeling, system analysis and optimization” (p. 262).

Because of the importance of quality in manufacturing today, there have been many studies about the quality of the PAC cut. Various researchers have studied the different aspects of quality and the variables involved. Many researchers have noted the lack of information about optimizing cut quality with the PAC process. In their theoretical study of plasma heat and energy movement, Dashkovskiy and Narimanyan (2007) stated, "Investigations are needed for the prediction and control of the above mentioned phenomena [poor cut quality] concerning the plasma arc cutting process" (p. 442). While the manufacturers of PAC machines provide guidelines for machine settings, they still expect the end-user to experiment with the variables to find the optimum settings. An example of this comes from a chart in the operating manual of the Hypertherm Powermax 1000 PAC machine:

> Maximum travel speeds are the fastest travel speeds possible to cut the material without regard to cut quality. Optimum travel speeds provide the best cut angle, least dross, and best cut surface finish. Remember that cut charts are intended to provide a good starting point for each different cut assignment. Every cutting system requires fine tuning for each cutting application to obtain the desired cut quality (Hypertherm, 2008, p. 17).

In a paper reviewing numerous PAC studies, Nemchinsky and Severance, (2006) discuss the need for more PAC studies. They wrote, "A full understanding of the phenomena of dross formation has not been achieved yet" (p. R435) and "By common practice there has developed some rules-of-thumb on how to improve the quality of cut, however, our understanding of the basic phenomena is very shallow" (p. R436). They also stated,

> Although the first PAC system was introduced half a century ago, very little has been done to explore and understand this process. Comparing PAC with welding, we see that while hundreds of papers are published on welding every year, only a few, if any, are

> annually dedicated to exploring PAC. The lack of scientific activity hampers the improvement of PAC technology. This is surprising, keeping in mind that many of the problems faced by PAC (electrode erosion, double arcing, dross formation) are common not only to PAC but to other industrial processes as well. (Nemchinsky & Severance, 2006, p. R437)

Ramakrishnan et al. (2000) examined how gas composition affects dross formation in PAC. They wrote.

> The physical mechanisms associated with the ejection of molten metal (in PAC) from the cut front, and the adhesion of some of the ejected molten metal to form dross at the bottom of kerf are complex, and only limited work on these topics have been reported. (p. 2297)

In an article titled "Improving Plasma Arc Cutting," Whiting (2007) discussed the need for PAC users to be more knowledgeable about this technology:

> The purpose of a PAC system is to inexpensively cut a part in the least amount of time with the best cut quality possible. Balancing the cost, the cut quality, and the speed of the system can become difficult when designing or improving a system's performance. Therefore, it is crucial that anyone who uses a PAC system be fully aware of its functionality. By understanding and optimizing the performance of each of its components, you can quickly and consistently create high-quality products at a relatively low operating cost. (p. 44)

The lack of trained technicians to operate PAC machines is addressed by Walsh (2005, ¶ 2) in his article on advancements in PAC technology. He stated, "It wasn't long ago that plasma cutting was the domain of seasoned metal fabrication veterans who knew just how to tweak the

gas settings and adjust torch height to get the best cut on a plasma cutting table. Today many of the highly trained technicians have left the shop floor."

In his paper outlining a PAC expert system, Yang (2000) addressed the issue of controlling the quality of cut with PAC:

> Plate cutting is one of the most important manufacturing processes for metal components making. The quality and the cost of cutting processes are often critical for final product quality and cost. It is estimated that the plasma cutting machine with a computer numerical controlled (CNC) torch movement is the optimal choice for 80% of the metal plate cutting processes. However, the quality of the plasma cutting process is often unpredictable largely due to the unknown effects of the different process parameters. Difficulty in quality control in one of the factors which affect the wide spread use of the plasma cutting process in industry (p. 438).

Since users do not understand the operating parameters on PAC machines, there are instances where these machines are underutilized. This is the situation at Cincinnati State Technical and Community College. The Center for Innovative Technologies at the college purchased a new CNC PAC machine in 2006. This machine has the potential to be used by hundreds of students in numerous programs throughout the college. Students in the Mechanical Engineering Technology, Civil Engineering Technology, Industrial Design Technology, and Electromechanical Engineering Technology programs can use this equipment in their courses and for their student projects. After four years, the machine has hardly been used, primarily due to the college faculty's poor understanding of the proper machine settings required to produce quality parts. The college faculty do not have the time to experiment with all of the combinations of variables involved in using this machine nor do they wish to waste expensive

materials as they experiment with the different machine settings. Therefore, this study will be useful for those at Cincinnati State and many other users.

Summary

PAC has become a very useful tool in the metalworking industry. It is a very versatile process that can be used to cut many different types and sizes of materials. The machine settings to control the speed and quality of the process are different for each application of the PAC process. While PAC equipment manufacturers give recommendations for machine settings, questions remain about how to balance the numerous operating parameters to achieve the best quality of cut. The proposed study is designed to determine the specific machine settings needed to minimize the formation of dross while cutting 1018 HR steel of various thicknesses.

Statement of Hypotheses

Many studies have shown that there are two types of dross: low-speed dross (LSD) and high-speed dross (HSD). They have also shown that there are speeds between those causing LSD and HSD that produce the best quality of cut. The challenge is to find this range of "dross-free" speeds for each application. The goal of this study is to determine the settings that minimize dross formation for a variety of thicknesses of 1018 HR steel material. This will be done by determining the lower limit of machine settings that will prevent the formation of LSD and the upper limit of machine settings that will prevent the formation of HSD. The following hypotheses will be used to determine the optimum machine settings to produce the least amount of dross on the work piece.

Null Hypotheses

H_{o1}: The formation of dross during plasma cutting is not linearly related to either amperage, cutting speed, or nozzle size when cutting 16-gauge 1018 HR steel ($B_1 = B_2 = B_3 = 0$).

H_{o2}: The formation of dross during plasma cutting is not linearly related to either amperage, cutting speed, or nozzle size when cutting 14-gauge 1018 HR steel ($B_1 = B_2 = B_3 = 0$).

H_{o3}: The formation of dross during plasma cutting is not linearly related to either amperage, cutting speed, or nozzle size when cutting 12-gauge 1018 HR steel ($B_1 = B_2 = B_3 = 0$).

H_{o4}: The formation of dross during plasma cutting is not linearly related to either amperage, cutting speed, or nozzle size when cutting 1/8" 1018 HR steel ($B_1 = B_2 = B_3 = 0$).

H_{o5}: The formation of dross during plasma cutting is not linearly related to either amperage, cutting speed, or nozzle size when cutting 3/16" 1018 HR steel ($B_1 = B_2 = B_3 = 0$).

H_{o6}: The formation of dross during plasma cutting is not linearly related to either amperage, cutting speed, or nozzle size when cutting 1/4" 1018 HR steel ($B_1 = B_2 = B_3 = 0$).

H_{o7}: The formation of dross during plasma cutting is not linearly related to either amperage, cutting speed, or nozzle size when cutting 3/8" 1018 HR steel ($B_1 = B_2 = B_3 = 0$).

Alternative Hypotheses

H_{A1}: The formation of dross on plasma-cut parts is linearly related to either amperage, cutting speed, or nozzle size when cutting 16-gauge 1018 HR steel ($B_j \neq 0$ for at least one j = 1, 2, 3).

H_{A2}: The formation of dross on plasma-cut parts is linearly related to either amperage, cutting speed, or nozzle size when cutting 14-gauge 1018 HR steel ($B_j \neq 0$ for at least one j = 1, 2, 3).

H_{A3}: The formation of dross on plasma-cut parts is linearly related to either amperage, cutting speed, or nozzle size when cutting 12-gauge 1018 HR steel ($B_j \neq 0$ for at least one j = 1, 2, 3).

H_{A4}: The formation of dross on plasma-cut parts is linearly related to either amperage, cutting speed, or nozzle size when cutting 1/8" 1018 HR steel ($B_j \neq 0$ for at least one j = 1, 2, 3).

H_{A5}: The formation of dross on plasma-cut parts is linearly related to either amperage, cutting speed, or nozzle size when cutting 3/16" 1018 HR steel ($B_j \neq 0$ for at least one j = 1, 2, 3).

H_{A6}: The formation of dross on plasma-cut parts is linearly related to either amperage, cutting speed, or nozzle size when cutting 1/4" 1018 HR steel ($B_j \neq 0$ for at least one j = 1, 2, 3).

H_{A7}: The formation of dross on plasma-cut parts is linearly related to either amperage, cutting speed, or nozzle size when cutting 3/8" 1018 HR steel ($B_j \neq 0$ for at least one j = 1, 2, 3).

Note: B is the regression coefficient for the independent variables amperage, cutting speed, and nozzle size.

Statement of Assumptions

1. The manufacturer's recommended values of torch standoff and air pressure give optimum results.
2. The machine performance will remain consistent during this study.
3. The measuring equipment will remain consistent during this study.

Statement of Limitations

1. Results of cutting 1018 HR steel may not be generalizable to other grades of steel.
2. Results obtained from this study may not be generalizable to other brands of PAC machines.

Statement of Delimitations

1. The testing will occur during a 1-month period of time.
2. Testing will be performed using a PlasmaCAM CNC machine with a Hypertherm Powermax 1000 PAC machine.
3. Testing will be limited to 1018 HR steel.
4. Testing will involve cutting 0.055", 0.075", 0.105", 0.125", 0.188", 0.250", & 0.375" material.

Terminology

1018 steel: Steel that is composed of iron and carbon only, with carbon content of 0.18%

Air plasma cutting: A thermal cutting process that uses a high-temperature jet of plasma gas to cut metal.

Automatic torch height control: An electronically controlled system that adjusts the torch height based on the voltage through the system. This system is used to keep the torch height constant in case the work piece warps as it is being cut.

Computer-aided drafting (CAD): The process of using computer software to generate engineering drawings.

Computer numerical control (CNC): The control process of using computer software and digital technology, based on numerical methods, to control movement or shapes. In the case of PAC, CNC consists of a computer controller used to drive a machine tool to cut a predetermined path.

Cut angle: The angle between the stream of ejected molten metal and the bottom surface of the work piece. The optimum cut angle is 90°.

Dross: Metal that resolidifies and attaches to the work piece during the cutting process.

Dross-free range: A range of operating parameters where dross is not formed.

Edge inclination or *edge squareness:* A measure of the perpendicularity of the edge of the cut piece with reference to the bottom or top surface of the work piece.

Expert system: Computer software that attempts to replace a human expert through the use of a knowledge base of collected information.

Heat affected zone (HAZ): The area around the cut edge where the metallurgical microstructure of the metal is affected, which in turn affects its mechanical properties.

High-tolerance plasma cutting (HTPAC): An advanced PAC process that is more complex and significantly more expensive than the traditional PAC process.

High-speed dross (HSD): Molten metal that reattaches to the work piece when the cutting speed is too high or the torch power is too low.

Hot rolled (HR): a metalworking process used to reduce the thickness of a metal by heating it above its recrystallization temperature and then forcing it between rollers until the appropriate cross section is achieved.

Ionized: When an atom of an element is transformed into an ion by adding or removing electrons.

Kerf: The width of the material removed during cutting.

Lag angle: The angle (less than 90˚) that the plasma jet is deflected behind the direction of torch travel.

Low-speed dross (LSD): The reattached metal that forms under the work piece when the cutting speed is too low or the torch power is too high.

Martensitic phase: The arrangement of the iron and carbon atoms within steel that causes the material to become hardened after heat treatment.

Mathematical model: An equation or set of equations that describe a physical phenomenon in mathematical terms.

Mild steel: Steel that is composed of iron and carbon only, with carbon content between 0.15% and 0.30%

Oxygen PAC: A PAC system that uses oxygen as the cutting gas.

Oxy–fuel cutting: A thermal cutting process using oxygen and another fuel gas to generate a high-temperature flame.

Plasma arc cutting (PAC): A process that uses high-temperature plasma generated by an electric arc to cut metal.

Plasma: The fourth state of matter where a gas becomes ionized when superheated.

Plasma jet: A stream of ionized gas.

Spectroscopic analysis: The identification of elements in a substance by examining the spectrum of light emitted from or absorbed by the material.

Splatter: Small particles of waste metal that randomly reattaches to the top of the work piece.

Swirl ring: A component of the torch that creates a swirling motion in the gas to help concentrate the flow to the work piece.

Tungsten inert gas (TIG) arc welding: An arc welding process that uses a nonconsumable tungsten electrode to heat the work piece while a filler rod is used to add material to the weld.

Torch height control: A feedback system incorporated into the machine controller that automatically adjusts the torch to the proper height above the work piece once cutting is initiated.

Torch standoff: The distance between the tip of the cutting nozzle and the work piece being cut.

Vortex: A spinning motion imparted to the cutting gas to produce a concentrated flow of gas.

Warpage: A distortion of the flatness of the material caused by exposure to extreme temperature changes, which is a quality parameter in PAC.

Work piece: The material being cut.

CHAPTER 2

REVIEW OF LITERATURE

The Process

As previously discussed, PAC is a dynamic process involving many variables that affect the quality and efficiency of the cutting process. Finding a balance of appropriate operating parameters can be a difficult task for the operator of a PAC system (Ramakrishnan, Gershenzon, Polivka, Kearney, & Rogozinski, 1997). The operator can use numerous settings to achieve the best quality of cut. The machining parameters include arc current, plasma-gas type, cutting speed, gas flow rate, pierce height, cut height (standoff), consumables, travel direction, nozzle size, material type, material thickness, and torch angle.

The operator of the PAC machine must determine the settings that will satisfy the output requirements. One of the biggest challenges is balancing all of the parameters to "achieve optimal cutting performance." The best possible scenario is to find the parameters that produce the highest quality of cut in the shortest time (Whiting, 2007). Thompson and Hachette (2003) wrote about the difficulties in controlling the PAC process:

> For many people, the world of plasma cutting is a complex and daunting place, with a cryptic set of rules that can be mastered only by highly trained technicians after weeks of training. For every change of material or thickness being cut, a long process ensues of resetting gas mixtures, tweaking pierce heights and pierce delays, and manually calibrating every last parameter to ensure a reliable result. (¶ 1)

Plasma Arc Cutting Quality

Quality is a very important aspect of manufacturing today. Several processing and quality issues must be addressed when using a plasma cutter. Measures of quality include edge squareness, kerf width, HAZ size, dimensional accuracy, material warpage, splatter, and dross formation (American Welding Society [AWS], 2006; Bini, Colosimo, Kutlu, & Monno, 2007; Bogorodski et al., 1991; Colt, 2002; Dashkovskiy, et al. & Narimanyan, 2007; Freton et al., 2001; Gane et al., 1994; Güllü & Atici, 2006; Iosub, Nagit, & Negoescu, 2008; Nemchinsky, 1997; Nemchinsky & Severance, 2006; Peters, 2006; Ramakrishnan et al., 2000; Vasil'ev, 2002; Zajac & Pfeifer, 2006). One of the most common problems with plasma cutting is the formation of dross, resolidified metal, on the cut edge (Sommer, 2000).

Dross is a by-product of all thermal-cutting techniques including PAC, oxy–fuel cutting, and laser cutting (Nemchinsky & Severance, 2006). The PAC process "tends to leave a bottom residue of recast metal that is sometimes difficult to remove" (Sommer, 2000, p. 227). Dross appears as a small, hard bead or a large, bubbly accumulation on the underside of the cut work piece (Landry, 1998) that results from incomplete expulsion of the melted material from the kerf (Tani, Tomesani, Campana, & Fortunato, 2003). By carefully controlling the operating parameters, the formation of dross on the work piece can be minimized. The reduction of dross greatly increases the quality of the part and the efficiency of the production process (Cook, 1998; Dashkovskiy & Narimanyan, 2007; Gane et al., 1994; Ramakrishnan et al., 1997).

PAC involves focusing a lot of power onto a small surface area of the material, producing an intense heating of the surface. Initially the material on the top surface melts and the molten metal is removed by the flow of high-speed gas. As the plasma cutter advances across the surface of the material, there is a greater degree of melting on the top of the work piece than at

the bottom, which can result in a poor quality cut due to the formation of dross on the bottom edge (Dashkovskiy & Narimanyan, 2007), as shown in Figure 5.

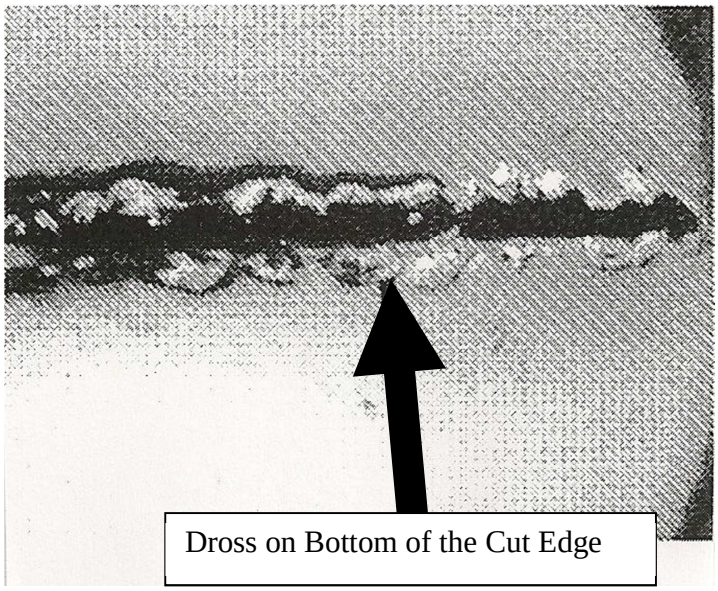

Figure 5. Dross attached to bottom of the work piece.
From *Plasma Cutting of Composite Materials*, by A. Iosub, Gh. Nagit, & F. Negoescu, 2008, paper presented at the 11th European Aviation Safety Agency conference on Material Forming, Lyons, France.

Dross formed on the cut edge of the work piece creates several problems for a manufacturer. Dross creates a jagged edge in the cut area as well as a protrusion on the top and bottom surfaces of the work piece. Due to the effect of the heat applied to the cut area, this dross can be very difficult to remove from the work piece (Nemchinsky & Severance, 2006; Sommer, 2000; Whiting, 2007). Removing the dross requires additional processing time as well as added costs in labor and tools (Davis, 2010). It is very important to achieve high precision in PAC cutting geometry in order to minimize the subsequent machining costs (Dashkovskiy & Narimanyan, 2007).

Eliminating Secondary Operations

Manufacturing companies using the CNC PAC process are concerned with the dimensional accuracy and physical appearance of the parts they produce (Güllü & Atici, 2006). The quality of plasma-arc cut parts also affects the overall efficiency of the manufacturing operation. One of the main reasons for optimizing the quality of PAC-produced parts is to minimize or eliminate the costs associated with secondary operations that may be required to remove dross from the work piece (Cook, 1998, 1999; Dashkovskiy & Narimanyan, 2007). In many cases, the time required to plasma cut the parts is less than the time taken by the secondary operations required to remove the dross from the parts (Bogorodski et al., 1991).

Dross Formation

Dross can be formed by a combination of operating parameters, but cutting speed has been identified by many studies as one of the leading causes of dross formation (Freton et al., 2001; Gane et al., 1994; Nemchinsky, 1997; Nemchinsky & Severance, 2006; Ramakrishnan et al., 2000; Zajac & Pfeifer, 2006). Colombo, Concetti, Ghedini, Dallavalle, and Vancini (2009) stated, “This phenomenon [dross formation] has been observed in the case of both too high and too low cutting speeds with respect to optimum conditions.” Because of the clear relationship between cutting speed and dross formation, the industry has identified two main types of dross formed when thermal cutting: LSD and HSD (Nemchinsky & Severance, 2006). The two types of dross are different in appearance and behavior, but they both reduce in the cut quality. The challenge is to find the proper cutting parameters to prevent the formation of both LSD and HSD during PAC.

Low-Speed Dross

LSD forms on the work piece when the cutting speed is too low. A low cutting speed widens the kerf and makes it more difficult for the pressurized jet to blow the molten metal away. This causes the excess molten material to accumulate and resolidify along the bottom edge of the work piece, forming LSD (Bini et al., 2007; Cook, 1998; Gane et al., 1994). LSD is relatively easy to remove by scraping (Whiting, 2007).

Depending on the other parameters being used, there is a minimum cutting speed below which LSD does not form on the work piece (Nemchinsky, 1997). The formation of dross on the bottom of the cut can be quite severe when the cutting speed is too low (Gane et al., 1994). Ramakrishnan et al. (2000) and Gane et al. (1994) observed that LSD formation is a combination of the effects of surface tension and the angle created by the arc as it meets the surface of the work piece as shown in Figure 6.

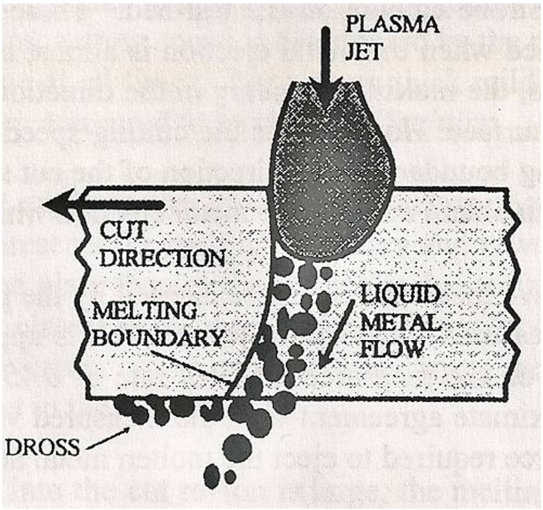

Figure 6. Formation of low-speed dross.
From *Quality of Cut in Air Plasma Cutting*, by N. Gane, M. W. Rogozinski, F. Polivka, A. G. Doolette, & S. Ramakrishnan, 1994, paper presented at the Washington Technology Industry Association 42nd annual National Welding Conference, Melbourne, Australia.

The other parameters that affect LSD formation are the arc current and torch standoff. According to Cook (1998, 1999), increasing the arc current or reducing the standoff affect LSD

formation similarly to reducing the cutting speed. All of these adjustments cause the added energy from the plasma jet to melt additional material in direct contact with the plasma arc without giving it enough energy to blow the melted material clear of the work piece.

High-Speed Dross

HSD forms when a higher cutting speed is used without an accompanying appropriate increase in the arc current. A cutting speed that is too high causes instability in the arc and an inability to remove material quickly enough. This situation allows the molten material to weld itself to the bottom of the work piece. HSD is much more difficult to remove, requiring extensive machining or grinding (Landry, 1998; Nemchinsky, 1997; Whiting, 2007). According to Nemchinsky and Severance (2006) "The phenomenon of high-speed dross formation is even less understood than that of low-speed dross" (p. R436).

HSD occurs at cutting speeds that are very close to the maximum cutting speed. Gane et al. (1994), Nemchinsky and Severance (2006), and Freton et al. (2001) studied the mechanism of dross formation and determined that high cutting speeds increase the cut angle relative to the bottom edge of the work piece. The optimum angle of ejection of the molten metal is 90° from the work piece; at high speeds, this angle is greatly reduced and causes the ejected metal to lag with respect to the direction of cut as shown in Figure 7.

The lag angle is created when cutting too fast and allows the formation of HSD. Because the molten metal leaving the work piece is almost parallel to the bottom of the plate, it has enough time to solidify while it is still in contact with the work piece. In addition to cutting speed, researchers have identified other variables that affect HSD formation (Cook, 1998, 1999; Nemchinsky, 1997; Vasil'ev, 2002). A worn nozzle, high torch standoff, or low arc amperage all reduce the energy of the plasma jet, which leads to HSD formation. For each material type and

thickness being cut, the PAC operator must determine the optimum settings for each of these parameters in order to reduce or eliminate HSD.

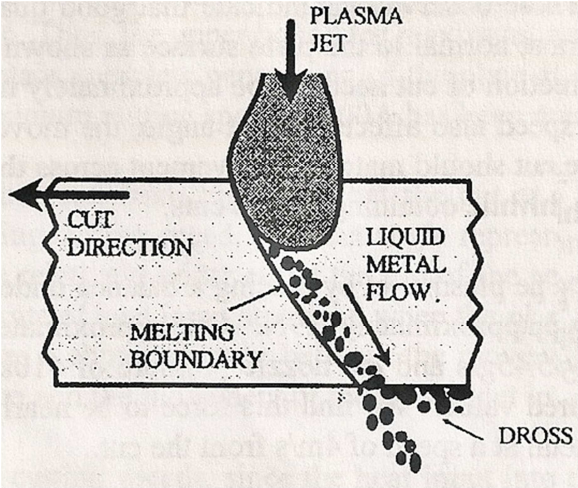

Figure 7. Formation of high-speed dross.
From *Quality of Cut in Air Plasma Cutting*, by N. Gane, M. W. Rogozinski, F. Polivka, A. G. Doolette, & S. Ramakrishnan, 1994, paper presented at the Washington Technology Industry Association 42nd annual National Welding Conference, Melbourne, Australia.

The Dross-Free Window

The dross-free interval or dross-free window is defined as the range between a maximum and minimum speed where little or no dross is formed on the work piece at a given power level. Higher quality cuts are produced when the PAC machine is operating within the dross-free window of speeds. As the work piece gets thicker, the window becomes narrower. A difference of a few inches per minute in cutting speed on thick plates can cause the work piece to go from LSD formation to HSD formation (Nemchinsky & Severance, 2006). In their studies, Nemchinsky (1997), Cook (1998), and Nemchinsky and Severance (2006) showed that the kind of plasma cutting gas used also affects the dross-free window. They found that air PAC has a relatively narrow dross-free window. The chemical composition of the material being cut also affects the dross-free window. Blankenship (1990) wrote, “Stainless steel and aluminum have

relatively wide dross-free operating ranges. Nickel copper, nickel chromium iron, and copper alloys form dross quite readily. Mild steel falls in between the two extremes" (p. 56).

A wider dross-free window is preferred because it allows the speed of the PAC machine to vary slightly without impacting dross formation. Cook (1998) stated, "Between the extremes of high- and low-speed dross is a window of dross-free or minimum dross cutting. Finding this window is the key to minimizing secondary operation requirements on plasma cut pieces" (p. 2). The window of dross-free speeds tends to widen with an increase in arc current and become narrower as the material gets thicker. According to Nemchinsky and Severance (2006), "A full understanding of the phenomena of dross formation has not been achieved yet" (p. R435).

Preventing Dross

In order to prevent dross formation, the PAC process needs to have a concentrated, high-energy, high-velocity plasma jet that can rapidly melt the work piece. The plasma jet must also exert enough force on the work piece to quickly remove the molten material before it resolidifies (Pardo, Gonzalez-Aguilar, Rodriguez-Yunta, & Calderon, 1999; Nemchinsky & Severance, 2006; Ramakrishnan & Rogozinski, 1997). Nemchinsky (1997) examined the forces acting upon the molten metal in the kerf and concluded that aerodynamic drag and surface tension are the predominant forces that must be overcome to prevent dross adhesion. According to Nemchinsky and Severance (2006), "One of the most important features of a good-quality cut is either a completely dross-free cut or, at the least, easy to remove dross" (p. R435). Gane et al. (1994) wrote, "For the process to be effective, a correct balance between the heat input into the work and the momentum of the jet is essential to remove all the molten material from the cut region" (p. 9). Table 1 summarizes the effects of the proposed test parameters on the formation of dross.

Table 1

How Test Parameters Affect Dross Formation

Parameter	Affect on dross
Cutting speed too slow	LSD formed
Cutting speed too fast	HSD formed
Optimum speed	No dross formed
Power setting too low	HSD formed
Power setting too high	LSD formed
Optimum power setting	No dross formed
Nozzle type	Dependent on speed and power settings

Research Studies

For many years, there has been a need in industry for guidelines about how to achieve the best quality of cut from the PAC process. There are many journal articles that address the issue of PAC parameters. These authors have examined the variables involved in the operation of a PAC machine and have reached various conclusions about the behavior of the PAC process under different operating conditions. The primary objective of all of these works was to determine how to achieve the best performance from a PAC machine.

In his efforts to create an expert system for controlling PAC parameters, Yang (2000) identified 120 process parameters that can affect the plasma cutting process. PAC studies have included mathematical modeling of the process, focused on specific properties, and examined the behavior of the plasma jet itself, as well as more practical experimental studies to evaluate the parameters that affect the quality of the cut produced with PAC. These studies can be classified into two main areas of concern: the properties and behavior of the plasma jet and the quality of the cut obtained with the PAC process.

Plasma-Jet Studies

Plasma-jet studies have been performed by Girard et al. (2006), Gonzalez-Aguilar et al. (1999), Kelly et al. (2004), Nemchinsky (1998), Pardo et al. (1999), Peters (2006), Ramakrishnan et al. (1997), Ramakrishnan and Rogozinski (1997), and Zhou et al. (2008). These studies examined such properties of the plasma jet as shape, temperature, and pressure. They were also performed to better understand the mechanics of the PAC process. Table 2 summarizes these studies.

Table 2

PAC Studies Involving Plasma-Jet Properties

Researcher(s)	Independent variables	Dependent variables	Results/conclusions
Girard et al. (2006)	Arc voltage, cutting speed, gas pressure	Temperature and plasma-jet pressure	Temperature and pressure of plasma jet are significantly affected by gas pressure, but not arc voltage or cutting speed.
Gonzalez-Aguilar et al. (1999)	Arc voltage, gas pressure	Flow properties of the plasma jet	Developed a 3-D model of the plasma jet.
Kelly et al. (2004)	Gas flow rate	Temperature and pressure of plasma jet	Results show affect of gas flow rate on plasma-jet properties.
Nemchinsky (1998)	Arc current, gas flow rate, nozzle diameter	Temperature, pressure, and power of plasma jet	Nozzle efficiency falls as the gas flow increases and as arc current increases.
Pardo et al. (1999)	Arc current, arc voltage	Temperature, pressure, and electron density of plasma jet	Pressure increases closer to the anode and decreases closer to the nozzle.
Peters (2006)	Arc current, gas flow rate, nozzle diameter	Temperature and electron density of plasma jet	Determined temperature and electron density throughout the plasma arc.
Ramakrishnan et al. (1997)	Arc current, gas flow rate, nozzle diameter	Arc radius, pressure, and arc voltage of plasma jet	Arc power for a given current can be increased by increasing the air flow rate or reducing the nozzle size.
Ramakrishnan & Rogozinski (1997)	Arc current	Arc voltage and nozzle pressure	With a constant gas flow rate, the plasma jet's pressure increases as the arc current increases.
Zhou et al. (2008)	Nozzle length, arc current, mass flow rate	Arc voltage, temperature, and velocity	Temperature and velocity of plasma jet is significantly affected by arc current and mass flow rate.

Girard et al. (2006) examined the effect of voltage, torch velocity, and gas pressure on "the macroscopic properties of the arc" in an oxygen PAC system. Data was collected on an actual cutting device and compared with tests performed on a rotating anode (simulated cutting). The arc current was a constant 60 amps while the cutting speed was varied from 50–140 cm/min while cutting 10-mm plates. The results showed that the temperature and pressure of the plasma jet was significantly influenced by the oxygen inlet pressure, but "not really affected" by the cutting speed or arc voltage.

Gonzalez-Aguilar et al. (1999) developed a 3-D model of an air PAC torch. This mathematical model was used to study the heat flow and compressible fluid flow of the arc. According to the authors, "the model gives some predictions about the behavior of plasma and useful quantities for the optimization design of plasma torches" (p. 270).

Using a low-current (30–40-amp) air PAC system, Kelly et al. (2004) examined the temperature and velocity of the plasma jet exiting the nozzle. They used a rotating steel cylinder as an anode to simulate cutting, a 0.8-mm nozzle orifice, air at 5 bar, and arc currents of 30 and 40 amps. The results showed the affect of mass flow rate on plasma-jet properties.

Nemchinsky (1998) examined how the torch nozzle affects plasma flow from the torch. This test involved creating a mathematical model to examine how the plasma arc is affected by changes in arc current, gas flow rate, and nozzle dimensions. Nozzle efficiency was found to be between 60% and 80%. The results also showed that larger nozzle sizes, increased arc current, and increased gas flow rates reduce the efficiency of the plasma jet.

Pardo et al. (1999) used spectroscopic analysis to analyze an air PAC torch. They varied arc current and arc voltage to obtain data on temperature, pressure, and electron density. Testing was performed using a Terwin 155/2 PAC system, 150-amp arc current, a gas flow rate of 20

liter/min, 5 bars at the inlet, and a rotating anode (no actual cutting). They determined that the pressure increases as the plasma jet approaches the work piece.

Peters (2006) also used spectroscopic diagnostics to investigate the behavior of the plasma arc. He varied the nozzle diameter, gas flow rate, and arc current and measured the temperature and electron densities across the width of the plasma arc to better understand the arc's behavior. He also examined how nozzle wear affects the constriction of the arc and determined that as the nozzle wears, the temperature of the arc is reduced.

Ramakrishnan et al. (1997) created a mathematical model to describe the thermal power and force of a plasma jet. This model was used to predict the plasma jet's arc radius, pressure, and arc voltage while varying the arc current, nozzle size, and air flow rate. Estimated values were then compared to experimental values. They used a Hypertherm Max 200 air PAC with a 1.3–1.7-mm nozzle, a constant arc current of 100 amps and a 5-mm torch standoff. The results showed that a sufficient amount of power and force must be applied to the work piece in order to melt and remove the metal from the cut. They concluded that arc power for a given current can be increased by increasing the air flow rate or by reducing the nozzle size. They also determined that "a balance between the power input and force is necessary to maintain dross-free cuts over a range of speeds" (p. 944). Additionally, they give some guidelines to estimate the operating parameters.

Ramakrishnan and Rogozinski (1997) developed a mathematical model to estimate the plasma arc radius, voltage, and pressure with respect to the arc current. Measurements were taken of arc voltage, nozzle voltage, air flow rate, and nozzle pressure while varying the arc current from 40 A to 160 A. They used a Hypertherm Max 200 with a 1.5-mm nozzle with no shield cap (to aid photography). Simulated cutting was done using a rotating, water-cooled

copper disc for the anode with a 5-mm standoff. The results showed that, with a constant flow of gas through the nozzle, the pressure at the nozzle exit increases as the arc current increases (inlet pressure is not critical).

Zhou et al. (2008) conducted a numerical simulation to study the influence of nozzle length, arc current, and mass flow rate on the plasma arc. The aim of the study was to provide new information to improve the design of the plasma arc process. They determined that nozzle length has a large effect on the arc voltage, and arc energy, which affect the cutting speed and cut quality. This study also found that high mass flow constricts the arc and increases the heat flux.

Studies on Cut Quality

While studies concentrating specifically on the plasma jet have been useful in understanding the process, the information in these studies has done little to help the PAC end-user. Many other researchers have examined the operating parameters that affect the overall performance of the PAC process and especially the quality of the parts produced with this process. There are numerous ways to examine cut quality on PAC-produced parts. Studies by Bini et al. (2007), Güllü and Atici (2006), Iosub et al. (2008); Vasil'ev (2002), and Zajac and Pfeifer (2006) have analyzed PAC cut quality in terms of the shape and size of the kerf as well as the HAZ. Table 3 presents a summary of PAC quality studies involving kerf width and HAZ.

Bini et al. (2007) used a high-tolerance plasma arc cutting system to examine how arc voltage, cutting speed, gas flow rate, and gas composition affect the shape and position of the kerf. Cuts were made on 15-mm mild steel material while varying the operating parameters. It was shown that "very good quality" can be achieved by properly setting the cutting speed and arc voltage only. They also concluded that the torch standoff distance is important for obtaining a good cut quality.

Table 3

PAC Quality Studies Involving Kerf and HAZ

Researcher(s)	Independent variables	Dependent variables	Results/conclusions
Bini et al. (2007)	Arc voltage, cutting speed, gas composition, gas flow rate	Cut quality: shape and position of kerf	Cutting speed & arc voltage are critical to cut quality.
Güllü & Atici (2006)	Cutting speed, cutting gas, standoff distance	Cut quality: hardness and HAZ	Cutting speed, cutting gas, & nozzle height affect HAZ.
Iosub et al. (2008)	Arc voltage, cutting speed, gas pressure, standoff distance	Cut quality: kerf width and surface finish	The results show the critical nature of proper cutting speed & arc voltage for cut quality.
Vasil'ev (2002)	Gas composition: O_2 content in cutting gas	Cut quality: edge squareness and HAZ	Results show that cutting with 70% O_2 & 30% N_2 gives best quality & reduced HAZ.
Zajac & Pfeifer (2006)	Arc current, cutting speed, cutting media	Cut quality:edge squareness and HAZ	The rate of cutting is the "fundamental parameter which determines cut quality"

Güllü and Atici (2006) examined the microstructure of plasma cut samples determine the effect of cutting speed, nozzle height, and cutting gas on hardness and the HAZ. They cut 304 stainless steel and St52 carbon steel samples of various thicknesses using either oxygen or nitrogen and using manufacturer-recommended cutting speeds. The results showed that the cutting speed, cutting gas, and nozzle height affect the width of the HAZ.

Iosub et al. (2008) investigated the performance of a PAC machine while cutting laminar composite materials consisting of two aluminum plates with a polyethylene core. Their goal was to find proper operating parameters to produce the highest quality cuts. They varied gas pressure, cutting speed, standoff distance, and arc voltage. They found effective settings for cutting this specialized material and also noted the critical nature of the proper cutting speed and arc voltage.

Vasil'ev (2002) examined the effects of oxygen content of the cutting gas on the cutting speed for the PAC process. The cut quality in terms of edge squareness and HAZ were evaluated

for the different gas compositions tested. Steel plate 1 and 2 mm thick were cut at 200–300 Amps and 1–3 m/min cutting speed. The results showed that the cuts produced at 70% oxygen and 30% nitrogen gave the best quality and reduced the HAZ. They found that variation in the HAZ was also dependent on cutting speed, arc current, arc voltage, gas flow rate, nozzle dimensions, and torch height.

Zajac and Pfeifer (2006) investigated how operating parameters and cutting medium, air or water, affect the HAZ when plasma arc cutting. They cut 8-mm 1H18N9T stainless steel material in air and water while varying the arc current and the cutting speed. The results showed that the "fundamental parameter which determines quality of the cut, edge squareness, is the rate of cutting" (p. 8). They also found that regardless of arc current and cutting medium, the width of the HAZ can be reduced significantly by increasing the cutting speed.

The prevention of dross continues to be a challenge for PAC users. Dross is such a major quality concern that numerous research projects have been completed to examine cut quality based on the presence of dross on plasma-cut parts. Studies by Colt (2002), Colombo et al. (2009), Freton et al. (2001), Gane et al. (1994), Nemchinsky (1997), Nemchinsky and Severance (2006), Nishiguchi and Matsuyama (1979), Ramakrishnan et al. (2000), Xu, Fang, and Lu (2005), and Xue, Kusumoto, and Nezu (2004) examined cut quality in terms of dross adhesion and other quality measures as shown in Table 4.

Table 4

PAC Quality Studies Involving Dross

Researcher(s)	Independent variables	Dependent variables	Results/conclusions
Colt (2002)	Nozzle wear	Cut quality: edge squareness and dross presence	Linear degradation of cut quality as the nozzle wears.
Colombo et al. (2009)	Arc current, gas flow rate	Cut quality: kerf and dross formation	Arc current and gas flow rate can affect cut quality due to shape of the arc and double arcing.
Freton et al. (2001)	Cutting speed, standoff distance	Cut quality: dross presence	Definite relationship between the amount of dross and the cut speed and torch standoff (at a constant arc current).
Gane et al. (1994)	Cutting speed, gas pressure, standoff distance	Cut quality: edge squareness and dross presence	Cut quality is mostly dependent on cutting speed and nozzle orifice condition (for 1 material thickness tested).
Nemchinsky (1997)	Alloys, material thickness, nozzle diameter	Cut quality: dross formation	Found max. and min. cutting speeds w/ O_2 PAC and constant current. Alloys affect dross.
Nemchinsky & Severance (2006)	Cutting speed, cutting gas, gas flow rate and swirl, standoff distance	Cut quality: dross formation and edge squareness	All of the parameters studied can be "used to achieve the best possible cut quality" (no specific machine settings given).
Nishiguchi & Matsuyama (1979)	Cutting gas, cutting speed	Cut quality: dross adhesion	Identified cutting conditions to minimize dross adhesion for 16-mm stainless steel.
Ramakrishnan et al. (2000)	Cutting gas: O_2, N_2, air	Cut quality: kerf width and dross adhesion	Amt. of melt does not vary linearly with cut speed; air has narrowest kerf, highest cut speed (at constant arc current).
Xu et al. (2002)	Magnetic forces applied to plasma jet	Dross formation	Operating parameters affect dross formation more than "secondary constriction" of jet.
Xue et al. (2004)	Cutting speed	Acoustic signal, kerf width, bevel angle, and dross formation	Acoustic signal varies with "cut quality."
Yang (2000)	Arc current, arc voltage, cutting speed, shield pressure	Accuracy, cut angle, surface finish, dross coverage, and dross removability	Expert-system quality predictions "agreed well" with experimental values, but the system needs more training with actual data.

Colt (2002) examined consumable wear and the effect on cut quality. Colt examined wear in the nozzle through a series of cuts. He found that as the nozzle orifice wears "there is a fairly linear degradation of cut quality to the point where cut quality is no longer acceptable" (p. 4) due to the straightness of the cut edge and the formation of dross.

Colombo et al. (2009) used a high-speed camera imaging to examine the PAC process, investigating kerf formation, dross, cathode erosion, pressure conditions, and piercing. Their qualitative results demonstrate that high-speed imaging can be a useful tool for gaining a better understanding of the PAC process. The authors concluded that arc current and gas flow rate can affect cut quality due to the shape of the arc and double arcing in the PAC process.

Freton et al. (2001) performed an experimental study on dross formation. Their experimental analysis consisted of cutting metal of three different thicknesses (2, 4, and 6 mm) at a constant arc current of 60 amps while varying the torch standoff distance and the cutting speed. They examined dross ejection and adhesion at various machine settings. Using three relatively thin samples and at a constant arc current, the results of this study showed a definite relationship between the amount of dross formed and the cutting speed and torch standoff.

Gane et al. (1994) performed an analysis of how cut quality and consumable wear are affected by cutting speed, standoff distance, and air pressure. Using an air PAC torch, arc current was held constant at 100 amps and 6-mm mild steel was cut. The results of this limited testing showed that quality of cut, measured as squareness of cut edge and amount of dross formation, is mostly dependent on the cutting speed. The quality was also strongly affected by the condition of the nozzle orifice in the cutting torch.

Nemchinsky (1997) examined an oxygen gas PAC system to determine the maximum and minimum cutting speeds possible without forming dross. The project involved calculating the theoretical speeds and then comparing these to experimental results. Testing for this study involved cutting 12.7–50.8-mm mild steel. The nozzle diameter was varied from 2.3 to 3.3 mm, while cutting with a constant 9.5-mm torch standoff. They also examined how alloys in the work piece affect dross formation. The report presented tabulated results of maximum and minimum

cuttings speeds at a constant arc current for the samples tested. In addition, the results showed that small amounts of silicon, selenium, and tellurium added to the steel can increase the dross-free window significantly.

Nemchinsky and Severance (2006) examined plasma-jet behavior, dross, and overall cut quality under limited test conditions. The authors stated, “There are several parameters in the operator’s possession to achieve the best possible cut quality. They are: arc current, … type of the plasma gas, cutting speed, gas flow rate, amount of the gas swirl, and torch-to-work-piece distance (stand-off)” (p. R436).

Nishiguchi and Matsuyama (1979) investigated the “heat input characteristics” and molten metal flow to better understand PAC kerf formation and dross adhesion. In this study, they cut 16-mm SS41 stainless material at a constant 200-A arc current while varying the cutting speed and cutting gas (air, nitrogen, oxygen). The results demonstrated how molten metal flows during cutting and identified cutting conditions to minimize dross adhesion for one thickness of stainless steel material at a constant arc current. They found that the best quality cuts were achieved at the proper cutting speed while using nitrogen or air as the cutting gas.

Ramakrishnan et al. (2000) compared the effect of air, oxygen, and nitrogen on the shape of the kerf and the leading edge of the actual plasma arc. Tests were performed on 6-mm mild steel at a constant 100-A arc current. Cutting speeds of 1, 2, 3, and 4 m/min were used for each plasma gas. Several conclusions were reached about this one thickness of steel at a constant arc current: The amount of metal melted does not vary linearly with cutting speed, air produces the narrowest kerf, and air has the highest cutting speed. They also found that using oxygen as the cutting gas produced less dross over a wider range of cutting speeds.

Studying plasma cutting of ceramic materials, Xu et al. (2002) examined the affect of constricting the plasma jet with magnetic fields. Their results showed that "secondary constriction" of the arc does not reduce dross formation as much as "coordination of the operating parameters" (p. 155). They also found a definite correlation between cutting quality and cutting speed when cutting a ceramic material.

Xue et al. (2004) examined the relationship between the PAC acoustic signal and cut quality. They measured how the sound pressure level (SPL) changed as kerf width, bevel angle, and dross formation vary. They made 80-mm cuts in 3.2-mm and 6-mm mild steel using an automatic oxygen PAC machine. Their results showed that the acoustic signal does vary with cut quality, confirming the validity of using this phenomenon to monitor cut quality.

Yang (2000) outlined the development of an expert system for the PAC process designed to predict the cut quality for given parameter settings. This study examined arc current, arc voltage, cutting speed, and shield pressure. According to Yang, these variables were chosen because "they are commonly regarded in industry as the main influential plasma cutting parameters" (p. 442). They observed the effect on five quality attributes: accuracy, cut angle, cut surface finish, dross coverage, and dross removability. Samples of 6-mm mild steel were cut using a Hypertherm HT 200 plasma cutter with oxygen as the cut gas. They used the cutting speeds recommended by Hypertherm and compared predicted values to actual measures of quality. This study involved cutting only seven actual samples to compare to predicted values. They concluded that the quality predictions from their expert system "agreed well" with experimental values, but admitted that they need to train their system with more actual data.

Summary

Current literature and research studies support the idea that there are numerous variables that affect PAC cut quality. The variables shown to be critical to cut quality are cutting speed, arc current, torch standoff, size and condition of the nozzle orifice, cutting gas, and material type and thickness. For most operations, the cutting gas and torch standoff are predetermined for the cutting operation. With this in mind, for a given material type and thickness, the PAC operator should be able to use cutting speed, arc current, and nozzle size to obtain high-quality cuts. The difficulty lies in determining the exact settings needed to produce high-quality cuts when cutting different material types and thicknesses.

None of the previous studies of cut quality and dross formation can be used to meet the objectives of this proposed study. Although Colt (2002) discusses the correlation between operating parameters and dross formation, he gives minimal specifics on test parameters. Freton et al. (2001) tested only very thin metal at a constant power setting. Gane et al. (1994) tested only 6-mm mild steel at a constant power setting of 100 Amps and cut only a few samples. Nemchinsky (1997) developed a mathematical model to minimize dross formation, but his study involved an oxygen (not air) torch as well as large diameter nozzles and thick steel material (1/2" to 2" thick). Nemchinsky and Severance (2006) and Ramakrishnan et al. (2000) concentrated on examining the affects of various cutting gases and gas flow on cut quality. The study performed by Nishiguchi and Matsuyama (1979) was limited to a constant power of 200 Amps while cutting only stainless steel material. Xu et al. (2002) examined the affect of magnetic forces while cutting a ceramic material. Xue et al. (2004) performed a qualitative study limited to only two thicknesses of mild steel. None of the previous studies involving PAC cutting quality provide detailed information on speed, power, and nozzle size for a range of different thickness

of steel. These studies do provide valuable information about the performance of PAC systems, some of which is foundation information for the current study.

It is clear from previous PAC studies that the cutting speed, power level, and nozzle size all affect the amount of dross produced during plasma arc cutting. The parameter identified in a majority of journal articles as the most critical for cut quality is the cutting speed. Secondary parameters that still significantly affect the quality of cut include the arc current, the torch nozzle size, and the torch height (AWS, 2006; Cook, 1998, 1999, 2000; Hypertherm, 2008; Landry, 1998; Keddell, 2007; Sommer, 2000; Whiting, 2007). These variables all work in conjunction to control the nature of the plasma jet, and the quantity of heat supplied to the work piece, all of which determine the quality of the cut produced with the PAC process (Zajac & Pfeifer, 2006).

There is also no published information that can provide specific machine settings applicable to the equipment that will be used in this proposed study. The fact remains that this study can make it possible to greatly improve the performance of this machine without forcing the users to spend valuable time and money experimenting with machine settings each time a different thickness of material is cut.

CHAPTER 3

METHODOLOGY

This research study investigated the relationship between operating parameters, stated below, and the formation of dross on plasma-cut parts. Samples of parts produced while varying selected operating parameters were collected and analyzed to determine the optimum settings needed to minimize the amount of dross formed on the cut edges. The operating parameters studied included cutting speed, arc current, material thickness, and diameter of the cutting nozzle. Parameters that were held constant throughout testing included material type, air pressure, and torch standoff. The air pressure was set to the manufacturer's recommended value of 70–80 pounds per square inch and the torch standoff was set to the recommended values of 0.063" for nozzles #1 (A60) and #2 (A40), and 0.080" for nozzle #3 (finecut). Multiple regression analysis was used to examine the effect of these variables on the formation of dross and to determine the optimum settings for each of the parameters tested. Mathematical models consisting of these parameters were developed for each thickness of steel plate being tested. These equations were then used to determine the optimum machine settings for each thickness that will minimize the formation of both LSD and HSD. Tables produced from these equations will allow the machine operator to readily determine the proper machine settings that will allow the PAC machine to operate in the dross-free range. The results of the analysis were used to determine whether to accept or reject the null hypotheses presented.

This study was performed using a CNC PAC machine located at Cincinnati State Technical and Community College in Cincinnati, Ohio, as seen in Figure 8. The PAC machine is a Hypertherm Powermax 1000 controlled by a PlasmaCAM CNC machine. The CNC controller was programmed to cut out the 4" specimens that were used to collect data for this study. The order in which each part was cut from different thicknesses of steel were randomly selected prior to starting the testing to minimize the chance of any trends forming in the machine operating process that could have influenced the results. With four independent variables being tested (amperage, cutting speed, nozzle size, and material thickness), a significant number of combinations could be created. A sample of these combinations was tested by randomly choosing the settings for each test cut throughout the study.

Figure 8. PlasmaCAM CNC plasma cutting machine.

The design of experiments concept was explored in an attempt to create a more systematic and efficient study; unfortunately a few characteristics of this particular study prevent

its use. Experience with the PAC process has shown that the amount of dross formed is not a purely linear function with relation to cutting speed and power. Using this concept to deal with a nonlinear process requires that all variables be quantitative to allow testing at the center points of each variable's range (Anderson & Whitcomb, 2000). The qualitative nature of the nozzle type variable creates a problem with using this concept. The other obstacle is the requirement for a balanced experimental design that does not have missing data points (Mathews, 2005). Due to the nature of plasma arc cutting, the range of power and speed settings varies significantly depending on the material thickness and nozzle type. This variation makes it difficult to create a balanced design with no missing data points. Therefore, a traditional statistical analysis using multiple regressions was used. Multiple regressions can deal with the degree of nonlinearity expected in this study.

Review of Hypotheses

The following hypotheses were tested in this study:

Null Hypotheses

H_{o1}: The formation of dross during plasma cutting is not linearly related to either amperage, cutting speed, or nozzle size when cutting 16-gauge 1018 HR steel ($B_1 = B_2 = B_3 = 0$).

H_{o2}: The formation of dross during plasma cutting is not linearly related to either amperage, cutting speed, or nozzle size when cutting 14-gauge 1018 HR steel ($B_1 = B_2 = B_3 = 0$).

H_{o3}: The formation of dross during plasma cutting is not linearly related to either amperage, cutting speed, or nozzle size when cutting 12-gauge 1018 HR steel ($B_1 = B_2 = B_3 = 0$).

H_{o4}: The formation of dross during plasma cutting is not linearly related to either amperage, cutting speed, or nozzle size when cutting 1/8" 1018 HR steel ($B_1 = B_2 = B_3 = 0$).

H_{o5}: The formation of dross during plasma cutting is not linearly related to either amperage, cutting speed, or nozzle size when cutting 3/16" 1018 HR steel ($B_1 = B_2 = B_3 = 0$).

H_{o6}: The formation of dross during plasma cutting is not linearly related to either amperage, cutting speed, or nozzle size when cutting 1/4" 1018 HR steel ($B_1 = B_2 = B_3 = 0$).

H_{o7}: The formation of dross during plasma cutting is not linearly related to either amperage, cutting speed, or nozzle size when cutting 3/8" 1018 HR steel ($B_1 = B_2 = B_3 = 0$).

Alternative Hypotheses

H_{A1}: The formation of dross on plasma-cut parts is linearly related to either amperage, cutting speed, or nozzle size when cutting 16-gauge 1018 HR steel ($B_j \neq 0$ for at least one j = 1, 2, 3).

H_{A2}: The formation of dross on plasma-cut parts is linearly related to either amperage, cutting speed, or nozzle size when cutting 14-gauge 1018 HR steel ($B_j \neq 0$ for at least one j = 1, 2, 3).

H_{A3}: The formation of dross on plasma-cut parts is linearly related to either amperage, cutting speed, or nozzle size when cutting 12-gauge 1018 HR steel ($B_j \neq 0$ for at least one j =1, 2, 3).

H_{A4}: The formation of dross on plasma-cut parts is linearly related to either amperage, cutting speed, or nozzle size when cutting 1/8" 1018 HR steel ($B_j \neq 0$ for at least one j = 1, 2, 3).

H_{A5}: The formation of dross on plasma-cut parts is linearly related to either amperage, cutting speed, or nozzle size when cutting 3/16" 1018 HR steel ($B_j \neq 0$ for at least one j = 1, 2, 3).

H_{A6}: The formation of dross on plasma-cut parts is linearly related to either amperage, cutting speed, or nozzle size when cutting 1/4" 1018 HR steel ($B_j \neq 0$ for at least one j = 1, 2, 3).

H_{A7}: The formation of dross on plasma-cut parts is linearly related to either amperage, cutting speed, or nozzle size when cutting 3/8" 1018 HR steel ($B_j \neq 0$ for at least one j = 1, 2, 3).

Note: B is the regression coefficient for the independent variables amperage, cutting speed, and nozzle size.

Steel Tested

Plasma arc cutting is capable of cutting any electrically conductive material (Nemchinsky & Severance, 2006). The only material involved in this study is SAE 1018 HR mild steel. The term mild steel refers to a group of low-carbon, low-alloy steels that are commonly used to manufacture many different components for consumer products, vehicles, and machine components. Mild steel's prevalence is due to its relatively high strength, low cost, machinability, availability, and weldability (Budinski & Budinski, 2005). Colt (p. 27) stated, "95% of all steel cut is carbon steel" p. 27). One of the most commonly plasma-cut materials is mild steel (Ramakrishnan et al. 2000). Concerning the cutting of mild steel, Colombo et al.

(2009) stated, “This process [PAC] is considered a challenging technology when compared with its main competitors, oxy–fuel and laser, in particular, for cutting mild steel (MS) in the 8–40-mm thickness range.”

SAE 1018 HR steel is a commonly used mild steel in many of the applications previously discussed, and is the most commonly used raw material at Cincinnati State. Table 5 lists the properties and chemical compositions of 1018 HR steel.

Table 5

Properties of 1018 HR Steel

Material	Ultimate strength	Yield strength	Elongation	Chemical composition
SAE 1018 HR	68900 psi	39900 psi	38%	0.14–0.20% Carbon, 98.81–99.26% Iron, 0.60–0.90% Manganese, <0.040% Phosphorous, <0.050% Sulfur

From: *Material Property Data*, 2009, retrieved from http://www.matweb.com/search/DataSheet.aspx?MatGUID=e60983fcde914b278ceffebb946995e6

A variety of different thicknesses of 1018 HR steel were examined in this study: 16 gauge (.055"), 14 gauge (.075"), 12 gauge (.105"), 1/8" (.125"), 3/16" (.188"), 1/4" (.250"), and 3/8" (.375"). These are standard steel sizes that are commonly used in manufacturing and fabrication industries and they are also the material thicknesses most often used at Cincinnati State to fabricate components for student projects. These sizes should adequately represent many of the common thicknesses of steel typically processed using plasma arc cutting. According to Colt (2002), “ninety percent of all carbon steel cut is less than one inch thick.”

The steel used in this study was purchased from a local steel supplier that has provided raw materials to Cincinnati State for many years. The material was obtained and prepared in a manner that balanced the requirements of the plasma cutting process, material handling issues, cost issues, and generally accepted manufacturing practices. Large sheets were purchased of each of the material thickness being tested. The 16-, 14-, and 12-gauge material was purchased

in 4' x 4' sheets. The 1/8", 3/16", 1/4", and 3/8" material was purchased in 1' x 4' sheets. Experience has shown that these are the most economical and practical sizes for use on the PAC machine. Each sheet of steel was cleaned with a nonflammable solvent called “Simple Green” to remove all oil and grease from the top and bottom surfaces. Clean steel reduces the amount of smoke and hazardous fumes and eliminates any possibility of a foreign substance on the steel affecting the cut quality (Hoult, Pashby, & Chan, 1995).

Specimen Size and Shape

While numerous studies have been completed to examine dross formation during plasma arc cutting, a review of current literature reveals that there is no generally accepted sample size or shape for these studies. Many researchers have used a rotating anode to test the plasma arc instead of performing actual cutting (Colombo et al., 2009; Freton et al., 2001; Girard et al., 2006; Kelly et al., 2004; Ramakrishnan et al., 1997; Ramakrishnan & Rogozinski, 1997). Studies involving actual cutting have used various cutting patterns, but the most prevalent practice involves making linear cuts in the material to evaluate cut quality (Bini et al., 2007; Gariboldi & Previtali, 2004; Hoult et al., 1995, Xue et al., 2004). Several researchers have discussed cut-quality problems associated with the PAC cutting of shapes with sharp corners (AWS, 2006; Gane et al., 1994; Ramakrishnan et al., 1997). Regardless of whether the corners are radiused or square, the deceleration and acceleration of the cutting head on the CNC tool carrier can significantly affect the quality of the cut edge (AWS, 2006). Previous research projects have avoided dealing with the issue of cut quality on sharp corners by only examining the dross formation on the straight-cut portions of the work piece (Bini et al., 2007; Gariboldi & Previtali, 2004; Hoult et al., 1995). There are additional adjustments available within the CNC

software that can be used to control the speed changes when cutting corners, but this is beyond the scope of this study. Dross-formation data was collected on straight cuts.

The specific sample size and shape chosen for this test were long, slender, rectangular shapes with dimensions of 4" long x 1/2" wide. A 3/16" diameter offset hole was also cut into one end of each specimen for identification purposes as shown in Figure 9.

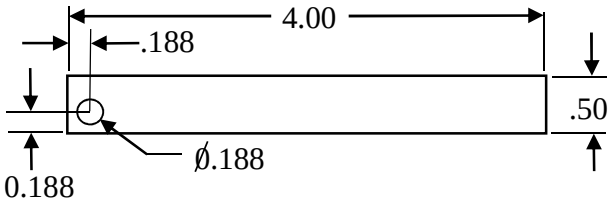

Figure 9. Dimensions of test specimens.

These are similar to the samples used by Zajac and Pfeifer (2006) in their study of the HAZ during PAC. The 4" length of each sample is sufficient to allow a continuous straight cut with no variation in power or cutting speed. The 1/2" width of each sample should prevent the cut quality on one side of the sample from being affected by the heat from the cut on the opposite side. This was supported by Zajac and Pfeifer, which showed that the width of the HAZ can extend up to 0.020" from the cut edge.

The hole in the part served as an attachment point for a cardboard identification tag attached to each sample immediately after cutting. These tags listed the specific operating parameters used to produce each sample as shown in Figure 10. Once the samples cooled sufficiently, they were also labeled with a permanent marker to further ensure that each sample remained properly identified until all data had been collected.

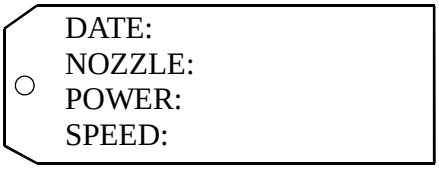

Figure 10. Tag used to identify samples.

Sample Size

It is important to obtain enough samples for the results to be generalized from each material to provide an accurate representation of each thickness of steel. Salkind (2000) recommended a sample size of 30 for most situations. Hair, Anderson, Tatham, and Black (1998) stated, "The ratio of observations to independent variables should never fall below 5 to 1" (p. 165). This study involved examining the four independent variables of material thickness, nozzle size, cutting speed, and power. Using these recommendations as a guideline a total of 30 samples of each material thickness were cut and examined for this study.

Environmental Conditions

The testing was performed in a laboratory space located at the Cincinnati State Technical and Community College. Due to the extremely high temperatures generated with the plasma cutter (on the order of 50,000 °F), the ambient room temperature has a negligible effect on the cutting process. The ordinary room conditions of the laboratory also are similar to those found in most fabrication facilities.

The PAC system used in this study is equipped with a powerful downdraft dust collection system to draw the smoke and dust out of the room through a filtration system. This is used to protect the operator and equipment from exposure to noxious fumes and dust created during the PAC process. This dust collector is powerful enough that it has the potential to affect the behavior of the gas flow that controls the plasma jet. To maintain constant test conditions the

downdraft system was turned on a minimum of 30 seconds before each test was initiated and remained on at least one minute after cutting was completed to assist in dust and fume removal.

Cutting Speed, Power, and Nozzle Sizes

The range of available speeds for the CNC table carrying the PAC torch is 1 to 1,000 in/min. The power on the PAC unit is adjustable from 20 to 60 amps. Three different nozzle sizes can be used to cut steel. As stated before, the combination of these three variables provides the potential for thousands of combinations of speed, power, and nozzle size. Accurate results for this study required random testing of logical values of each of these three variables for each thickness of material tested.

The manufacturer of the PAC machine provides a chart of maximum cutting speeds for selected levels of power for a limited variety of material types and thicknesses. There is a note at the bottom of the table stating "Remember that cut charts are intended to provide a *good starting point* for each different cut assignment" (emphasis added; Hypertherm, 2008, p. 17). Experience has shown that in most cases these values are not optimal for minimizing the formation of dross. The manufacturers' recommended maximum machine settings were used as guidelines for establishing a range of test values for speed and power. An example of the manufacturers' chart of recommended settings is shown in Table 6.

The speed range for each material thickness, nozzle size, and power setting were determined through a pilot study. The pilot study identified a viable range of speeds based on the manufacturers' maximum and optimal speed recommendations verified on the equipment being used for the study. Cutting speed was tested within the practical range of cutting speeds in increments of one inch per minute. The plasma cutter power level was tested throughout a range of values from 25 to 60 amps. The machine can be set in increments of 5 amps so values of 25,

30, 35, 40, 45, 50, 55, and 60 amps were tested. The three different nozzle sizes were tested through a range of speeds and power settings to determine appropriate test settings for the actual study. This range was based on finding a minimum cutting speed just above the point where excessive LSD was formed and a maximum cutting speed below where excessive HSD was formed. The results of the pilot study are shown in Appendix A.

Table 6

Recommended Settings for Nozzle #2 (40 amp)

			Material thickness		*Maximum travel speeds*		*Optimum travel speeds*	
Arc current	Arc voltage	*Pierce delay*	Inches	mm	IPM	mm/min	IPM	mm/min
25	147	0	26 GA	0.5	638	16205	415	10541
	148	0	22 GA	0.8	500	12700	325	8255
	152	0	16 GA	1.5	176	4470	114	2896
40	144	0.25	14 GA	1.9	640	16256	221	5613
	146	0.50	10 GA	3.4	151	3835	98	2489
	147	0.75	3/16"	4.7	97	2464	63	1600
	149	1.00	1/4"	6.4	74	1880	48	1219

Note. Maximum travel speeds are the fastest travel speeds possible to cut the material without regard to cut quality. Optimum travel speeds provide the best cut angle, least dross and best cut surface finish. **Remember that cut charts are intended to provide a *good starting point* for each different cut assignment.** Every cutting system requires "fine tuning" for each cutting application in order [to achieve] the desired cut quality.

The three different nozzle sizes are labeled by the manufacturer as "60 amp," "40 amp," and "finecut." These nozzles vary by dimensions and in the case of the finecut nozzle, also by material composition. The 60-amp and 40-amp nozzles are dimensionally similar with the exception of the diameter of the hole in the bottom of the nozzles. The 60-amp nozzle shown in Figure 11 has a 0.042" diameter cylindrical hole in the bottom of the conical section that opens up to a 0.056" diameter hole at the very bottom of the nozzle. The 40-amp nozzle shown in Figure 12 has a 0.033" diameter cylindrical hole in the bottom of the conical section that opens up to a 0.045" diameter hole as the very bottom of the nozzle. The finecut nozzle shown in

Figure 13 has a significantly different shape and is manufactured from a different material. The opening in the finecut nozzle is also smaller than both the 60-amp and the 40-amp nozzle with a diameter of 0.029". The size and shape of the nozzle governs the size and shape of the plasma jet. A cut-away drawing of the entire nozzle assembly is shown in Figure 1. To eliminate any confusion in this study due to the "amp" notation, the nozzles will be referred to as #1 (60 amp), #2 (40 amp), and #3 (finecut). All test values were randomly chosen from the range of predetermined settings previously discussed.

Figure 11. Nozzle #1 (60 amp).

Figure 12. Nozzle #2 (40 amp).

Figure 13. Nozzle #3 (finecut).

Selection of Specific Test Parameters

The manufacturers' recommendations for the applicable nozzle sizes, range of possible cutting speeds, and power settings were used to identify test settings for this study. The results of the pilot study were used to determine the appropriate nozzle sizes, power settings, and speed settings for each material thickness. Information learned during the pilot study was also used to establish a process for determining specific settings for each sample collected.

A random-number generator was used to determine the specific values of material thickness, nozzle size, power setting, and speed setting for each test. The following selection procedure was used.

1. Each thickness was assigned a numeric value 1 through 7; 1 = 16 gauge, 2 = 14 gauge, 3 = 12 gauge, 4 = 1/8", 5 = 3/16", 6 = 1/4", 7 = 3/8". A random-number generator was used to choose a material thickness to test.
2. Each nozzle was assigned a numerical value 1 through 3; 1 = "60-amp" nozzle, 2 = "40-amp" nozzle, 3 = "finecut" nozzle. A random-number generator was used to select the specific nozzle to use for the material thickness chosen in Step 1.
3. A random-number generator was used to choose the power setting from a predetermined range of power settings based on the results of the pilot study and the material thickness and nozzle selected in Steps 1 and 2.
4. A random-number generator was used to choose a cutting speed from the predetermined range of speeds for the steel thickness, nozzle size, and power setting chosen in the previous three steps based on the results of the pilot study.

A summary of test parameters is shown in Table 7

Table 7

Test Parameters for Cutting SAE 1018 Steel

Parameter	Potential values to test
Material Thickness	16 gauge, 14 gauge, 12 gauge, 1/8", 3/16". 1/4", 3/8"
Nozzle Size	#1 (A60), #2 (A40), #3 (Finecut)
Power Setting	20, 25, 30, 35, 40, 45, 50, 55, 60 amps
Speed Setting	10–800 inches per minute (ipm) in increments of 1 ipm

Table 8 shows the actual range of parameters that were used to test 16-gauge steel. Similar data was produced for each steel thickness. The primary differences between the material thicknesses were the maximum and minimum cutting speeds, and the minimum power settings. These values were determined in the pilot study as shown in Appendix A.

Table 8

Potential Test Settings for 16-Gauge Material

Nozzle size	Power (amps)	Cutting speed (in/min)
#1 (A60)	40	100 –325
#1 (A60)	45	175–425
#1 (A60)	50	200–525
#1 (A60)	55	275–575
#1 (A60)	60	350–650
#2 (A40)	30	40–140
#2 (A40)	35	60–150
#2 (A40)	40	100–230
#2 (A40)	45	100–240
#2 (A40)	50	150–375
#3 (Finecut)	40	80–180
#3 (Finecut)	45	80–180
#3 (Finecut)	50	100–220
#3 (Finecut)	55	100–280
#3 (Finecut)	60	120–330

Collecting and Analyzing the Samples

Once the samples were cut, they were carefully labeled as previously described, collected, and stored in a manner described below. While the dross that is attached from plasma cutting is rather tenaciously attached, it is important not to chip any of the dross from the parts prior to measuring and collecting data from the samples. To preserve the quality of the samples, they were stored and transported in boxes, and each layer of parts was separated by layers of packing material. The boxes used were plastic trays with individual divided sections typically used to store and transport fasteners, hardware, and small tools. The dimensions of the boxes were 14" x 11" x 2". The packing material used was 1/16" plastic designed for shipping fragile items. This storage method was successfully used to collect and store all samples in all stages of this study.

Despite the fact that dross formation is a potential problem for any of the thermal cutting processes (AWS, 2006; Nemchinsky & Severance, 2006), there is no accepted standard for classifying or measuring dross on plasma-cut surfaces. Researchers examining laser beam cut quality also faced this problem. Caristan (2003) stated, “There are no internationally or even nationally recognized standards for laser-cut edge quality” (p. 210). An examination of the various international standards on thermal-cut quality reveals that while these standards recognize the existence of dross as a quality parameter, they have not adopted any specific standards for measuring dross adhesion. The most recent thermal cutting standard, *DIN EN ISO 9013 Thermal Cutting–Classification of Thermal Cuts–Geometric Product Specification and Quality Tolerances,* lists dross as a “quality characteristic,” but it provides no information on quantifying dross (AWS, 2006).

Current PAC studies note the lack of standards for quantifying dross. Gane et al. (1994) stated, “A quantitative measure of the extent of dross formation on the underside of the plate is difficult to make” (p. 6). In their study on plasma-arc cut quality, they initially assessed the amount of dross formation qualitatively as either *severe* or *negligible*. In later experiments, measurements of the maximum height of the dross were made to evaluate cut quality. Another more abstract measure of dross involves ‘dross removability’ as discussed by Yang (2000) in a study of an expert system for controlling a PAC system. Freton et al. (2001) used the mean height of dross as a measure of cut quality in their experimental study of a PAC torch. In their study of how the gas composition affects PAC cut quality, Ramakrishnan et al. (2000) wrote, “Quantifying the dross formed during cutting is difficult because the characteristics of the dross formed at various cutting speeds differ in amount, height, width, and removability” (p. 2292). Xue et al. (2004) wrote, “Until now, no clearly unified standard has been suggested to evaluate the cut quality by plasma arc. Therefore, the cut quality standard WES2801 used for flame cutting are referred” (p. 450). This Japanese Welding Engineering Society standard classifies cut quality into one of three categories: dross-free, attached dross, or dross bridge. Many researchers have used a grading system to identify the presence of dross by using a range of numbers to classify the existence of, and the amount of dross, or the lack of dross (Bogorodski et al., 1991; Nemchinsky, 1997; Nemchinsky & Severance, 2006; Ramakrishnan et al., 2000).

This study involved quantifying the amount of dross formed to a much greater degree than most previous studies reported in the literature review. This study measured the height of the dross using digital calipers along the bottom surface of the straight cut edge of each sample. This method provided a much more accurate indication of any dross attached to the cut edge of each sample. This thickness or “height” of dross is illustrated in Figure 14. Figure 15 shows an

actual measurement being taken on a test specimen. This is similar to the procedures used by Freton et al. (2001), Gane et al. (1994), and Güllü and Atici (2006) in their studies of plasma-cut quality. To eliminate the possibility of variation in the material thickness adversely affecting the test results, the thickness of each sheet of steel was measured at five places and found to have a consistent thickness within a total tolerance of 0.003".

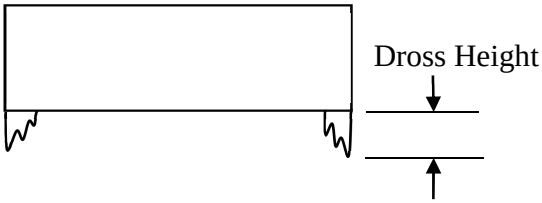

Figure 14. Dross height measurement.

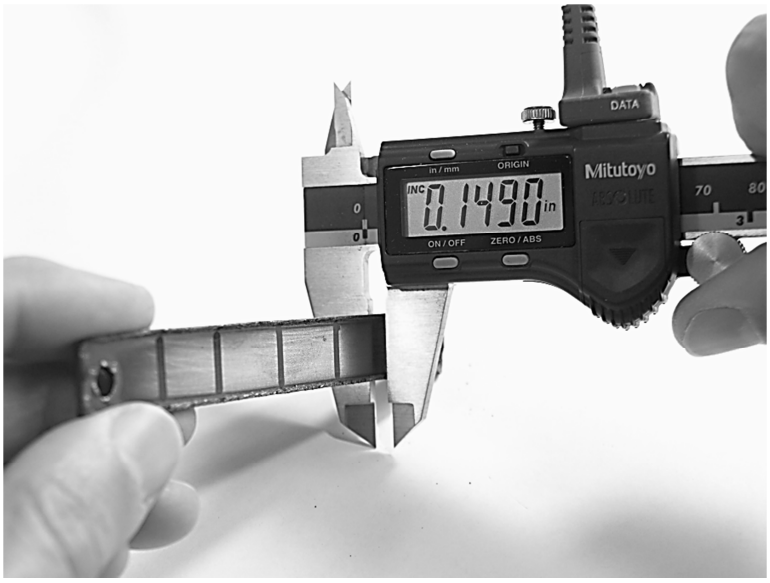

Figure 15. Measuring dross using digital calipers.

Weighing the specimens was also considered as a possible means of quantifying the amount of dross formed. As previously discussed, the corners of a cut part tend to behave differently from the straight sections and depending on the machine settings may tend to accumulate excessive amounts of dross. This added variable would complicate the analysis of

the data obtained during the study. Another problem is that occasionally molten metal randomly splashes back and attaches to the material being cut during piercing which would add another variable to the study. Measuring the dross with calipers eliminated these variables and allowed an accurate indication of dross that is attached to the edges of the part.

Another issue to address is the number of measurements to take on the edge of each specimen. The American Welding Society (AWS, 2006) wrote, "The number and location of the measuring points depends on the shape and size of the work piece, and sometimes on the intended use. The number and location of the measuring points shall be defined by the manufacturer." For this study, the 4" length of the specimens was divided into five measuring points and calipers were used to measure the total thickness of the work piece including any attached dross as shown in Figure 16.

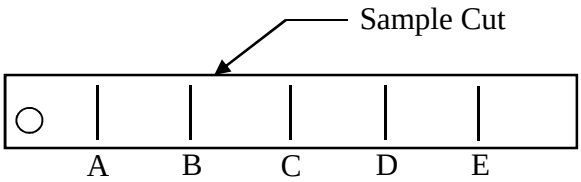

Figure 16. Data measurement points identified as A–E.

The following procedure was used to determine the amount of dross attached to each specimen.

1. Measure the thickness of the specimen plus any dross attached to the cut edge as shown in Figure 15. Measurements were taken at five equally spaced points along the length of the specimen, labeled A, B, C, D, and E in Figure 16.
2. Calculate the average of the five measurements for each specimen.
3. Subtract the sheet thickness from the average measurement.

4. The resulting value was used as the average amount of dross attached to the cut edge of the specimen.

This process was used to find the average amount of dross on each cut edge and these values were ultimately used to determine the affects of the parameters being studied. This method is similar to that used by Bini et al. (2007) in their study of kerf width. Photographs of actual test specimens are shown in Figures 17 and 18. Figure 17 shows a 14-gauge steel specimen with minimal amounts of dross attached to the cut edges. Figure 18 shows a 14-gauge steel specimen with excessive amounts of dross attached to the cut edges.

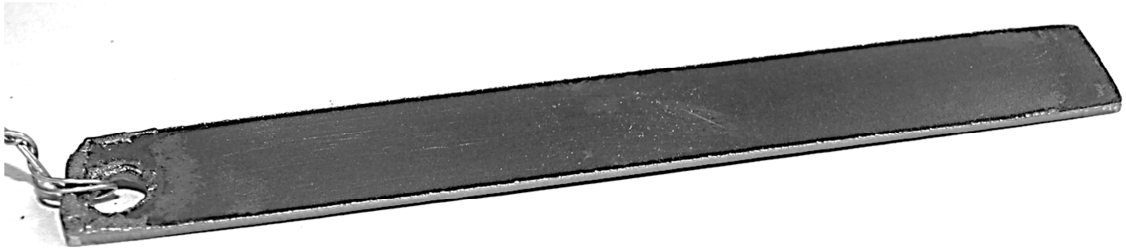

Figure 17. 14-gauge steel sample with minimal dross.

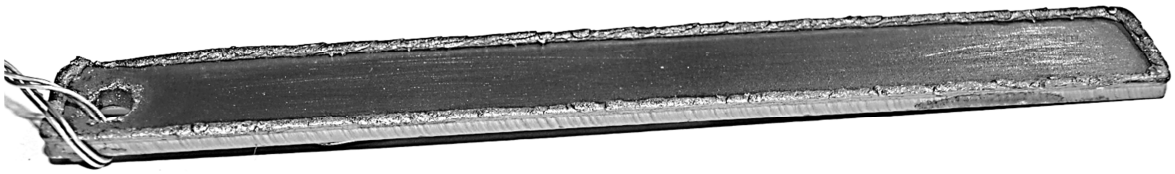

Figure 18. 14-gauge steel sample with excessive dross.

Data Analysis

The data collected was analyzed using SPSS software and the statistical functions of multiple regression analysis. One of the requirements of multiple regression analysis is that there be a linear relationship between the independent and dependent variables (Triola, 2004). Statistical analyses of the data collected proved that there was a linear relationship between the variables being tested, which validated the use of multiple regression analysis.

The data collected was used to determine how the variables of material thickness, nozzle size, cutting speed, and arc current affected the formation of dross on the 1018 HR steel samples. These results were used to determine whether to accept or reject the null hypotheses of the study. Furthermore, the results of this study were used to determine one equation for each thickness of 1018 HR steel that could then be used to determine the optimum machine operating parameters that produce parts with the least dross.

CHAPTER 4

RESULTS

The following chapter discusses the results of the research investigating dross formation when plasma cutting. This research examined the effects of the process parameters cutting speed, power, and nozzle size on the formation of dross when cutting seven different thicknesses of 1018 steel with a CNC PAC machine. The data was generated using a random sampling technique to collect 210 samples. The amount of dross formed on the samples at five different points across the length of each sample was measured and these values were used to determine an average dross value for each of the samples. The complete data set is shown in Appendix B.

Regression Analysis of Data

The goal of this analysis was to determine if there is a significant linear relationship between the dross formed during plasma cutting and the parameters power, speed, and nozzle size. Multiple regression analysis was used to examine the effect of these parameters on dross formation. The software used to perform the statistical analysis was SPSS version 16. An alpha value of .05 was used for each analysis. This allows the possibility that there is a 5% chance of rejecting the null hypothesis when it is actually true. This is a reasonable risk to take in this analysis, and has been used by other researchers in similar fields (Bini et al., 2007; Nagarajan, 2000; Rajaram, Sheikh-Ahmad, & Cheraghi, 2002; Sundar et al., 2007).

According to Berry (1993), multiple regression analysis imposes eight requirements:

- The values of the independent variables must be randomly selected—The existing data set was collected from randomly chosen values of material thickness, power setting, speed setting, and nozzle size. A random-number generator was used to select each of the values of the independent variables until a total of 210 samples had been collected as described in Chapter 3.
- The variables must be measured accurately and reliably—A strict data-collection plan was used and great care was taken in the process of collecting all data. The operation of the equipment, collection and transportation of the samples, and the gathering of all data was performed meticulously as described in Chapter 3.
- The variables must be normally distributed—The means and medians of each of the variable sets should be equal if they are normally distributed. The skewness is another value that can help to identify normality. These values were examined for each data set, and are shown in Appendix C.
- The data must be in terms of interval or ratio values—Dross, speed, and power are all ratio data, and the nozzle type was coded to work within the parameters of linear regression.
- The dependent and independent variables must have a purely linear relationship—Scatterplots of each of the independent and dependent variables gave a good indication that there is some linear relationship that exists. The strength of these relationships was examined for each data set as shown in Appendix C.
- The prediction error must be random and normally distributed—Probability (P–P) plots are a good indicator of normality and random prediction error. These plots were

produced for each data set and examined to determine normality and random prediction error and are shown in Appendix C.

- There must not be collinearity between the variables—The variance inflation factor (VIF) was used to examine the existence of multicollinearity. An acceptable VIF value is less than 10. In each case the VIF values were below 10 as shown in Appendix C.
- The data must exhibit homoscedasticity—This is true when the error variance is constant. Homoscedasticity can be demonstrated by examining the P–P plots for variation around the line on the chart. In each case, approximately equal variation indicated homoscedasticity as shown in Appendix C.

Data collected for each thickness of steel was analyzed individually. Each data set was examined for normality and linearity, and these results are shown in Appendix C. Each data set was examined and found to fit all of the requirements for the use of multiple regression analysis. The equations that best describe the relationships between the independent variables and the formation of dross were determined through regression analysis for each thickness of material tested.

Results for 16-Gauge Steel

Table 9 displays the ANOVA statistics for 16-gauge steel. In general, these results show two outcomes:

- For 16-gauge steel the significant variables involved in the formation of dross are the A40 nozzle, and the power setting.
- The calculated *F* value was compared to the critical *F* value to determine whether to accept or reject the null hypothesis. The calculated *F* value of 59.13 from the

ANOVA table is greater than the critical *F* value of 3.39 (Best & Kahn, 2003), which indicates that the null hypothesis should be rejected: The formation of dross during plasma cutting of 16-gauge steel is linearly related to the nozzle size and power setting.

Table 9

ANOVA Statistics for 16-Gauge Steel[a]

	Model	Squares	*df*	Mean square	*F*	Sig.
1	Regression	.005	1	.005	89.972	.000[b]
	Residual	.001	26	.000		
	Total	.006	27			
2	Regression	.005	2	.002	59.130	.000[c]
	Residual	.001	25	.000		
	Total	.006	27			

Note. a. Dependent variable: Dross (inches); b. Predictors: (constant), A40; c. Predictors: (constant), A40, power (amps).

The model summary shown in Table 10 displays the *R* value and R^2 value, which indicate the strength of the relationship between the variables. The values of both *R* and R^2 range from 0 to 1 with 1 indicating a perfect relationship. The computed *R* value of .909 and R^2 value of .825 indicate a very strong relationship (Salkind, 2000) between power, A40 nozzle, and the amount of dross formed. This indicates that 82.5% of the variation is explained by these two variables.

Table 10

R and R^2 Values for 16-Gauge Steel: Model Summary[a]

Model	*R*	R^2	Adjusted R^2	Std. error of the estimate	Durbin–Watson
1	.881[b]	.776	.767	.0071866	
2	.909[c]	.825	.812	.0064660	1.974

Note. a. Dependent variable: Dross (inches); b. Predictors: (constant), A40; c. Predictors: (constant), A40, power (amps).

Table 11 displays the variables that are significant in the formation of dross for 16-gauge steel. The variables that contribute to the formation of dross were used to create a mathematical model that describes their relationship. In the case of 16-gauge steel, the formula that describes this relationship is: Dross = 0.0359 + 0.01873(*N*) - 0.000505(Power),

Where *N* = 1 when using the A40 nozzle, and *N* = 0 when using the A60 or finecut nozzle, where power is in amps, and dross is in thousandths of an inch. While the factors shown in the formula above appear to be very small, this is due to the relatively large values of power (40–60 amps) when compared to the relatively small values of dross (thousandths of an inch). This was the case for all thicknesses of steel tested. Additional examination of data and results including scatterplots, P–P plots, and Durbin–Watson values are shown in Appendix C.

Table 11

Regression Analysis Results for 16-Gauge Steel: Coefficients

		Unstandardized coefficients		Standardized coefficients			Collinearity statistics	
	Model	*B*	Std. error	Beta	*t*	Sig.	Tolerance	VIF
1	(Constant)	7.859E-03	.002		4.509	.000		
	A40	2.638E-02	.003	.881	9.485	.000	1.000	1.000
2	(Constant)	3.593E-02	.011		3.377	.002		
	A40	1.873E-02	.004	.626	4.926	.000	.433	2.311
	Power (amps)	-5.05E-04	.000	-.339	-2.668	.013	.433	2.311

Note. Dependent variable: Dross (inches).

Summary of Results for 16-Gauge Steel

The analysis indicates that the null hypothesis should be rejected and the alternate hypothesis should be accepted. When cutting 16-gauge steel, there is a linear relationship between the amount of dross formed and the power setting and nozzle type. The results also show that nozzle type A40 produces more dross than nozzles A60 or finecut.

Results for 14-Gauge Steel

Table 12 displays the ANOVA statistics for 14-gauge steel. In general, these results show two outcomes:

- For 14-gauge steel the significant variables involved in the formation of dross are finecut nozzle and speed.
- The calculated *F* value was compared to the critical *F* value to determine whether to accept or reject the null hypothesis. The calculated *F* value of 10.862 from the ANOVA table is greater than the critical *F* value of 3.40 (Best & Kahn, 2003), which indicates that the null hypothesis should be rejected: The formation of dross during plasma cutting of 14-gauge steel is linearly related to the nozzle size and cutting speed.

Table 12

ANOVA Statistics for 14-Gauge Steel[a]

	Model	Sum of squares	*df*	Mean square	*F*	Sig.
1	Regression	.001	1	.001	12.273	.002[b]
	Residual	.002	25	.000		
	Total	.003	26			
2	Regression	.001	2	.001	10.862	.000[c]
	Residual	.002	24	.000		
	Total	.003	26			

Note. a. Dependent variable: Dross (inches); b. Predictors: (constant), finecut; c. Predictors: (constant), finecut, speed (in/min).

The model summary shown in Table 13 displays the *R* and R^2 values, which indicate the strength of the relationship between the variables. The computed *R* value of .689 and R^2 value of .475 indicate a strong relationship between speed, finecut nozzle, and the amount of dross formed. This indicates that 47.5% of the variation is explained by these two variables.

Table 13

R and R^2 Values for 14-Gauge Steel: Model Summary[a]

Model	*R*	R^2	Adjusted R^2	Std. error of the estimate	Durbin–Watson
1	.574[b]	.329	.302	.0088342	
2	.689[c]	.475	.431	.0079761	2.145

Note. a. Dependent variable: Dross (inches); b. Predictors: (constant), finecut; c. Predictors: (constant), finecut, speed (in/min).

Table 14 displays the variables that are significant in the formation of dross for 14-gauge steel. In the case of 14-gauge steel, the formula that describes this relationship between the variables tested is: Dross = 0.03194 - 0.0184(*N*) - 0.0000633(Speed),

Where *N* = 1 when using finecut nozzle, *N* = 0 when using A60 nozzle or A40 nozzle. Additional examination of data and results including scatterplots, P–P plots, and Durbin–Watson values are shown in Appendix C.

Table 14

Regression Analysis Results for 14-Gauge Steel: Coefficients

		Unstandardized coefficients		Standardized coefficients			Collinearity statistics	
	Model	*B*	Std. error	Beta	*T*	Sig.	Tolerance	VIF
1	(Constant)	1.689E-02	.002		7.885	.000		
	FINECUT	-1.23E-02	.004	-.574	-3.503	.002	1.000	1.000
2	(Constant)	3.194E-02	.006		5.203	.000		
	FINECUT	-1.84E-02	.004	-.858	-4.654	.000	.643	1.554
	Speed (in/min)	-6.33E-05	.000	-.476	-2.582	.016	.643	1.554

Note. Dependent variable: Dross (inches).

Summary of Results for 14-Gauge Steel

The analysis indicates that the null hypothesis should be rejected and the alternate hypothesis should be accepted. When cutting 14-gauge steel, there is a linear relationship

between the amount of dross formed and the cutting speed and nozzle type. The results also show that the finecut nozzle produces the least dross of the three nozzles tested.

Results for 12-Gauge Steel

Table 15 displays the ANOVA statistics for 12-gauge steel. In general, these results show two outcomes:

- For 12-gauge steel, the significant variables involved in the formation of dross are finecut nozzle and the product of speed and power.
- The calculated *F* value was compared to the critical *F* value to determine whether to accept or reject the null hypothesis. The calculated *F* value of 17.437 from the ANOVA table is greater than the critical *F* value of 3.39 (Best & Kahn, 2003), which indicates that the null hypothesis should be rejected: The formation of dross during plasma cutting of 12-gauge steel is linearly related to the nozzle size, cutting speed, and power setting.

Table 15

ANOVA Statistics for 12-Gauge Steel[a]

	Model	Sum of squares	*df*	Mean square	*F*	Sig.
1	Regression	.003	1	.003	15.296	.000[b]
	Residual	.006	32	.000		
	Total	.009	33			
2	Regression	.005	2	.002	17.437	.000[c]
	Residual	.004	31	.000		
	Total	.009	33			

Note. a. Dependent variable: Dross (inches); b. Predictors: (constant), finecut; c. Predictors: (constant), finecut, SPEEDPOW.

The model summary shown in Table 16 displays the *R* and R^2 values, which indicate the strength of the relationship between the variables. The computed *R* value of .728 and R^2 value of .529 indicate a strong relationship between finecut nozzle and the product of speed and power

and the amount of dross formed. This indicates that 52.9% of the variation is explained by these three variables.

Table 16

R and R^2 Values for 12-Gauge Steel: Model Summary[a]

Model	*R*	R^2	Adjusted R^2	Std. error of the estimate	Durbin–Watson
1	.569[b]	.323	.302	.0140269	
2	.728[c]	.529	.499	.0118854	1.743

Note. a. Dependent variable dross (inches); b. Predictors: (constant), finecut; c. Predictors: (constant), finecut, SPEEDPOW.

Table 17 displays the variables that are significant in the formation of dross for 12-gauge steel. In the case of 12-gauge steel, the formula that describes the relationship between the variables tested is: Dross = 0.05538 - 0.0253(*N*) - 0.00000361(Speed X Power),

Where *N* = 1 when using finecut nozzle, *N* = 0 when using A60 nozzle or A40 nozzle. Additional data and results, scatterplots, P–P plots, and Durbin–Watson values are shown in Appendix C.

Table 17

Regression Analysis Results for 12-Gauge Steel: Coefficients

		Unstandardized coefficients		Standardized coefficients			Collinearity statistics	
	Model	*B*	Std. error	Beta	*t*	Sig.	Tolerance	VIF
1	(Constant)	3.299E-02	.004		9.409	.000		
	FINECUT	-1.88E-02	.005	-.569	-3.911	.000	1.000	1.000
2	(Constant)	5.538E-02	.007		8.187	.000		
	FINECUT	-2.53E-02	.004	-.764	-5.696	.000	.844	1.185
	SPEEDPOW	-3.61E-06	.000	-.494	-3.684	.001	.844	1.185

Note. Dependent variable: Dross (inches).

Summary of Results for 12-Gauge Steel

The analysis indicates that the null hypothesis should be rejected and the alternate hypothesis should be accepted. When cutting 12-gauge steel, there is a linear relationship

between the amount of dross formed, and the nozzle type and the product of cutting speed and power. The results also indicate that the finecut nozzle produces less dross than the other two nozzles tested.

Results for 1/8" Steel

Table 18 displays the ANOVA statistics for 1/8" steel. In general, these results show two outcomes:

- For 1/8" steel, the variables that are significant are power, finecut nozzle, and speed.
- The calculated *F* value was compared to the critical *F* value to determine whether to accept or reject the null hypothesis. The calculated *F* value of 24.251 from the ANOVA table is greater than the critical *F* value of 3.01 (Best & Kahn, 2003), which indicates that the null hypothesis should be rejected: Dross formation while plasma cutting 1/8" steel is linearly related to nozzle size, cutting speed, and power setting.

Table 18

ANOVA Statistics for 1/8" Steel[a]

	Model	Sum of squares	*df*	Mean square	*F*	Sig.
1	Regression	.004	1	.004	16.298	.000[b]
	Residual	.007	26	.000		
	Total	.011	27			
2	Regression	.007	2	.004	24.795	.000[c]
	Residual	.004	25	.000		
	Total	.011	27			
3	Regression	.008	3	.003	24.251	.000[d]
	Residual	.003	24	.000		
	Total	.011	27			

Note. a. Dependent variable: Dross (inches); b. Predictors: (constant), power (amps); c. Predictors: (constant), power (amps) finecut; d. Predictors: (constant), power (amps), finecut, speed (in/min).

The model summary shown in Table 19 displays the *R* and R^2 values, which indicate the strength of the relationship between the variables. The computed *R* value of .867 and R^2 value of

.752 indicate a strong relationship between finecut nozzle, speed, and power and the amount of dross formed. This indicates that 75.2% of the variation is explained by these three variables.

Table 19

R and R^2 Values for 1/8" Steel: Model Summary[a]

Model	*R*	R^2	Adjusted R^2	Std. error of the estimate	Durbin–Watson
1	.621[b]	.385	.362	.0159036	
2	.815[c]	.665	.638	.0119761	
3	.867[d]	.752	.721	.0105153	2.399

Note. a. Dependent variable: Dross (inches); b. Predictors: (constant), power (amps); c. Predictors: (constant), power (amps) finecut; d. Predictors: (constant), power (amps), finecut, Speed (in/min).

Table 20 displays the variables that are significant in the formation of dross for 1/8" steel. The variables that contribute to the formation of dross were used to create a mathematical model that describes their relationship.

Table 20

Regression Analysis Results for 1/8" Steel: Coefficients

		Unstandardized coefficients		Standardized coefficients			Collinearity statistics	
	Model	*B*	Std. error	Beta	*t*	Sig.	Tolerance	VIF
1	(Constant)	9.957E-02	.019		5.229	.000		
	Power (amps)	-1.49E-03	.000	-.621	-4.037	.000	1.000	1.000
2	(Constant)	0.105	.014		7.327	.000		
	Power (amps)	-1.47E-03	.000	-.611	-5.276	.000	1.000	1.000
	FINECUT	-2.21E-02	.005	-.529	-4.566	.000	1.000	1.000
3	(Constant)	9.972E-02	.013		7.792	.000		
	Power (amps)	-9.13E-04	.000	-.380	-2.942	.007	.620	1.613
	FINECUT	-2.89E-02	.005	-.690	-5.956	.000	.771	1.298
	Speed (in/min)	-1.55E-04	.000	-.406	-2.903	.008	.528	1.895

Note. Dependent variable: Dross (inches).

In the case of 1/8" steel the formula that describes this relationship is:

Dross = 0.09972 - 0.000913(Power) - 0.0289(*N*) - 0.000155(Speed),

Where *N* = 1 when using finecut nozzle, *N* = 0 when using A60 nozzle or A40 nozzle.

Additional examination of data and results including scatterplots, P–P plots, and Durbin–Watson values are shown in Appendix C.

Summary of Results for 1/8" Steel

The analysis indicates that the null hypothesis should be rejected and the alternate hypothesis should be accepted. When cutting 1/8" steel, there is a linear relationship between the amount of dross formed, and the cutting speed, power, and nozzle type. The results also show that the finecut nozzle produces the least amount of dross of the three nozzles tested.

Results for 3/16" Steel

Table 21 displays the ANOVA statistics for 3/16" steel. In general, these results show two outcomes:

- For 3/16" steel, the variables that are significant are speed and power.
- The calculated *F* value is compared to the critical *F* value to determine whether to accept or reject the null hypothesis. The calculated *F* value of 12.921 from the ANOVA table is greater than the critical *F* value of 2.72 (Best & Kahn, 2003), which indicates that the null hypothesis should be rejected: The formation of dross during plasma cutting of 3/16" steel is linearly related to the cutting speed and power.

The model summary shown in Table 22 displays the *R* and R^2 values, which indicate the strength of the relationship between the variables. The computed *R* value of .706 and R^2 value of .498 indicate a strong relationship between speed and power and the amount of dross formed. This indicates that 49.8% of the variation is explained by these two variables.

Table 21

ANOVA Statistics for 3/16" Steel[a]

	Model	Sum of squares	*df*	Mean square	*F*	Sig.
1	Regression	.008	1	.008	13.598	.001[b]
	Residual	.015	27	.001		
	Total	.023	28			
2	Regression	.011	2	.006	12.921	.000[c]
	Residual	.011	26	.000		
	Total	.023	28			

Note. a. Dependent variable: Dross (inches); b. Predictors: (constant), speed (in/min); c. Predictors: (constant), speed (in/min), power (amps).

Table 22

R and R^2 Values for 3/16" Steel: Model Summary[a]

Model	*R*	R^2	Adjusted R^2	Std. error of the estimate	Durbin–Watson
1	.579[b]	.335	.310	.0235895	
2	.706[c]	.498	.460	.0208752	1.834

Note. a. Dependent variable: Dross (inches); b. Predictors: (constant), speed (in/min); c. Predictors: (constant), speed (in/min), power (amps).

Table 23 displays the variables that are significant in the formation of dross for 3/16" steel. The variables that contribute to the formation of dross were used to create a mathematical model that describes their relationship. In the case of 3/16" steel, the formula that describes this relationship is: Dross = 0.172 - 0.000453(Speed) - 0.00203(Power).

Additional examination of data and results including scatterplots, P–P plots, and Durbin–Watson values are shown in Appendix C.

Table 23

Regression Analysis Results for 3/16" Steel: Coefficients

		Unstandardized coefficients		Standardized coefficients			Collinearity statistics	
	Model	*B*	Std. error	Beta	*t*	Sig.	Tolerance	VIF
1	(Constant)	7.560E-02	.013		6.039	.000		
	Speed (in/min)	-5.77E-04	.000	-.579	-3.688	.001	1.000	1.000
2	(Constant)	.172	.035		4.919	.000		
	Speed (in/min)	-4.53E-04	.000	-.454	-3.125	.004	.913	1.095
	Power (amps)	-2.03E-03	.001	-.423	-2.912	.007	.913	1.095

Note. Dependent variable: Dross (inches).

Summary of Results for 3/16" Steel

The analysis indicates that the null hypothesis should be rejected and the alternate hypothesis should be accepted. When cutting 3/16" steel, there is a linear relationship between the amount of dross formed and the cutting speed and power setting.

Results for 1/4" Steel

Table 24 displays the ANOVA statistics for 1/4" steel. In general, these results show two outcomes:

- For 1/4" steel, the variable that is significant is speed.
- The calculated *F* value is compared to the critical *F* value to determine whether to accept or reject the null hypothesis. The calculated *F* value of 36.953 from the ANOVA table is greater than the critical *F* value of 4.16 (Best & Kahn, 2003), which indicates that the null hypothesis should be rejected: The formation of dross during plasma cutting of 1/4" steel is linearly related to the cutting speed.

The model summary shown in Table 25 displays the *R* and R^2 values, which indicate the strength of the relationship between the variables. The computed *R* value of .737 and R^2 value of

.544 indicate a strong relationship between speed and the amount of dross formed. This indicates that 54.4% of the variation is explained by this variable.

Table 24

ANOVA Statistics for 1/4" Steel[a]

	Model	Sum of squares	*df*	Mean square	*F*	Sig.
1	Regression	.033	1	.033	36.953	.000[b]
	Residual	.027	31	.001		
	Total	.060	32			

Note. a. Dependent variable: Dross (inches); b. Predictors: (constant), speed (in/min).

Table 25

R and R^2 Values for 1/4" Steel: Model Summary[a]

Model	*R*	R^2	Adjusted R^2	Std. error of the estimate	Durbin–Watson
1	.737[b]	.544	.529	.0297796	2.308

Note. a. Dependent variable: Dross (inches); b. Predictors: (constant), speed (in/min).

Table 26 displays the variable that is significant in the formation of dross for 1/4" steel. The variable that contributes to the formation of dross was used to create a mathematical model that describes their relationship. In the case of 1/4" steel, the formula that describes this relationship is: Dross = 0.128 - 0.00128(Speed).

Table 26

Regression Analysis Results for 1/4" Steel: Coefficients

		Unstandardized coefficients		Standardized coefficients			Collinearity statistics	
	Model	*B*	Std. error	Beta	*t*	Sig.	Tolerance	VIF
1	(Constant)	.128	.011		11.890	.000		
	Speed (in/min)	-1.28E-03	.000	-.737	-6.079	.000	1.000	1.000

Note. Dependent variable: Dross (inches).

Additional examination of data and results including scatterplots, P–P plots, and Durbin–Watson values are shown in Appendix C.

Summary of Results for 1/4" Steel

The analysis indicates that the null hypothesis should be rejected and the alternate hypothesis should be accepted. When cutting 1/4" steel, there is a linear relationship between the amount of dross formed and the cutting speed.

Results for 3/8" Steel

Table 27 displays the ANOVA statistics for 3/8" steel. In general, these results show two outcomes:

- For 3/8" steel, the variable that is significant is speed.
- The calculated *F* value is compared to the critical *F* value to determine whether to accept or reject the null hypothesis. The calculated *F* value of 22.979 from the ANOVA table is greater than the critical *F* value of 4.18 (Best & Kahn, 2003), which indicates that the null hypothesis should be rejected: The formation of dross during plasma cutting of 3/8" steel is linearly related to the cutting speed.

Table 27

ANOVA Statistics for 3/8" Steel[a]

	Model	Sum of squares	*df*	Mean square	*F*	Sig.
1	Regression	.020	1	.020	22.979	.000[b]
	Residual	.025	29	.001		
	Total	.046	30			

Note. a. Dependent variable: Dross (inches); b. Predictors: (constant), speed (in/min).

The model summary shown in Table 28 displays the *R* and R^2 values, which indicates the strength of the relationship between the variables. The computed *R* value of .665 and R^2 value of

.442 indicates a strong relationship between speed and the amount of dross formed. This indicates that 44.2% of the variation is explained by this variable.

Table 28

R and R^2 Values for 3/8" Steel: Model Summary[a]

Model	*R*	R^2	Adjusted R^2	Std. error of the estimate	Durbin–Watson
1	.665[b]	.442	.423	.0296304	1.915

Note. a. Dependent variable: Dross (inches); b. Predictors: (constant), speed (in/min).

Table 29 displays the variable that is significant in the formation of dross for 3/8" steel. The variable that contributes to the formation of dross was used to create a mathematical model that describes their relationship. In the case of 3/8" steel the formula that describes this relationship is: Dross = 0.102 - 0.000926(Speed).

Table 29

Regression Analysis Results for 3/8" Steel: Coefficients

		Unstandardized coefficients		Standardized coefficients			Collinearity statistics	
	Model	*B*	Std. error	Beta	*t*	Sig.	Tolerance	VIF
1	(Constant)	.102	.012		8.798	.000		
	Speed (in/min)	-9.26E-04	.000	-.665	-4.794	.000	1.000	1.000

Note. Dependent variable: Dross (inches).

Additional examination of data and results including scatterplots, P–P plots, and Durbin–Watson values are shown in Appendix C.

Summary of Results for 3/8" Steel

The analysis indicates that the null hypothesis should be rejected and the alternate hypothesis should be accepted. When cutting 3/8" steel, there is a linear relationship between the amount of dross formed and the cutting speed.

Summary of Results

The results of the statistical analysis discovered some interesting facts. Linear regression analysis determined that there was a generally a linear relationship between some of the variables involved in the formation of dross for each thickness of steel tested with this particular PAC machine. Each thickness of material showed a different strength in this linear relationship, but there was some consistency in terms of the magnitude of the calculated R^2 value. The results of the analysis are summarized in Table 30. As shown in Table 30 all of the material tested except for the 16-gauge material showed a definite relationship to the cutting speed.

Table 30

Results of Statistical Analysis of Each Metal Thickness

	Material thickness						
	16 gauge	14 gauge	12 gauge	1/8"	3/16"	1/4"	3/8"
Total R^2	0.825	0.475	0.529	0.752	0.498	0.544	0.442
Significant variables	Nozzle type, power	Speed, nozzle type	Nozzle type, speed X power	Speed, power, nozzle type	Speed, power	Speed	Speed

Using the data collected from the study, the results for each thickness of material were first analyzed in terms of all of the data regardless of whether the dross formed was HSD or LSD. The results of this analysis revealed R^2 values varying from .442 to .825 with a mean value of .581. The significant variables in the process were also identified.

The uniqueness of this particular study makes it difficult to compare these values to any previous studies. For purposes of comparison, a study involving kerf width when using a HTPAC system performed by Bini et al. (2007) produced an R^2 value of .73, and studies on

surface finish when laser cutting steel produced R^2 values of .697 (Sundar et al., 2007), .739 (Rajaram et al., 2002), and .74 (Nagarajan, 2000).

The statistical analysis also identified which of the three variables have the most effect on dross for each of the different thicknesses of steel. Testing at the 95% confidence level determined that for the seven thicknesses of material tested cutting speed was a significant variable for six of the seven materials tested. Nozzle size was significant for four of the seven materials tested, and power was significant for four of the seven materials tested.

An additional analysis was performed on the data collected by examining the difference between LSD and HSD. The nature of dross formation is that LSD is formed when cutting too slowly and HSD is formed when cutting too quickly. For each thickness of steel, there is a maximum cutting speed above which the plasma arc is unable to sever the material. This is not an issue when cutting at slower than optimum speeds as there is rarely a cutting speed that is too slow to cut through the material. In an effort to find more accurate relationships between the variables, the data were used to further examine this phenomenon by individually analyzing the LSD data by itself. Table 31 shows results of this analysis. Table 32 shows a comparison of the results of the analysis of all data and the analysis of only the LSD data. The result of the analysis of LSD data shows no significant improvement in the relationship between the independent variables compared to the previous analysis that combined the LSD and HSD data.

Table 31

Results of Statistical Analysis of LSD Data Only

	Material thickness						
	16 gauge	14 gauge	12 gauge	1/8"	3/16"	1/4"	3/8"
LSD R^2	0.708	0.531	0.54	0.742	0.495	0.56	0.43
Significant variables	Power	Speed, nozzle type	Power, nozzle type	Power, nozzle type	Speed, power	Speed	Speed X power

Table 32

Comparison of R^2 Values

	Material thickness						
	16 gauge	14 gauge	12 gauge	1/8"	3/16"	1/4"	3/8"
Total R^2	0.825	0.475	0.529	0.752	0.498	0.544	0.442
LSD R^2	0.708	0.531	0.54	0.742	0.495	0.56	0.43

Removing Outliers

Examination of scatterplots of each data set revealed the presence of outlying data points. These outliers could negatively affect the accuracy of the mathematical model that describes the relationship between the independent and dependent variables for each material thickness. Examples of the outliers identified for the 1/8" steel are shown in Figures 19–21. In this case the data points 10 and 24 appear to be outliers on all three scatterplots. When these two data points were removed, the *R* value decreased from .867 to .852, and the R^2 value decreased from .752 to .725, indicating that these two points should be included in the analysis. For each thickness of steel tested, the scatterplots were examined carefully to identify potential outliers. These data points were removed and the statistical analyses were performed without them in an effort to boost the *R* and R^2 values.

The results of removing the outliers for each thickness of steel are shown in Table 33. The results of the analysis with the outliers removed showed little to no improvement over the data that included these points. The mathematical models from the original regression analysis appear to be the most accurate at describing the behavior of the variables in the study.

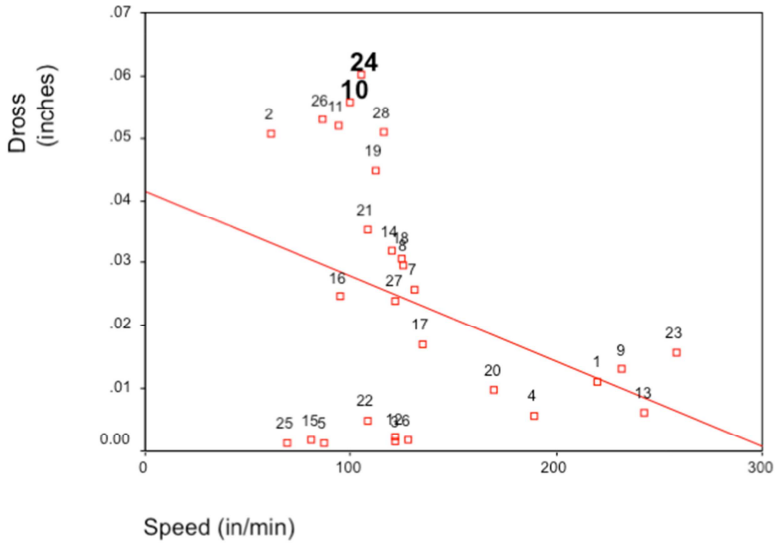

Figure 19. Scatterplot of dross vs. speed for 1/8"-thick steel.

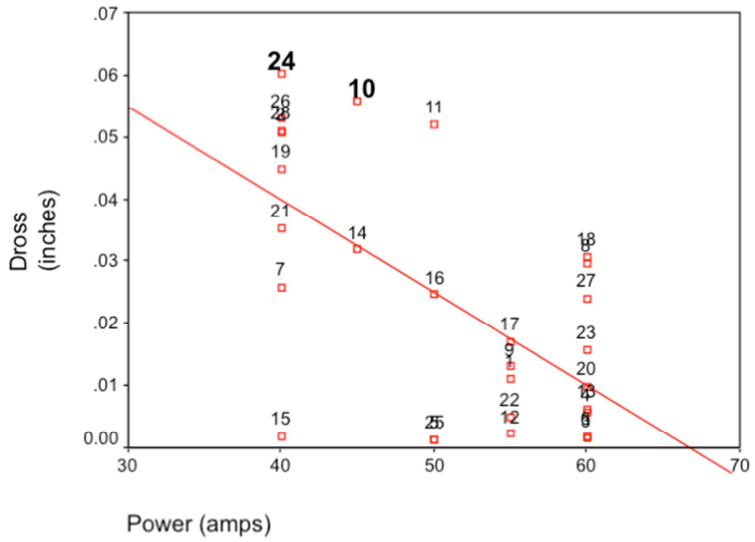

Figure 20. Scatterplot of dross vs. power for 1/8"-thick steel.

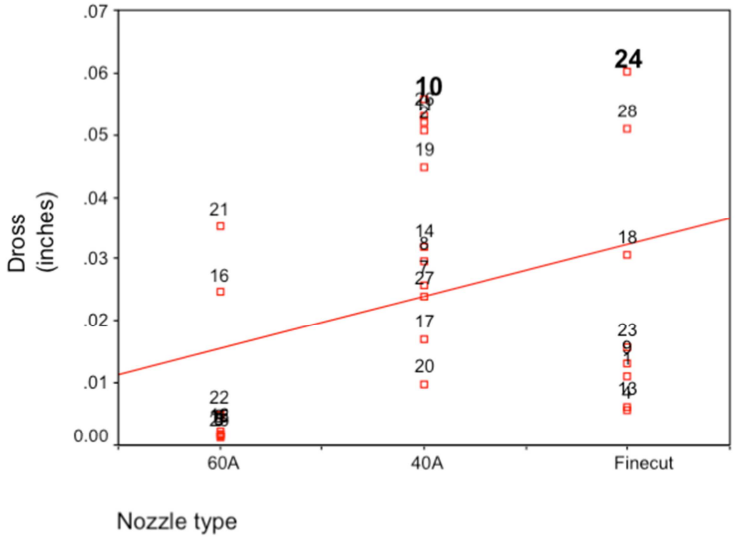

Figure 21. Scatterplot of dross vs. nozzle type for 1/8"-thick steel.

Table 33

Comparison of R^2 Values Without Outliers

	Material thickness						
	16 gauge	14 gauge	12 gauge	1/8"	3/16"	1/4"	3/8"
Total R^2	0.825	0.475	0.529	0.752	0.498	0.544	0.442
Total R^2 with outliers removed	0.83	0.468	0.507	0.725	0.533	0.521	0.429

Summary of Key Findings From Data Analysis

Key findings from this study and the subsequent data analysis are discussed below. Conclusions from these results are found in the following chapter.

- Multiple regression analysis determined that all of the independent variables tested were found to significantly affect the amount of dross formed on at least some of the material thicknesses tested.

  - The nozzle type was found to be significant in dross formation for four of the seven thicknesses tested.
  - The power was found to be significant in dross formation for four of the seven thicknesses tested.
  - The cutting speed was found to be significant in dross formation for six of the seven thicknesses tested.
- A multiple regression analysis determined that the amount of variation explained by the three independent variables tested varied between 44.2% and 82.5%.
- Each material thickness is affected by a different combination of speed, power, and nozzle type and to a different degree.
- LSD data alone is not a better predictor of dross formation than a combination of LSD and HSD.
- On 1/8" or thinner material, the finecut nozzle produced the least amount of dross of the three nozzles tested.

CHAPTER 5

CONCLUSIONS AND RECOMMENDATIONS

This research investigated how selected process parameters affect the formation of dross when plasma cutting steel. The objective of this research was to determine the optimum machine settings that will minimize the formation of dross when cutting 1018 steel with a CNC PAC machine. This chapter focuses on the research hypotheses developed to address this objective and to provide conclusions based on the statistical analyses performed. Recommendations for future research are also contained in this chapter.

Conclusions on the Research Hypotheses

Each of the hypotheses developed for this study involved the effect of selected parameters on the formation of dross on the individual material thicknesses examined. The conclusions to each hypothesis were determined based on the results of the statistical analysis.

Null Hypothesis 1

The formation of dross during plasma cutting is not linearly related to either amperage (power), cutting speed, or nozzle size when cutting 16-gauge HR steel.

Conclusion 1

Multiple regression analysis indicates that there is a linear relationship between dross formation and the nozzle size and the power setting. The multiple regression correlation coefficient (R) value of .909 and the coefficient of determination (R^2) value of .825 indicate a very strong correlation between these variables and that the multiple regression model is a good

predictor of dross formation. Regression analysis revealed that the variables nozzle size and power are statistically significant at the .013 level. The model for 16-gauge steel uses the nozzle size and the power setting to explain 82.5% of the variation in dross formation. Based on this model, the optimum machine settings for 16-gauge steel are Nozzle: A60 nozzle; Power: 60 amps; Speed: 502 ipm.

Null Hypothesis 2

The formation of dross during plasma cutting is not linearly related to either amperage, cutting speed, or nozzle size when cutting 14-gauge HR steel.

Conclusion 2

Multiple regression analysis indicates that there is a linear relationship between dross formation and the nozzle size and cutting speed. The multiple regression correlation coefficient (R) value of .689 and the coefficient of determination (R^2) value of .475 indicate a strong correlation between these variables and that the multiple regression model is a good predictor of dross formation. Regression analysis revealed that the variables nozzle size and speed are statistically significant at the .016 level. The model for 14-gauge steel uses the nozzle size and the cutting speed to explain 47.5% of the variation in dross formation. Based on this model, the optimum machine settings for 14-gauge steel are Nozzle: Finecut nozzle; Power: 40 amps; Speed: 214 ipm.

Null Hypothesis 3

The formation of dross during plasma cutting is not linearly related to either amperage, cutting speed, or nozzle size when cutting 12-gauge HR steel.

Conclusion 3

Multiple regression analysis indicates that there is a linear relationship between dross formation and the nozzle size and the product of speed and power. The multiple regression correlation coefficient (R) value of .728 and the coefficient of determination (R^2) value of .529 indicate a strong correlation between these variables and that the multiple regression model is a good predictor of dross formation. Regression analysis revealed that the variables nozzle size and the product of speed and power are statistically significant at the .001 level. The model for 12-gauge steel uses the nozzle size and the power and speed settings to explain 52.9% of the variation in dross formation. Based on this model, the optimum machine settings for 12-gauge steel are Nozzle: Finecut nozzle; Power: 40 amps; Speed: 208 ipm.

Null Hypothesis 4

The formation of dross during plasma cutting is not linearly related to either amperage, cutting speed, or nozzle size when cutting 1/8" HR steel.

Conclusion 4

Multiple regression analysis indicates that there is a linear relationship between dross formation and the nozzle size, the cutting speed, and the power setting. The multiple regression correlation coefficient (R) value of .867 and the coefficient of determination (R^2) value of .752 indicate a very strong correlation between these variables and that the multiple regression model is a good predictor of dross formation. Regression analysis revealed that the variables nozzle size, cutting speed, and power are statistically significant at the .008 level. The model for 1/8" steel uses the nozzle size, the cutting speed, and the power setting to explain 75.2% of the variation in dross formation. Based on this model, the optimum machine settings for 1/8" steel are Nozzle: Finecut nozzle; Power: 50 amps; Speed: 162 ipm.

Null Hypothesis 5

The formation of dross during plasma cutting is not linearly related to either amperage, cutting speed, or nozzle size when cutting 3/16" HR steel.

Conclusion 5

Multiple regression analysis indicates that there is a linear relationship between dross formation and the cutting speed and the power setting. The multiple regression correlation coefficient (R) value of .706 and the coefficient of determination (R^2) value of .498 indicate a strong correlation between these variables and that the multiple regression model is a good predictor of dross formation. Regression analysis revealed that the variables cutting speed and power are statistically significant at the .007 level. The model for 3/16" steel uses the nozzle size and the power setting to explain 49.8% of the variation in dross formation. Based on this model, the optimum machine settings for 3/16" steel are Nozzle: A60 nozzle; Power: 60 amps; Speed: 110 ipm.

Null Hypothesis 6

The formation of dross during plasma cutting is not linearly related to either amperage, cutting speed, or nozzle size when cutting 1/4" HR steel.

Conclusion 6

Multiple regression analysis indicates that there is a linear relationship between dross formation and the cutting speed. The multiple regression correlation coefficient (R) value of .737 and the coefficient of determination (R^2) value of .544 indicate a strong correlation between these variables and that the multiple regression model is a good predictor of dross formation. Regression analysis revealed that the variable cutting speed is statistically significant at the .000 level. The model for 1/4" steel uses cutting speed to explain 54.4% of the variation in dross

formation. Based on this model, the optimum machine settings for 1/4" steel are Nozzle: A60 nozzle; Power: 60 amps; Speed: 100 ipm.

Null Hypothesis 7

The formation of dross during plasma cutting is not linearly related to either amperage, cutting speed, or nozzle size when cutting 3/8" HR steel.

Conclusion 7

Multiple regression analysis indicates that there is a linear relationship between dross formation and the cutting speed. The multiple regression correlation coefficient (R) value of .665 and the coefficient of determination (R^2) value of .442 indicate a strong correlation between these variables and that the multiple regression model is a good predictor of dross formation. Regression analysis revealed that the variable cutting speed is statistically significant at the .000 level. The model for 3/8" steel uses cutting speed to explain 44.2% of the variation in dross formation. Based on this model, the optimum machine settings for 3/8" steel are Nozzle: A60 nozzle; Power: 60 amps; Speed: 110 ipm.

Discussion of Significant Results

Plasma arc cutting involves using a carefully controlled plasma jet to melt and vaporize the work piece and expel the molten metal quickly enough to prevent the material from reattaching itself to the base metal. This study identifies and quantifies the specific parameters that minimize the formation of dross when plasma arc cutting. Results of this research provide the users of PAC machines with quantified information to improve their manufacturing process. Table 34 suggests that the sheet thicknesses can be grouped into three groups, namely 16 gauge as one group, 14-gauge, 12-gauge, and 1/8" steel as another group, and 3/16", 1/4", and 3/8" steel as the third group. We can label these as group 1, 2, and 3, respectively.

Table 34

Optimum Machine Settings Derived from Study

Group	Thickness	Nozzle	Power (amps)	Speed (ipm)
1	16 gauge	A60	60	502
2	14 gauge	Finecut	40	214
2	12 gauge	Finecut	40	208
2	1/8"	Finecut	50	162
3	3/16"	A60	60	110
3	1/4"	A60	60	100
3	3/8"	A60	60	110

Findings Specific to Each Thickness Group

1. Findings specific to 16-gauge steel, Group 1: Analysis of the data collected for the 16-gauge steel revealed that dross can be minimized by using the highest power setting of 60 amps and using the A60 nozzle. The *R* value of .91 and R^2 value of .825 indicate a very strong relationship between the power setting, nozzle type, and dross formation which is markedly higher than for the other thicknesses tested. A possible explanation for this reduced variability in dross formation may be the small amount of net dross being formed. As explained by numerous studies, there is a subtle balance of speed and power that is required to produce the proper energy in the plasma jet to effectively melt and remove the material from the cut area. The optimum speed for 16-gauge steel was found to be 502 ipm, which is a relatively high cutting speed for this process. The thin gauge steel appears to be susceptible to LSD formation, which would explain why the cutting speed is so high. While the higher power setting of 60 amps quickly melts the material, hence quickly piercing the sheet,

the high cutting speed prevents prolonged exposure of the molten material to the plasma jet, thus preventing LSD formation. Table 34 shows that the optimum settings found for this thickness are markedly different from other thicknesses. Further studies of thinner steel may reveal more insight in this behavior.

2. Findings specific to 14-gauge, 12-gauge, and 1/8" steel, Group 2: The optimum conditions for these thicknesses are found to be finecut nozzle, 40–50-amp power, and progressively reduced cutting speeds from 214 to 162 inches per minute. The *R* values of .689, .728, and .867, respectively for the increasing thicknesses, suggest there is a stronger correlation with increasing thickness in this group, but not as high as for the 16-gauge sheet. This increased variability could be the result of increased amounts of dross as compared to the 16-gauge material. The reduced variability for the 1/8" material could be the result of increased power settings. The finecut nozzle produces the least amount of dross for this group. This may be because the nozzle focuses the plasma arc into a smaller area, which produces less molten material and thus less dross. The finecut nozzle may also produce a higher velocity at its tip due to the smaller orifice. This higher velocity may reduce dross formation by forcing the vaporized material away from the cut area. The highest power setting was not required to minimize dross formation for these thicknesses of steel and ranged from 40 to 50 amps. This suggests that the amount of energy is sufficient at these power levels. The additional material that is present with increasing thickness is more difficult to melt, vaporize, and remove from the kerf without forming dross. Consequently as the thickness increases more time is needed to melt and remove the metal requiring lower cutting speeds.

3. Findings specific to 3/16", 1/4", and 3/8" steel, Group 3: The optimum conditions for these thicknesses are found to be A60 nozzle, 60-amp power, and 110 ipm cutting speed. The *R* values for this group are .706, .737, and .665, respectively for the increasing thicknesses, hence there is a stronger correlation with increasing thickness for the 3/16" and 1/4" material, but not as high as for the 16-gauge steel. Again, this variability could be the result of increased dross formation as the material thickness increases. The results suggest that the 60-amp power level is more than sufficient to melt and vaporize the metal even for the thickest material tested. Similarly, the larger nozzle size of A60 is needed to deliver more energy for the thicker materials. The amount of material being vaporized may be too much to be evacuated from the kerf due to velocity alone, and therefore the larger nozzle is required to provide more relief to the kerf. It should be noted that the recommended cutting speed for the 3/8" steel is higher than for the 1/4" steel. This does not follow the pattern of thicker material requiring a lower cutting speed. The *R* and R^2 values indicate a correlation between the independent variables and the dependent variable, dross, but the relationship is not 100% correlated. This particular value of cutting speed may be slightly out of trend, but it is not significant enough to change the overall results or conclusions.

General Findings on Plasma Arc Cutting

This research resulted in the following significant findings for plasma cutting in general.

1. For each material thickness used in this study, the analysis performed determined that there is a correlation between some of the variables tested and the formation of dross.

Mathematical models for each thickness of steel were developed and these equations were used to determine the optimum settings for each thickness.

2. The mathematical models determined in the analyses of the data indicate a correlation between the variables tested and the formation of dross. The correlation coefficients vary between .442 and .825, indicating that much of the variation in the amount of dross formed can be attributed to one or more of the variables studied.
3. The analysis of the data clearly shows the nature of the relationships between cutting speed, power, and dross formation as shown in Figure 16. In almost every case as the thickness of the steel increases, the required power increases, and the optimum speed decreases. These trends are further supported by the statistical analysis: cutting speed as a significant variable in dross formation for six of the seven thicknesses tested and power is a significant variable in dross formation for four of the seven thicknesses tested. Clearly, speed is an important factor in reducing the formation of dross. In general, the cutting speed decreases as the material thickness increases. This may be due to the need for more time under the plasma jet to melt and vaporize the increasing amount of material in the kerf as the work piece gets thicker.
4. The resulting optimum machine settings determined from the analysis of the data show that the minimum amount of dross was produced when using either the A60 or the Finecut nozzle (depending on the material thickness). One conclusion that can be drawn from these results is that the A40 nozzle should not be used when cutting these thicknesses of steel.
5. In the above discussions, the volume of material to be melted and vaporized has been used as the main causal factor to possibly explain the results. Another factor to be

considered is heat conduction. During the process of cutting, heat is conducted away from the cut. The conduction of heat is explained by Fourier's law (Eastop, 1993). Fourier's law can be expressed as

$$H = C \Delta T A$$

H = the amount of heat being conducted away from the cut

C = Thermal conductivity of the material (constant, since all sheets are made of the same steel)

ΔT = Temperature difference (between the melting point of steel and room temperature)

A = Cross section area of material being cut

In the case of plasma arc cutting, this formula explains that as the material gets thicker it will conduct more heat away from the cut area. This will require additional energy to be supplied to compensate for the heat conducted away from the kerf. This further explains why more power, a larger nozzle, and lower cutting speeds are needed as the material thickness increases, as shown in Figure 22.

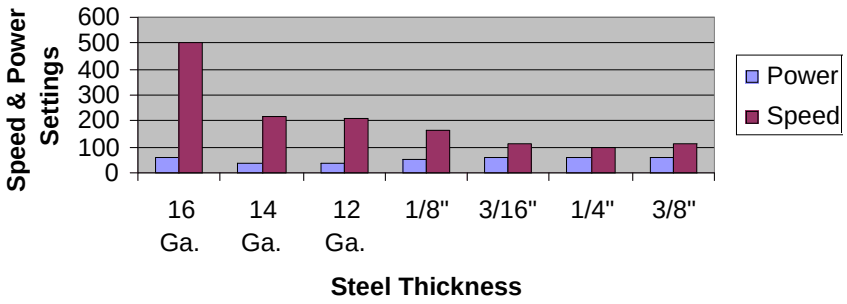

Figure 22. Recommended machine settings.

6. Dross consists of molten metal droplets that resolidify and weld onto the steel surface. During testing, it was noted that the dross was very hard and tenaciously attached to the specimens. It was so hard that a file would not remove it, indicating that the

surface of the dross was harder than the file. 1018 carbon steel melts at about 2700 °F (Material Property Data, 2009). Since the plasma-jet temperature (~50,000 °F) is much greater than the melting point of the 1018 steel, the metal is quickly melted and vaporized during plasma arc cutting. As the molten steel droplets rapidly cool, they oxidize to create a very hard, oxide covered martensitic phase material that is now welded to the base material. It is this welding and martensitic phase that may explain the tenacity and hardness of the dross. This can be verified through metallurgical studies, but it is beyond the scope of this project.

Limitations of the Study

The results of this study can only be used to make generalizations involving this specific brand, and model of CNC plasma cutting machinery. The PlasmaCAM CNC table and Hypertherm Powermax 1000 PAC machine are a unique combination that may not represent other CNC plasma cutting machines. The results are also limited to cutting selected thicknesses of 1018 HR steel with this machinery. While the results may provide guidelines for other similar equipment and materials, extrapolating these results to other machinery or materials is not recommended.

Recommendation Based Upon the Findings

The results from this study have the potential to improve the manufacturing process with this particular CNC PAC machine. The use of proper machine settings has been shown to result in the reduction of dross formation. The reduction of dross can reduce manufacturing time and the associated costs involved (Bogorodski et al., 1991; Cook, 1999; Dashkovskiy & Narimanyan, 2007). While the PAC equipment manufacturer provides recommended machine settings that are “intended to provide a good starting point for each cut assignment” (Hypertherm, 2008), the

results of this study have identified more specific machine settings that should ensure reduced dross on plasma-cut components. By using the settings shown in Table 34, the formation of dross should be minimized when cutting 1018 steel using this PAC machine.

Technology managers in organizations involved in manufacturing should consider, and should have sufficient technical background to fully understand similar studies for optimizing the equipment and processes in their company. As this study demonstrates, there are many potential improvements to be found through careful analysis of machine operating parameters. One of the unexpected results of this study of plasma arc cutting was the finding that the A40 nozzle produced the most dross of the three nozzles tested and therefore is not needed when cutting any of the steel thicknesses tested. This is one less piece of tooling that must be purchased and stored by the users of this machine.

Recommendations for Future Research

The following recommendations for future research were developed based on the experience gained from the research study and the analyses performed.

1. The obvious topic of further research is to conduct experiments to understand the PAC process to explain the results found, especially for materials thinner than 16 gauge. This would involve metallurgical studies to see the effects of heat conduction and the metallurgical nature of the dross as well as kerf quality.
2. The specific objective of this study was to find the parameters that minimize dross formation, with no regard given to other manufacturing issues. Manufacturers must find ways to maximize the quality of their product and minimize costs and production time, and these recommendations may help achieve these goals.

a. Future research may be performed to find parameters that stress the reduction in cutting time while still attempting to minimize dross formation.
b. Future research may examine how machine parameters affect energy use while still minimizing dross formation.
c. Future research may examine how to minimize dross formation while maximizing the life of PAC consumables.

3. While this study was limited to cutting specific thicknesses of 1018 steel, the plasma cutting process works equally well with many types and thicknesses of metals. Future studies can be performed to examine the optimum machine settings when cutting other thicknesses of steel, other steel alloys, or materials such as aluminum and stainless steel.
4. Experience with the plasma arc cutting process has shown that any oil or grease on the surface of the material affects the cutting process by producing excessive smoke. This suggests that surface coatings on the material may affect dross formation as well. Further studies could be performed to examine the use of a specific surface coating to reduce the adhesion of dross on the underside of the material being cut.
5. Cutting steel with the PAC process requires that the equipment being used be large enough to handle the thickness of material being cut. While the equipment used in this study is rated by the manufacturer to cut steel up to 1" thick this does not guarantee the quality of the cut produced. Experience in collecting and analyzing the data in this study has shown that the thicker the steel being cut, the more critical the machine settings become. Further studies could be performed to determine the maximum thickness of steel that can be cut while still minimizing dross formation.

REFERENCES

American Welding Society. (2006). Thermal cutting—Cssification of thermal cuts—Geometric product specification and quality tolerances. AWS C4.6-M:2006 (ISO 9013:2002 IDT). Miami, FL: Author.

Anderson, M., & Whitcomb, P. (2000). *Doe simplified.* Portland, OR: Productivity.

Berry, W. D. (1993). Understanding regression assumptions (Sage University Paper series on Quantitative Applications in the Social Sciences, 07-092). Newbury Park, CA: Sage.

Best, J., & Kahn, J. (2003). Research in education (9th ed.). Boston, MA: Pearson.

Bini, R., Colosimo, B. M., Kutlu, A. E., & Monno, M. (2007). Experimental study of the features of the kerf generated by a 200 A high tolerance plasma cutting system. *Journal of Materials Processing Technology, 196*, 345–355.

Blankenship. G. (1990). Plasma arc cutting popularity on the rise. *Welding Journal, 69*(2), 53–56.

Bogorodski, Y.A. & Rossomakho, Y.V., Olennikpov, E.F. (1991). Precision plasma arc cutting. *Weld. World*. 29 (5-6), 139-143.

Budinski, K., & Budinski, M. (2005). *Engineering materials, properties and selection.* Upper Saddle River, NJ: Pearson Education.

Caristan, C. L. (2003). *Laser cutting guide for manufacturing.* Dearborn, MI: Society of Manufacturing Engineers.

Centralized control architecture for a plasma arc system. (2008). Retrieved from http://www.freepatentsonline.com/6772040.html

Colombo, V., Concetti, A., Ghedini, E., Dallavalle, S., & Vancini, M. (2009). High speed imaging in plasma arc cutting: A review and new developments. *Plasma Sources Science Technology, 18*, 023001. doi: 10.1088/0963-0252/18/2/023001/

Colt, J. (2002). Matters of the fourth state—Technology advances pump up the energy density levels of plasma cutters. *Cutting Technology*. Retrieved from http://www.zakmet.pl /source/cutting%20technology%20Hypertherm.pdf

Cook, D. (1998). Plasma arc cutting—Cut quality problems. *Welding Design and Fabrication*. Retrieved from http://www.centricut.com/TA_CutQuality Problems.htm

Cook, D. (1999). Solving PAC cut quality problems—Dimensional inaccuracies. *Welding Design and Fabrication*. Retrieved from http://www.centricut.com/TA _SolvingPACCutQualityProb.htm

Cook, D. (2000). Illustrated guide to plasma gas selection: How to choose the best gases. *Welding Design and Fabrication*. *February*.

Dashkovskiy, S., & Narimanyan, A. (2007). Thermal plasma cutting. Part I: Modified mathematical model. *Mathematical Modelling and Analysis, 12,* 441–458.

Davis, D. (2010). Eliminating slag time in plasma cutting. *The Fabricator, 40*(8), 58–59.

Eastop, T. D. (1993). *Applied thermodynamics for engineering technologists.* Essex, UK: Wiley.

Fernicola, R. C. (1998). A guide to manual plasma arc cutting. *Welding Journal, 77*, 52–55.

Freton, P., Gonzales, J. J., Gleizes, A., Camy Peyret, F., Caillibotte, G., & Delzenne, M. (2001). Numerical and experimental study of a plasma cutting torch. *Journal of Physics D: Applied Physics*, *35*, 115–131.

Gane, N., Rogozinski, M. W., Polivka, F., Doolette, A. G., & Ramakrishnan, S. (1994, October). *Quality of cut in air plasma cutting.* Paper presented at the Washington Technology

Industry Association 42nd annual National Welding Conference, Melbourne, Australia.

Gariboldi E., Previtali B. (2004). High tolerance plasma arc cutting of commercially pure titanium. *Journal of Materials Processing Technology*, 160, pp.77-89.

Girard, L., Teulet, Ph., Razafinimanana, M., Gleizes, A., Camy-Peyret, F., Baillot, E., & Richard, F. (2006). Experimental study of an oxygen plasma cutting torch. *Journal of Physics D: Applied Physics, 39*, 1543–1556.

Gonzalez-Aguilar, J., Pardo, C., Rodriquez-Yunta, A., & Calderon, M. A. G. (1999). A theoretical study of a cutting air plasma torch. *IEEE Transactions in Plasma Science, 27*, 264–271.

Goodwin, D. (1989). Air-plasma—A growing force in metal cutting. *Welding and Metal Fabrication, 57*(8), 389, 391–392.

Güllü, A., & Atici, U. (2006). Investigation of the effects of plasma arc parameters on the structure variation of AISI 304 and St 52 Steels, *Materials and Design, 27*, 1157–1162.

Hair, J. F., Anderson, R. E., Tatham, R. L., & Black, W. C. (1998). Multivariate data analysis (5th ed.). Upper Saddle River, NJ: Prentice-Hall.

Harris, D., & Lowery, J. (1996). High tolerance plasma arc cutting. *Welding in the World, 37*(6); 283–287.

Hoult, A. P., Pashby, I. R., & Chan, K. (1995). Fine plasma cutting of advanced aerospace materials. *Journal of Materials Processing Technology, 48*, 825–831.

Hussary, N., & Renault, T. (2006). Correlations between system parameters and process responses in plasma cutting. *Proceedings of the 33rd IEEE International Conference, Plasma Science, 2006, ICOPS 2006, IEEE Conference Record—abstracts*, 383.

Hypertherm. (2007). *Powermax 1000 plasma are cutting system*. Hanover, NH: Author.

Hypertherm. (2008). Powermax 1000 plasma arc cutting system. In *Hypertherm operators manual* (pp. 804290). Hanover, NH: Author.

Indiana State University. (2009). *PhD in technology management.* Retrieved from http://www .indstate.edu/consortphd/

Iosub, A., Nagit, Gh., & Negoescu, F. (2008, April). *Plasma cutting of composite materials.* Paper presented at the 11th European Aviation Safety Agency Conference on Material Forming, Lyons, France.

Keddell, D. (2007). Improving manual plasma cutting quality. *The Fabricator*. Retrieved from http://www.thefabricator.com/PlasmaCutting/PlasmaCutting_Article.cfm?ID=1575

Kelly, H., Mancinelli, B., Prevosto, L., Minotti, F. O., & Marquez, A. (2004). Experimental characterization of a low-current cutting torch. *Brazilian Journal of Physics, 34*, 1518–1522.

Landry, C. (1997). Improving plasma cutting in sheet metal applications. *MetalForming Magazine*, (September), 27–32.

Landry, C. (1998). Elements of plasma arc cut quality. *MetalForming Magazine*. Retrieved from http://archive.metalformingmagazine.com/1998/05/plasma/plasma.htm

Linde Group. (1955). Linde universal inert gas tungsten-arc cutting of aluminum. *Welding Journal, 34*, 1097–1098.

Lucas, R. (2005). Hypertherm stays hot on metalcutting technology. *Gases & Welding Distributor*. Retrieved from http://gwd.weldingmag.com/mag/gwd_11350/

Material Property Data. (2009). Retrieved from http://www.matweb.com/search/DataSheet .aspx? MatGUID= e60983fcde914b278ceffebb946995e6

Mathews, P. (2005). *Design of experiments with MINITAB.* Milwaukee, WI: Quality Press.

Matsuyama, K. (1997). Current status of high tolerance plasma arc cutting in Japan. *Welding in the World*. 39(4); 165-171.

Nagarajan, R. (2000). *Parametric study of the effect of laser cutting variables on the cut quality.* (Unpublished master's thesis). Wichita State University, Wichita, KS.

Nemchinsky, V. A. (1997). Dross formation and heat transfer during plasma arc cutting. *Journal of Physics D: Applied Physics, 30,* 2566–2572.

Nemchinsky, V. A. (1998). Plasma flow in a nozzle during plasma arc cutting. *Journal of Physics D: Applied Physics, 31,* 3102–3107.

Nemchinsky, V. A., & Severance, W. S. (2006). What we know and what we do not know about plasma arc cutting. *Journal of Physics D: Applied Physics, 39,* R423–R438.

Nishiguchi, K., & Matsuyama, K. (1979). Kerf formation and dross adhesion in plasma arc cutting. *Welding in the World, 17,* 232–239.

Pardo, C., Gonzalez-Aguilar, J., Rodriguez-Yunta, A., & Calderon, M. A. G. (1999). Spectroscopic analysis of an air plasma cutting torch. *Journal of Physics D: Applied Physics, 32,* 2181–2189.

Pellecchia, M. (1995). Select the best process: laser or precision plasma. *Welding Design and Fabrication, 68,* 19–26.

Peters, J. (2006). *Effects of torch design and operating conditions on plasma properties in a plasma cutting system* (Unpublished doctoral dissertation). University of Minnesota, Minneapolis.

Rajaram, N., Sheikh-Ahmad, J., & Cheraghi, S. H. (2002). CO_2 laser cut quality of 4130 steel. *International Journal of Machine Tools & Manufacture, 43,* 351–358.

Ramakrishnan, S., Gershenzon, M., Polivka, F., Kearney, T. N., & Rogozinski, M. W. (1997). Plasma generation for plasma cutting process. *IEEE Transactions on Plasma Science, 25,* 937–946.

Ramakrishnan, S., & Rogozinski, M. W. (1997). Properties of electric arc plasma for metal cutting. *Journal of Physics D: Applied Physics, 30,* 636–644.

Ramakrishnan, S., Shrinet, V., Polivka, F. B., Kearney, T. N., & Koltun, P. (2000). Influence of gas composition on plasma arc cutting of steel. *Journal of Physics D: Applied Physics, 33,* 2288–2299.

Renault, T., & Hussary, N. (2007). The life and times of plasma cutting. *The Fabricator, 37*(11), 47–50.

Salkind, N. J. (2000). *Statistics for people who think they hate statistics.* Thousand Oaks, CA: Sage.

Sommer, C. (2000). *Nontraditional machining handbook.* Houston, TX: Advanced.

Sundar, M., Nath, A. K., Bandyopadhyay, D. K., Chaudhuri, S. P., Dey, P. K., & Misra, D. (2007). Effect of process parameters on the cutting quality in LASOX cutting of mild steel. *International Journal of Advanced Manufacturing Technology, 40,* 865–874.

Tani, G., Tomesani, L., Campana, G., & Fortunato, A. (2003). Quality factors assessed by analytical modeling in laser-cutting. *Thin Solid Films, 453–454,* 486–491.

Teulet, P., Girard, L., Razafinimanana, M., Gleizes, A., Bertrand, P., Camy-Peyret, F., … Richard, F. (2006). *Journal of Physics D: Applied Physics, 39,* 1557–1573.

Thompson, B., & Hanchette, K. (2003). Making plasma cutting easier using CNC automation technology. *The Fabricator*. Retrieved from http://www.thefabricator.com/PlasmaCutting/PlasmaCutting_Article.cfm?ID=675

Triola, M. (2004). *Elementary statistics.* Boston, MA: Pearson Addison Wesley.

Vasil'ev, K. V. (2002). Plasma arc cutting—A promising method of thermal cutting. *Welding International, 17,* 147–151.

Venkatramani, N. (2002). Industrial plasma torches and applications. *Current Science, 83,* 254–262.

Walsh, M. (2005). Plasma cutting: then and now. *The Fabricator*. Retrieved from http://www.thefabricator.com/PlasmaCutting/PlasmaCutting_Article.cfm?ID=1142

Whiting, T. (2007). Improving plasma cut quality. *The Fabricator*. Retrieved from http://www.thefabricator.com/PlasmaCutting/PlasmaCutting_Article.cfm?ID=1703

Xu, W. J., Fang, J. C., & Lu, Y. S. (2002). Study on ceramic cutting by plasma arc. *Journal of Materials Processing Technology, 129,* 152–156.

Xue, W., Kusumoto, K., & Nezu, K. (2004). Measurement and analysis of plasma arc cutting acoustic signal. *Material Science Forum, 449–452,* 313–316.

Yang, S. Y. S. (2000, November). An expert system for plasma cutting process quality prediction and optimal parameter suggestion. In Mo J. P. T. & Nemes, L. (Eds.), *Global engineering, manufacturing and enterprise networks* (pp. 438–445). Dordrecht, The Netherlands: Kluwer Academic.

Zajac, A., & Pfeifer, T. (2006). Restricting the heat-affected zone during plasma cutting of high alloy steels. *Welding International, 20,* 23–27.

Zhou, Q., Li, H., Liu, F., Guo, S., Guo, W., & Xu, P. (2008). Effects of nozzle length and process parameters on highly constricted oxygen plasma cutting arc. *Plasma Chemistry Plasma Process, 28,* 729–747.

APPENDIX A: PILOT STUDY RESULTS

Table A1

Range of Test Settings Determined From Pilot Study

Material thickness	Nozzle size	Power (amps)	Cutting speed (in/min)
16 gauge	#1 (A60)	40	100–325
16 gauge	#1 (A60)	45	175–425
16 gauge	#1 (A60)	50	200–525
16 gauge	#1 (A60)	55	275–575
16 gauge	#1 (A60)	60	350–650
16 gauge	#2 (A40)	30	40–140
16 gauge	#2 (A40)	35	60–150
16 gauge	#2 (A40)	40	100–230
16 gauge	#2 (A40)	45	100–240
16 gauge	#2 (A40)	50	150–375
16 gauge	#3 (Finecut)	40	80–180
16 gauge	#3 (Finecut)	45	80–180
16 gauge	#3 (Finecut)	50	100–220
16 gauge	#3 (Finecut)	55	100–280
16 gauge	#3 (Finecut)	60	120–330

Material thickness	Nozzle size	Power (amps)	Cutting speed (in/min)
14 gauge	#1 (A60)	40	120–240
14 gauge	#1 (A60)	45	140–260
14 gauge	#1 (A60)	50	160–300
14 gauge	#1 (A60)	55	180–400
14 gauge	#1 (A60)	60	180–450
14 gauge	#2 (A40)	40	80–260
14 gauge	#2 (A40)	45	100–350
14 gauge	#2 (A40)	50	120–380
14 gauge	#2 (A40)	55	140–400
14 gauge	#2 (A40)	60	160–400
14 gauge	#3 (Finecut)	40	60–145
14 gauge	#3 (Finecut)	45	80–160
14 gauge	#3 (Finecut)	50	90–210
14 gauge	#3 (Finecut)	55	100–220
14 gauge	#3 (Finecut)	60	120–240

Material thickness	Nozzle size	Power (amps)	Cutting speed (in/min)
12 gauge	#1 (A60)	40	80–150
12 gauge	#1 (A60)	45	80–170
12 gauge	#1 (A60)	50	80–220
12 gauge	#1 (A60)	55	100–260
12 gauge	#1 (A60)	60	120–350
12 gauge	#2 (A40)	35	30–100
12 gauge	#2 (A40)	40	30–130
12 gauge	#2 (A40)	45	40–150
12 gauge	#2 (A40)	50	50–160
12 gauge	#2 (A40)	55	60–180
12 gauge	#2 (A40)	60	70 -180
12 gauge	#3 (Finecut)	40	40–90
12 gauge	#3 (Finecut)	45	50–130
12 gauge	#3 (Finecut)	50	60–130
12 gauge	#3 (Finecut)	55	70–140
12 gauge	#3 (Finecut)	60	80–150

Material thickness	Nozzle size	Power (amps)	Cutting speed (in/min)
1/8"	#1 (A60)	40	80–150
1/8"	#1 (A60)	45	80–170
1/8"	#1 (A60)	50	90–200
1/8"	#1 (A60)	55	100–240
1/8"	#1 (A60)	60	120–260
1/8"	#2 (A40)	35	30–100
1/8"	#2 (A40)	40	60–160
1/8"	#2 (A40)	45	60–160
1/8"	#2 (A40)	50	80–200
1/8"	#2 (A40)	55	80–220
1/8"	#2 (A40)	60	100–250
1/8"	#3 (Finecut)	40	30–120
1/8"	#3 (Finecut)	45	50–140
1/8"	#3 (Finecut)	50	60–150
1/8"	#3 (Finecut)	55	60–150
1/8"	#3 (Finecut)	60	70–160

Material thickness	Nozzle size	Power (amps)	Cutting speed (in/min)
3/16"	#1 (A60)	40	No Cut
3/16"	#1 (A60)	45	No Cut
3/16"	#1 (A60)	50	50 - 90
3/16"	#1 (A60)	55	60 - 130
3/16"	#1 (A60)	60	70 - 150
3/16"	#2 (A40)	40	30 - 90
3/16"	#2 (A40)	45	30 - 100
3/16"	#2 (A40)	50	40 - 120
3/16"	#2 (A40)	55	50 - 120
3/16"	#2 (A40)	60	60 - 120
3/16"	#3 (Finecut)	40	No Cut
3/16"	#3 (Finecut)	45	No Cut
3/16"	#3 (Finecut)	50	15 - 35
3/16"	#3 (Finecut)	55	30 - 70
3/16"	#3 (Finecut)	60	30 - 80

Material thickness	Nozzle size	Power (amps)	Cutting speed (in/min)
1/4"	#1 (A60)	40	No Cut
1/4"	#1 (A60)	45	No Cut
1/4"	#1 (A60)	50	20–50
1/4"	#1 (A60)	55	30–80
1/4"	#1 (A60)	60	40–100
1/4"	#2 (A40)	40	No Cut
1/4"	#2 (A40)	45	No Cut
1/4"	#2 (A40)	50	No Cut
1/4"	#2 (A40)	55	No Cut
1/4"	#2 (A40)	60	No Cut
1/4"	#3 (Finecut)	40	No Cut
1/4"	#3 (Finecut)	45	No Cut
1/4"	#3 (Finecut)	50	10–40
1/4"	#3 (Finecut)	55	10–40
1/4"	#3 (Finecut)	60	10–40

Material thickness	Nozzle size	Power (amps)	Cutting speed (in/min)
3/8"	#1 (A60)	40	No Cut
3/8"	#1 (A60)	45	No Cut
3/8"	#1 (A60)	50	20–40
3/8"	#1 (A60)	55	20–50
3/8"	#1 (A60)	60	20–60
3/8"	#2 (A40)	40	No Cut
3/8"	#2 (A40)	45	No Cut
3/8"	#2 (A40)	50	No Cut
3/8"	#2 (A40)	55	No Cut
3/8"	#2 (A40)	60	No Cut
3/8"	#3 (Finecut)	40	No Cut
3/8"	#3 (Finecut)	45	No Cut
3/8"	#3 (Finecut)	50	No Cut
3/8"	#3 (Finecut)	55	No Cut
3/8"	#3 (Finecut)	60	No Cut

APPENDIX B: RAW DATA

Table B1

Dross Data

Sample	1	2	3	4	5	6	7	8
Mat'l	0.1840	0.0990	0.1170	0.0720	0.3660	0.0570	0.2560	0.3660
Nozzle	60A	Fine	60A	40A	Fine	60A	60A	60A
Power	60	40	55	55	55	60	60	60
Speed	117	49	220	342	23	608	85	56
Thick. A	0.1890	0.1495	0.1220	0.0785	0.4710	0.0650	0.2925	0.4185
Thick. B	0.1900	0.1500	0.1250	0.0785	0.4500	0.0675	0.2855	0.4085
Thick. C	0.1990	0.1435	0.1305	0.0790	0.4475	0.0690	0.3320	0.3860
Thick. D	0.2000	0.1530	0.1305	0.0785	0.4570	0.0690	0.2875	0.3870
Thick. E	0.2045	0.1440	0.1325	0.0780	0.4590	0.0615	0.2860	0.3940
Avg. Thick.	0.1965	0.1480	0.1281	0.0785	0.4569	0.0664	0.2967	0.3988
Dross	0.0125	0.0490	0.0111	0.0065	0.0909	0.0094	0.0407	0.0328

Sample	9	10	11	12	13	14	15	16
Mat'l	0.1170	0.0570	0.0720	0.2560	0.0990	0.1840	0.0990	0.0720
Nozzle	40A	60A	FINE	60A	40A	FINE	FINE	40A
Power	40	55	40	60	40	55	55	55
Speed	61	361	187	55	116	62	126	187
Thick. A	0.1600	0.0620	0.0830	0.2795	0.1490	0.1875	0.1095	0.1055
Thick. B	0.1655	0.0620	0.0840	0.2815	0.1545	0.1880	0.1000	0.1065
Thick. C	0.1675	0.0615	0.0860	0.3015	0.1545	0.1880	0.1000	0.1050
Thick. D	0.1695	0.0620	0.0820	0.2880	0.1480	0.1890	0.1000	0.1040
Thick. E	0.1760	0.0620	0.0805	0.2925	0.1490	0.1900	0.1005	0.1100
Avg. Thick.	0.1677	0.0619	0.0831	0.2886	0.1510	0.1885	0.1020	0.1062
Dross	0.0507	0.0049	0.0111	0.0326	0.0520	0.0045	0.0030	0.0342

Sample	17	18	19	20	21	22	23	24
Mat’l	0.0570	0.1170	0.3660	0.2560	0.1840	0.2560	0.1170	0.3660
Nozzle	60A	FINE	60A	60A	FINE	60A	60A	Fine
Power	60	60	50	50	55	55	60	55
Speed	360	122	33	41	51	77	189	27
Thick. A	0.0650	0.1195	0.4865	0.2950	0.1855	0.2955	0.1220	0.5060
Thick. B	0.0650	0.1190	0.4270	0.2880	0.1850	0.2850	0.1220	0.4395
Thick. C	0.0655	0.1185	0.3965	0.2890	0.1850	0.3155	0.1240	0.4565
Thick. D	0.0640	0.1175	0.4350	0.3090	0.1850	0.3175	0.1235	0.4560
Thick. E	0.0640	0.1185	0.4375	0.2935	0.2050	0.3015	0.1215	0.4860
Avg. Thick.	0.0647	0.1186	0.4365	0.2949	0.1891	0.3030	0.1226	0.4688
Dross	0.0077	0.0016	0.0705	0.0389	0.0051	0.047	0.0056	0.1028

Sample	25	26	27	28	29	30	31	32
Mat’l	0.1840	0.0720	0.0570	0.0990	0.0990	0.1840	0.1170	0.0570
Nozzle	40A	60A	FINE	FINE	FINE	40A	FINE	60A
Power	55	45	55	40	55	45	50	45
Speed	98	182	197	65	101	95	87	307
Thick. A	0.1915	0.0980	0.0575	0.1175	0.1	0.1985	0.1180	0.0670
Thick. B	0.1900	0.0970	0.0570	0.1155	0.1035	0.2015	0.1180	0.0660
Thick. C	0.1925	0.0960	0.0570	0.1155	0.0995	0.1975	0.1175	0.0665
Thick. D	0.1945	0.0970	0.0570	0.1155	0.1005	0.2435	0.1195	0.0665
Thick. E	0.1910	0.0985	0.0570	0.1180	0.0995	0.2150	0.1185	0.0670
Avg. Thick.	0.1919	0.0973	0.0571	0.1164	0.1006	0.2112	0.1183	0.0666
Dross	0.0079	0.0253	0.0001	0.0174	0.0016	0.0272	0.0013	0.0096

Sample	33	34	35	36	37	38	39	40
Mat’l	0.3660	0.0720	0.2560	0.0720	0.1170	0.0570	0.0990	0.1840
Nozzle	60A	FINE	FINE	FINE	FINE	60A	FINE	FINE
Power	50	45	60	60	60	60	55	50
Speed	72	153	38	123	128	584	129	24
Thick. A	0.3980	0.0730	0.3060	0.0740	0.1185	0.0635	0.1120	0.2965
Thick. B	0.3880	0.0735	0.3340	0.0760	0.1180	0.0650	0.1200	0.3005
Thick. C	0.3785	0.0735	0.3350	0.0740	0.1185	0.0630	0.1305	0.2940
Thick. D	0.3895	0.0735	0.3190	0.0770	0.1195	0.0640	0.1165	0.3155
Thick. E	0.3875	0.0740	0.3370	0.0765	0.1195	0.0640	0.1130	0.3140
Avg. Thick.	0.3883	0.0735	0.3262	0.0755	0.1188	0.0639	0.1184	0.3041
Dross	0.0223	0.0015	0.0702	0.0035	0.0018	0.0069	0.0194	0.1201

Sample	41	42	43	44	45	46	47	48
Mat’l	0.3660	0.2560	0.1840	0.0990	0.0570	0.3660	0.0720	0.2560
Nozzle	60A	FINE	60A	60A	60A	60A	FINE	60A
Power	60	50	50	55	60	55	50	55
Speed	140	13	51	183	561	60	192	44
Thick. A	0.3935	0.4120	0.2215	0.1030	0.0620	0.4025	0.0730	0.2880
Thick. B	0.3945	0.4100	0.2235	0.1040	0.0660	0.4020	0.0735	0.2935
Thick. C	0.3935	0.4155	0.2150	0.1030	0.0655	0.3895	0.0735	0.3315
Thick. D	0.3950	0.4145	0.2315	0.1060	0.0640	0.4030	0.0735	0.2940
Thick. E	0.3880	0.4260	0.2260	0.1045	0.0635	0.4020	0.0735	0.3065
Avg. Thick.	0.3929	0.4156	0.2235	0.1041	0.0642	0.3998	0.0734	0.3027
Dross	0.0269	0.1596	0.0395	0.0051	0.0072	0.0338	0.0014	0.0467

Sample	49	50	51	52	53	54	55	56
Mat’l	0.1170	0.0720	0.0990	0.2560	0.3660	0.1840	0.0720	0.1170
Nozzle	40A	FINE	40A	60A	Fine	60A	40A	40A
Power	40	55	55	60	60	55	60	60
Speed	131	127	149	61	34	109	188	126
Thick. A	0.1420	0.0735	0.1065	0.2950	0.4030	0.1900	0.0735	0.1445
Thick. B	0.1440	0.0735	0.1065	0.2845	0.4165	0.1925	0.0755	0.1575
Thick. C	0.1435	0.0730	0.1075	0.2840	0.3985	0.1875	0.0720	0.1465
Thick. D	0.1420	0.0735	0.1075	0.3040	0.3995	0.1890	0.0720	0.1455
Thick. E	0.1420	0.0740	0.1065	0.2895	0.3990	0.1880	0.0725	0.1395
Avg. Thick.	0.1427	0.0735	0.1069	0.2914	0.4033	0.1894	0.0731	0.1467
Dross	0.0257	0.0015	0.0079	0.0354	0.0373	0.0054	0.0011	0.0297

Sample	57	58	59	60	61	62	63	64
Mat’l	0.0990	0.2560	0.0990	0.1840	0.1170	0.3660	0.0720	0.0990
Nozzle	FINE	60A	60A	60A	60A	Fine	FINE	FINE
Power	60	60	50	50	55	55	45	50
Speed	88	77	80	66	232	46	103	63
Thick. A	0.1000	0.2840	0.1465	0.2040	0.1285	0.4750	0.0740	0.1220
Thick. B	0.1000	0.2970	0.1275	0.2010	0.1315	0.4670	0.0740	0.1185
Thick. C	0.1005	0.3035	0.1295	0.2020	0.1285	0.4470	0.0740	0.1195
Thick. D	0.1000	0.3070	0.1370	0.2020	0.1295	0.4675	0.0740	0.1015
Thick. E	0.1005	0.3195	0.1420	0.2010	0.1320	0.4685	0.0750	0.1015
Avg. Thick.	0.1002	0.3022	0.1365	0.2020	0.1300	0.4650	0.0742	0.1126
Dross	0.0012	0.0462	0.0375	0.0180	0.0130	0.0990	0.0022	0.0136

Sample	65	66	67	68	69	70	71	72
Mat'l	0.0570	0.0720	0.1840	0.2560	0.3660	0.1170	0.3660	0.0570
Nozzle	40A	40A	FINE	FINE	Fine	40A	Fine	40A
Power	50	50	50	55	60	45	60	40
Speed	350	233	28	20	12	100	35	152
Thick. A	0.0680	0.0760	0.2550	0.3770	0.5490	0.1680	0.4350	0.0900
Thick. B	0.0685	0.0765	0.2575	0.3880	0.5160	0.1685	0.4385	0.0925
Thick. C	0.0680	0.0765	0.2695	0.3735	0.5210	0.1765	0.4355	0.0905
Thick. D	0.0695	0.0765	0.2675	0.3840	0.5105	0.1745	0.4370	0.0930
Thick. E	0.0680	0.0780	0.2725	0.3930	0.5050	0.1765	0.4340	0.0925
Avg. Thick.	0.0684	0.0767	0.2644	0.3831	0.5203	0.1728	0.4360	0.0917
Dross	0.0114	0.0047	0.0804	0.1271	0.1543	0.0558	0.0700	0.0347

Sample	73	74	75	76	77	78	79	80
Mat'l	0.1840	0.0990	0.1170	0.2560	0.0990	0.0570	0.2560	0.1840
Nozzle	40A	60A	40A	FINE	FINE	60A	FINE	60A
Power	55	60	50	50	45	60	55	55
Speed	51	135	94	10	36	622	38	126
Thick. A	0.2	0.1315	0.1695	0.4230	0.1155	0.0725	0.3130	0.1940
Thick. B	0.2045	0.1300	0.1680	0.4025	0.1135	0.0845	0.3145	0.1985
Thick. C	0.2015	0.1245	0.1720	0.3970	0.1100	0.0755	0.3130	0.1970
Thick. D	0.2065	0.1290	0.1660	0.3910	0.1130	0.0655	0.3075	0.1990
Thick. E	0.2055	0.1365	0.1695	0.4035	0.1120	0.0620	0.3205	0.1940
Avg. Thick.	0.2036	0.1303	0.1690	0.4034	0.1128	0.0720	0.3137	0.1965
Dross	0.0196	0.0313	0.0520	0.1474	0.0138	0.0150	0.0577	0.0125

Sample	81	82	83	84	85	86	87	88
Mat'l	0.0720	0.0990	0.3660	0.1170	0.0990	0.2560	0.1840	0.1170
Nozzle	40A	60A	60A	FINE	FINE	FINE	60A	60A
Power	60	45	60	55	50	60	55	60
Speed	252	143	104	122	66	16	73	243
Thick. A	0.0890	0.1240	0.3755	0.1195	0.1185	0.4010	0.2370	0.1240
Thick. B	0.0880	0.1215	0.3745	0.1200	0.1190	0.4010	0.2370	0.1240
Thick. C	0.0890	0.1165	0.3735	0.1195	0.1165	0.4120	0.2405	0.1245
Thick. D	0.0870	0.1190	0.3775	0.1185	0.1160	0.4285	0.2380	0.1220
Thick. E	0.0865	0.1195	0.3770	0.1185	0.1150	0.4030	0.2570	0.1215
Avg. Thick.	0.0879	0.1201	0.3756	0.1192	0.1170	0.4091	0.2419	0.1232
Dross	0.0159	0.0211	0.0096	0.0022	0.018	0.1531	0.0579	0.0062

Sample	89	90	91	92	93	94	95	96
Mat'l	0.0570	0.0720	0.3660	0.0720	0.3660	0.0990	0.0990	0.2560
Nozzle	40A	60A	Fine	60A	60A	FINE	60A	60A
Power	40	50	60	45	60	40	40	60
Speed	176	259	14	157	31	63	101	65
Thick. A	0.0910	0.0835	0.5240	0.1075	0.4360	0.1100	0.1445	0.3245
Thick. B	0.0935	0.0825	0.5235	0.1020	0.4325	0.1095	0.1380	0.3230
Thick. C	0.0900	0.0825	0.5220	0.1000	0.4345	0.1100	0.1395	0.3130
Thick. D	0.0890	0.0820	0.5145	0.0995	0.4355	0.1110	0.1405	0.3040
Thick. E	0.0920	0.0795	0.5225	0.0995	0.4370	0.1110	0.1430	0.3020
Avg. Thick.	0.0911	0.0820	0.5213	0.1017	0.4351	0.1103	0.1411	0.3133
Dross	0.0341	0.0100	0.1553	0.0297	0.0691	0.0113	0.0421	0.0573

Sample	97	98	99	100	101	102	103	104
Mat’l	0.1170	0.0570	0.1840	0.2560	0.0990	0.0570	0.0720	0.2560
Nozzle	40A	FINE	FINE	60A	FINE	60A	FINE	FINE
Power	45	60	55	50	60	40	50	55
Speed	120	187	39	45	131	269	107	26
Thick. A	0.1550	0.0615	0.2345	0.3025	0.1140	0.0730	0.0740	0.3565
Thick. B	0.1450	0.0610	0.2315	0.3040	0.1140	0.0715	0.0735	0.3525
Thick. C	0.1485	0.0610	0.2135	0.3075	0.1210	0.0705	0.0740	0.3455
Thick. D	0.1475	0.0610	0.2155	0.2960	0.1150	0.0710	0.0735	0.3435
Thick. E	0.1480	0.0610	0.2105	0.3015	0.1215	0.0700	0.0735	0.3465
Avg. Thick.	0.1488	0.0611	0.2211	0.3023	0.1171	0.0712	0.0737	0.3489
Dross	0.0318	0.0041	0.0371	0.0463	0.0181	0.0142	0.0017	0.0929

Sample	105	106	107	108	109	110	111	112
Mat’l	0.1170	0.3660	0.0570	0.2560	0.1840	0.0990	0.3660	0.1170
Nozzle	FINE	60A	FINE	60A	60A	FINE	60A	FINE
Power	40	50	60	55	50	45	55	50
Speed	81	55	304	34	78	94	78	95
Thick. A	0.1180	0.4225	0.0570	0.3825	0.2115	0.1775	0.4155	0.1610
Thick. B	0.1180	0.4080	0.0575	0.3725	0.2215	0.1175	0.4205	0.1550
Thick. C	0.1185	0.4175	0.0570	0.3640	0.2050	0.1095	0.4095	0.1460
Thick. D	0.1200	0.4225	0.0565	0.3630	0.2120	0.1205	0.4135	0.1280
Thick. E	0.1200	0.4180	0.0570	0.3675	0.2100	0.1220	0.4180	0.1180
Avg. Thick.	0.1189	0.4177	0.0570	0.3699	0.2120	0.1294	0.4154	0.1416
Dross	0.0019	0.0517	0.0000	0.1139	0.028	0.0304	0.0494	0.0246

Sample	113	114	115	116	117	118	119	120
Mat’l	0.3660	0.2560	0.0720	0.1840	0.3660	0.0570	0.0990	0.3660
Nozzle	60A	FINE	40A	FINE	Fine	40A	FINE	60A
Power	50	60	60	55	60	30	45	55
Speed	81	28	311	43	36	97	75	44
Thick. A	0.3845	0.3380	0.0825	0.2055	0.4035	0.1030	0.1170	0.4185
Thick. B	0.3865	0.3310	0.0830	0.2065	0.3995	0.1050	0.1170	0.4145
Thick. C	0.3850	0.3570	0.0840	0.2115	0.4020	0.1050	0.1165	0.4095
Thick. D	0.3870	0.3665	0.0835	0.2100	0.4100	0.1050	0.1210	0.4105
Thick. E	0.3775	0.3690	0.0835	0.2150	0.4095	0.1065	0.1140	0.4125
Avg. Thick.	0.3841	0.3523	0.0833	0.2097	0.4049	0.1049	0.1171	0.4131
Dross	0.0181	0.0963	0.0113	0.0257	0.0389	0.0479	0.0181	0.0471

Sample	121	122	123	124	125	126	127	128
Mat’l	0.1170	0.0570	0.2560	0.0990	0.1840	0.0720	0.3660	0.0570
Nozzle	40A	FINE	60A	FINE	60A	40A	60A	40A
Power	55	40	50	55	50	50	55	40
Speed	135	97	27	79	83	71	49	198
Thick. A	0.1375	0.0665	0.3400	0.1165	0.2370	0.1005	0.3895	0.0890
Thick. B	0.1345	0.0640	0.3260	0.1115	0.2385	0.1000	0.3915	0.0885
Thick. C	0.1335	0.0635	0.3455	0.1115	0.2360	0.0980	0.3985	0.0820
Thick. D	0.1320	0.0655	0.3270	0.1025	0.2380	0.0970	0.3995	0.0815
Thick. E	0.1330	0.0685	0.3240	0.1005	0.2475	0.0955	0.3990	0.0830
Avg. Thick.	0.1341	0.0656	0.3325	0.1085	0.2394	0.0982	0.3956	0.0848
Dross	0.0171	0.0086	0.0765	0.0095	0.0554	0.0262	0.0296	0.0278

Sample	129	130	131	132	133	134	135	136
Mat’l	0.1170	0.2560	0.0720	0.0990	0.1840	0.1840	0.0990	0.2560
Nozzle	60A	FINE	40A	FINE	40A	60A	FINE	60A
Power	60	60	60	55	40	60	60	55
Speed	125	27	333	91	30	82	84	60
Thick. A	0.1455	0.3535	0.0915	0.1000	0.2830	0.1975	0.1250	0.2965
Thick. B	0.1485	0.3560	0.0915	0.1000	0.2795	0.1960	0.1180	0.2920
Thick. C	0.1480	0.3565	0.0910	0.0995	0.2870	0.1945	0.1225	0.2860
Thick. D	0.1485	0.3585	0.0880	0.1000	0.2815	0.1955	0.1185	0.2905
Thick. E	0.1475	0.3790	0.0885	0.1000	0.2835	0.1920	0.1005	0.2880
Avg. Thick.	0.1476	0.3607	0.0901	0.0999	0.2829	0.1951	0.1169	0.2906
Dross	0.0306	0.1047	0.0181	0.0009	0.0989	0.0111	0.0179	0.0346

Sample	137	138	139	140	141	142	143	144
Mat’l	0.0570	0.1170	0.0720	0.1840	0.0990	0.2560	0.3660	0.0720
Nozzle	40A	40A	60A	60A	FINE	60A	60A	40A
Power	40	40	55	60	50	55	50	40
Speed	121	112	329	101	62	65	43	156
Thick. A	0.0895	0.1620	0.0785	0.1990	0.1190	0.3020	0.4205	0.1110
Thick. B	0.0905	0.1625	0.0780	0.2085	0.1115	0.2925	0.4185	0.1085
Thick. C	0.0905	0.1565	0.0770	0.2115	0.1020	0.2930	0.4115	0.1055
Thick. D	0.0910	0.1585	0.0765	0.2055	0.1015	0.2990	0.4095	0.1060
Thick. E	0.0905	0.1690	0.0770	0.2040	0.1160	0.2940	0.4075	0.1060
Avg. Thick.	0.0904	0.1617	0.0774	0.2057	0.1100	0.2961	0.4135	0.1074
Dross	0.0334	0.0447	0.0054	0.0217	0.0110	0.0401	0.0475	0.0354

Sample	145	146	147	148	149	150	151	152
Mat’l	0.1170	0.1840	0.0570	0.3660	0.0990	0.0570	0.2560	0.0720
Nozzle	40A	60A	FINE	Fine	40A	FINE	FINE	FINE
Power	60	50	60	55	60	60	55	40
Speed	170	62	297	39	174	152	29	107
Thick. A	0.1265	0.2015	0.0590	0.4235	0.1155	0.0650	0.3670	0.0775
Thick. B	0.1260	0.2040	0.0585	0.4255	0.1155	0.0750	0.3535	0.0765
Thick. C	0.1265	0.2020	0.0585	0.4265	0.1165	0.0800	0.3510	0.0760
Thick. D	0.1275	0.2025	0.0585	0.4305	0.1160	0.0750	0.3590	0.0775
Thick. E	0.1270	0.2020	0.0575	0.4185	0.1195	0.0705	0.3535	0.0760
Avg. Thick.	0.1267	0.2024	0.0584	0.4249	0.1166	0.0731	0.3568	0.0767
Dross	0.0097	0.0184	0.0014	0.0589	0.0176	0.0161	0.1008	0.0047

Sample	153	154	155	156	157	158	159	160
Mat’l	0.1840	0.1170	0.3660	0.0570	0.2560	0.0720	0.3660	0.0990
Nozzle	40A	FINE	60A	40A	FINE	40A	Fine	40A
Power	40	40	60	30	60	45	55	55
Speed	81	108	80	86	11	212	35	158
Thick. A	0.2330	0.1525	0.3730	0.0985	0.3965	0.0885	0.4105	0.1280
Thick. B	0.2380	0.1530	0.3745	0.0995	0.4020	0.0890	0.4160	0.1250
Thick. C	0.2355	0.1525	0.3695	0.1000	0.4050	0.0890	0.4105	0.1235
Thick. D	0.2360	0.1505	0.3725	0.0990	0.4165	0.0880	0.4065	0.1210
Thick. E	0.2325	0.1530	0.3745	0.1015	0.4215	0.0865	0.4050	0.1225
Avg. Thick.	0.2350	0.1523	0.3728	0.0997	0.4083	0.0882	0.4097	0.1240
Dross	0.0510	0.0353	0.0068	0.0427	0.1523	0.0162	0.0437	0.0250

Sample	161	162	163	164	165	166	167	168
Mat’l	0.1170	0.1840	0.0990	0.3660	0.0570	0.3660	0.2560	0.1170
Nozzle	FINE	60A	FINE	60A	FINE	60A	FINE	60A
Power	55	55	55	60	55	55	60	60
Speed	108	96	115	81	243	52	35	258
Thick. A	0.1225	0.2075	0.0990	0.3715	0.0670	0.3885	0.3100	0.1320
Thick. B	0.1235	0.2060	0.0995	0.3720	0.0740	0.3935	0.3210	0.1330
Thick. C	0.1210	0.2070	0.0995	0.3715	0.0770	0.3895	0.3035	0.1340
Thick. D	0.1215	0.2105	0.1000	0.3720	0.0570	0.3965	0.2925	0.1320
Thick. E	0.1215	0.2095	0.0990	0.3725	0.0570	0.3855	0.3035	0.1330
Avg. Thick.	0.1220	0.2081	0.0994	0.3719	0.0664	0.3907	0.3061	0.1328
Dross	0.0050	0.0241	0.0004	0.0059	0.0094	0.0247	0.0501	0.0158

Sample	169	170	171	172	173	174	175	176
Mat’l	0.0990	0.1840	0.0570	0.3660	0.2560	0.0720	0.2560	0.0720
Nozzle	40A	40A	FINE	60A	60A	FINE	FINE	FINE
Power	40	55	60	50	60	45	60	50
Speed	67	80	163	99	115	116	19	197
Thick. A	0.1485	0.2260	0.0675	0.4075	0.2830	0.0855	0.3860	0.0750
Thick. B	0.1495	0.2085	0.0620	0.4085	0.2805	0.0830	0.3710	0.0740
Thick. C	0.1530	0.2075	0.0625	0.4070	0.2795	0.0820	0.3825	0.0805
Thick. D	0.1485	0.2105	0.0615	0.4090	0.2770	0.0815	0.4115	0.0775
Thick. E	0.1470	0.1975	0.0630	0.4125	0.2725	0.0815	0.4055	0.0895
Avg. Thick.	0.1493	0.2100	0.0633	0.4089	0.2785	0.0827	0.3913	0.0793
Dross	0.0503	0.0260	0.0063	0.0429	0.0225	0.0107	0.1353	0.0073

Sample	177	178	179	180	181	182	183	184
Mat’l	0.0570	0.2560	0.3660	0.1170	0.1847	0.0990	0.1840	0.1170
Nozzle	40A	60A	60A	60A	40A	40A	40A	FINE
Power	45	55	55	40	40	60	45	50
Speed	201	53	32	105	82	132	99	69
Thick. A	0.0805	0.2800	0.4945	0.1730	0.2425	0.1445	0.2120	0.1185
Thick. B	0.0850	0.2835	0.4855	0.1880	0.2385	0.1405	0.2120	0.1175
Thick. C	0.0830	0.2780	0.4725	0.1745	0.2430	0.1380	0.2165	0.1180
Thick. D	0.0900	0.2790	0.4755	0.1760	0.2370	0.1455	0.2195	0.1185
Thick. E	0.0795	0.2800	0.4735	0.1745	0.2340	0.1385	0.2245	0.1185
Avg. Thick.	0.0836	0.2801	0.4803	0.1772	0.2390	0.1414	0.2169	0.1182
Dross	0.0266	0.0241	0.1143	0.0602	0.0543	0.0424	0.0329	0.0012

Sample	185	186	187	188	189	190	191	192
Mat’l	0.0990	0.0570	0.3660	0.2560	0.0990	0.1170	0.0720	0.0990
Nozzle	60A	40A	60A	60A	40A	40A	60A	40A
Power	50	40	60	50	60	40	55	60
Speed	92	115	60	49	67	86	305	103
Thick. A	0.1575	0.0975	0.4060	0.2760	0.1385	0.1680	0.0810	0.1315
Thick. B	0.1575	0.0975	0.4120	0.2825	0.1375	0.1640	0.0835	0.1395
Thick. C	0.1530	0.0990	0.3870	0.2805	0.1380	0.1765	0.0835	0.1420
Thick. D	0.1565	0.0985	0.4085	0.2755	0.1365	0.1675	0.0810	0.1155
Thick. E	0.1685	0.0955	0.3995	0.2785	0.1370	0.1740	0.0800	0.1190
Avg. Thick.	0.1586	0.0976	0.4026	0.2786	0.1375	0.1700	0.0818	0.1295
Dross	0.0596	0.0406	0.0366	0.0226	0.0385	0.053	0.0098	0.0305

Sample	193	194	195	196	197	198	199	200
Mat’l	0.2560	0.2560	0.0570	0.1840	0.0990	0.1170	0.1840	0.0720
Nozzle	FINE	Fine	60A	60A	40A	40A	60A	40A
Power	60	60	55	50	50	60	60	55
Speed	34	34	399	64	72	122	73	303
Thick. A	0.2935	0.2990	0.0690	0.2015	0.1270	0.1425	0.2015	0.0940
Thick. B	0.3005	0.2965	0.0705	0.1995	0.1165	0.1445	0.2045	0.0975
Thick. C	0.2880	0.2960	0.0695	0.2015	0.1165	0.1395	0.2000	0.0935
Thick. D	0.2850	0.2925	0.0705	0.2045	0.1155	0.1405	0.2085	0.1085
Thick. E	0.2995	0.2935	0.0690	0.2000	0.1150	0.1375	0.2015	0.0915
Avg. Thick.	0.2933	0.2955	0.0697	0.2014	0.1181	0.1409	0.2032	0.0970
Dross	0.0373	0.0395	0.0127	0.0174	0.0191	0.0239	0.0192	0.0250

Sample	201	202	203	204	205	206	207	208
Mat’l	0.3660	0.2560	0.0570	0.2560	0.1840	0.0990	0.3660	0.0570
Nozzle	60A	60A	40A	60A	60A	60A	60A	40A
Power	60	55	45	60	60	40	50	45
Speed	56	59	159	90	129	138	49	169
Thick. A	0.3865	0.2900	0.0965	0.3085	0.1885	0.1445	0.3895	0.1015
Thick. B	0.3860	0.2915	0.0965	0.3030	0.1895	0.1445	0.3875	0.0945
Thick. C	0.3845	0.2860	0.0945	0.3085	0.1910	0.1480	0.3885	0.0965
Thick. D	0.3870	0.2840	0.0935	0.3080	0.1890	0.1465	0.3875	0.0925
Thick. E	0.3835	0.2965	0.0945	0.3140	0.1915	0.1510	0.3900	0.0965
Avg. Thick.	0.3855	0.2896	0.0951	0.3084	0.1899	0.1469	0.3886	0.0963
Dross	0.0195	0.0336	0.0381	0.0524	0.0059	0.0479	0.0226	0.0393

Sample	209	210
Mat’l	0.0720	0.1170
Nozzle	60A	60A
Power	45	40
Speed	223	116
Thick. A	0.0850	0.1690
Thick. B	0.0850	0.1665
Thick. C	0.0840	0.1710
Thick. D	0.0835	0.1695
Thick. E	0.0845	0.1640
Avg. Thick.	0.0844	0.1680
Dross	0.0124	0.0510

APPENDIX C: REGRESSION ANALYSIS

The data was examined for normality, linearity, and homoscedasticity, and these results are shown in Appendix C. Each data set was examined and found to fit all of the requirements for the use of multiple regression analysis. The result of each analysis was used to determine the equation that best describes the relationship between the independent and the formation of dross.

Analysis of 16-Gauge Steel Statistics

The 16-gauge data was analyzed for normality by comparing the mean, median, and skewness for each variable. In each case the mean and median values are essentially equal. Values of skewness are used to determine a normal distribution based on the following guidelines:

- Skewness between -.5 and .5 indicates a distribution that is approximately symmetric.
- Skewness between -1 and +1 and outside the above range indicates that the distribution is moderately skewed.
- Skewness less than -1 or greater than +1 indicates that the distribution is skewed.

For 16-gauge steel the skewness value indicated a normal symmetric distribution. The values of mean, median, and skewness are shown in Table C1.

Table C1

Statistics for 16-Gauge Steel: Statistics

		Dross (inches)	Nozzle type	Power (amps)	Speed (in/min)
N	Valid	28	28	28	28
	Missing	0	0	0	0
Mean		.018221	2.04	49.64	269.11
Median		.012050	2.00	52.50	199.50
Skewness		.623	-.066	-.404	1.065
Std. Error of Skewness		.441	.441	.441	.441
Kurtosis		-1.103	-1.374	-1.145	.180
Std. Error of Kurtosis		.858	.858	.858	.858

Scatterplots were examined to determine the existence of a linear relationship between each independent variable and the dependent variable, dross. The resulting diagrams show that there may be a linear relationship between each of the variables as seen in the scatterplots in Figures C1–C3.

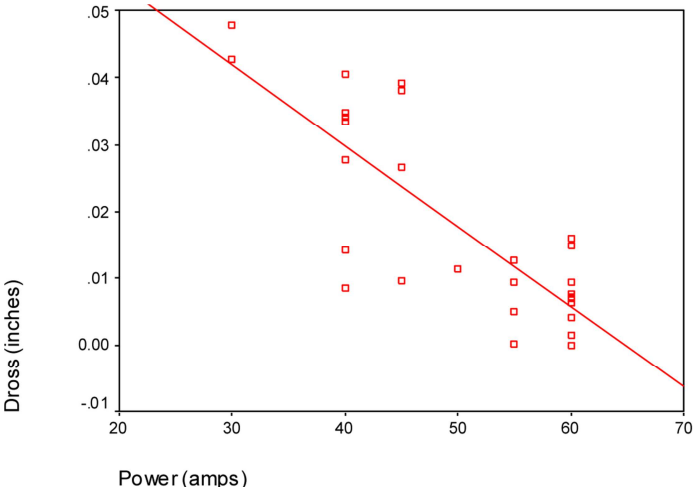

Figure C1. Dross vs. power for 16-gauge steel.

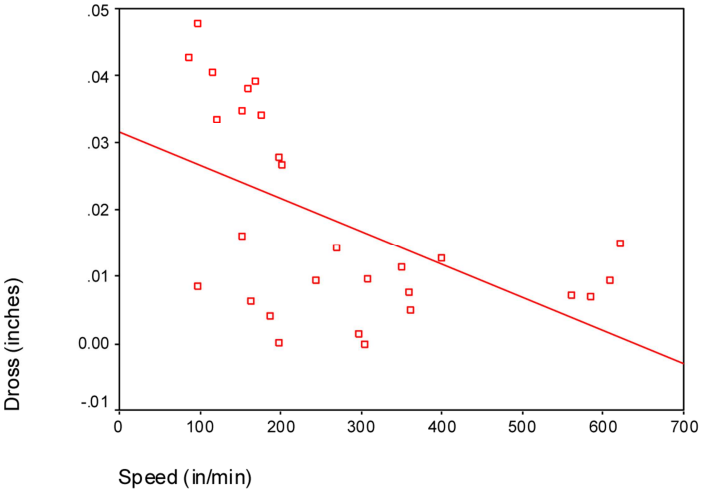

Figure C2. Dross vs. speed for 16-gauge steel.

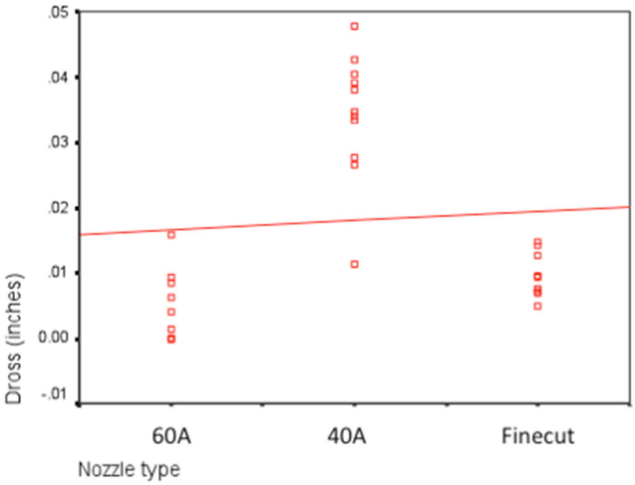

Figure C3. Dross vs. nozzle type for 16-gauge steel.

The P–P plots shown in Figures C4–C6 were examined as indicators of normality, random prediction error, and homoscedasticity. The relationships are all approximately linear which indicates normality and random prediction error, and equal variation about the line on the chart indicates homoscedasticity.

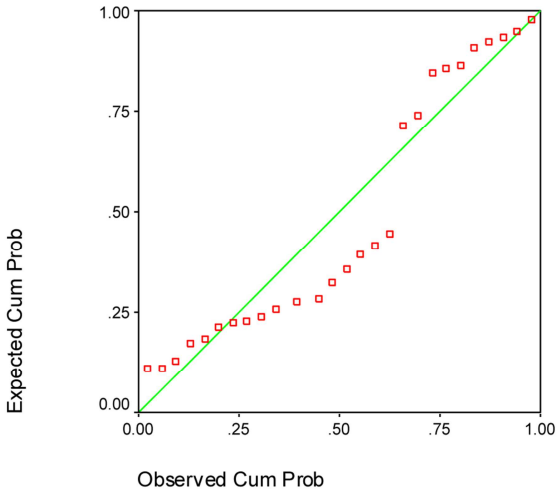

Figure C4. Normal P–P plot of dross for 16-gauge steel.

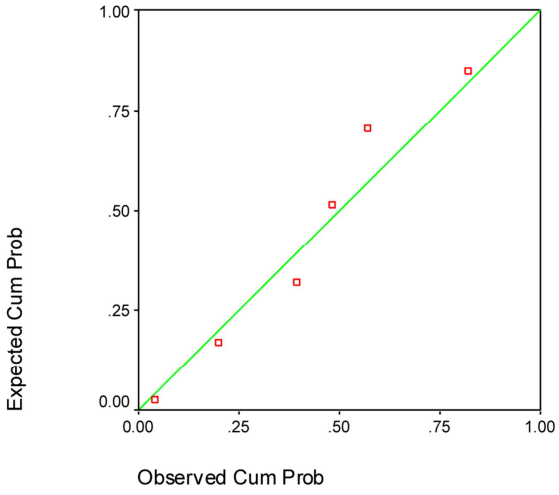

Figure C5. Normal P–P plot of power for 16-gauge steel.

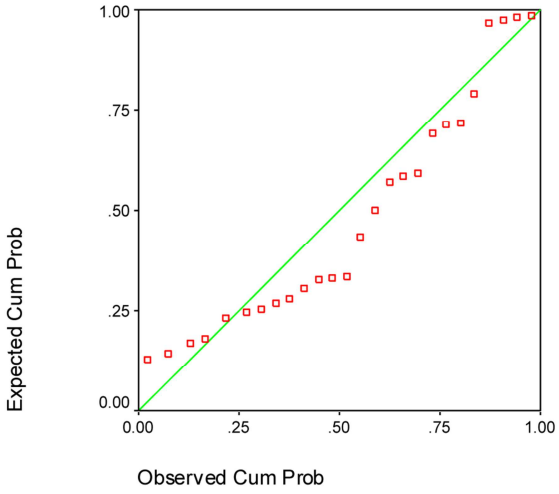

Figure C6. Normal P–P plot of speed for 16-gauge steel.

The VIF values were examined to determine if there is collinearity between the variables. As shown in Table C2, the VIF value of 2.311 for Model 2 indicates no collinearity.

Table C2

Coefficients and VIF Values for 16-Gauge Steel

Model		Unstandardized Coefficients		Standardized Coefficients	t	Sig.	Collinearity Statistics	
		B	Std. Error	Beta			Tolerance	VIF
1	(Constant)	7.859E-03	.002		4.509	.000		
	A40	2.638E-02	.003	.881	9.485	.000	1.000	1.000
2	(Constant)	3.593E-02	.011		3.377	.002		
	A40	1.873E-02	.004	.626	4.926	.000	.433	2.311
	Power (amps)	-5.05E-04	.000	-.339	-2.668	.013	.433	2.311

a. Dependent Variable: Dross (inches)

As previously discussed, the analysis of the initial results has shown that multiple regression is an appropriate test for this data. The coefficients that represent the relationship between the independent and dependent variables for 16-gauge steel are also shown in Table C2.

The ANOVA shown in Table C3 indicates several important values:

- Comparison of the regression value to the residual value: A high ratio of regression to residual indicates that the model accounts for most of the variation in the dependent variable (.005/.001) = 5. A ratio >1 is acceptable.
- Examination of the significance value: If the significance value of the *F* statistic is smaller than 0.05, then the independent variables explain the variation in the dependent variable. (For (constant), nozzle A40, and power, the sig. value = .000.)

Table C3

ANOVA Table for 16-Gauge Steel[c]

Model		Sum of Squares	df	Mean Square	F	Sig.
1	Regression	.005	1	.005	89.972	.000[a]
	Residual	.001	26	.000		
	Total	.006	27			
2	Regression	.005	2	.002	59.130	.000[b]
	Residual	.001	25	.000		
	Total	.006	27			

a. Predictors: (Constant), A40

b. Predictors: (Constant), A40, Power (amps)

c. Dependent Variable: Dross (inches)

The Durbin–Watson value was used to test for the autocorrelatation between residuals. One of the assumptions of regression analysis is that the residuals for consecutive observations are uncorrelated. A Durbin–Watson statistic of 2 indicates no autocorrelation. As indicated in Table C4, the calculated value of 1.974 shows no autocorrelation between power, nozzle type, and dross.

Table C4

Durbin–Watson Value for 16-Gauge Steel

Model	R	R Square	Adjusted R Square	Std. Error of the Estimate	Durbin-Watson
1	.881[a]	.776	.767	.0071866	
2	.909[b]	.825	.812	.0064660	1.974

a. Predictors: (Constant), A40

b. Predictors: (Constant), A40, Power (amps)

c. Dependent Variable: Dross (inches)

Analysis of 14-Gauge Steel Statistics

The 14-gauge data was analyzed for normality by comparing the mean, median, and skewness for each variable. For 14-gauge steel the mean and median values are essentially equal

and the skewness values indicate a normal symmetric distribution. The values of mean, median, and skewness are shown in Table C5.

Table C5

Statistics for 14-Gauge Steel

		Dross (inches)	Nozzle type	Power (amps)	Speed (in/min)
N	Valid	27	27	27	27
	Missing	0	0	0	0
Mean		.012326	1.85	50.56	202.04
Median		.010000	2.00	50.00	188.00
Skewness		.892	.267	.001	.328
Std. Error of Skewness		.448	.448	.448	.448
Kurtosis		-.306	-1.214	-1.120	-.959
Std. Error of Kurtosis		.872	.872	.872	.872

Scatterplots were examined to determine the existence of a linear relationship between each independent variable and the dependent variable, dross. The resulting diagrams show that there may be a linear relationship between each of the variables as seen in the scatterplots in Figures C7–C9.

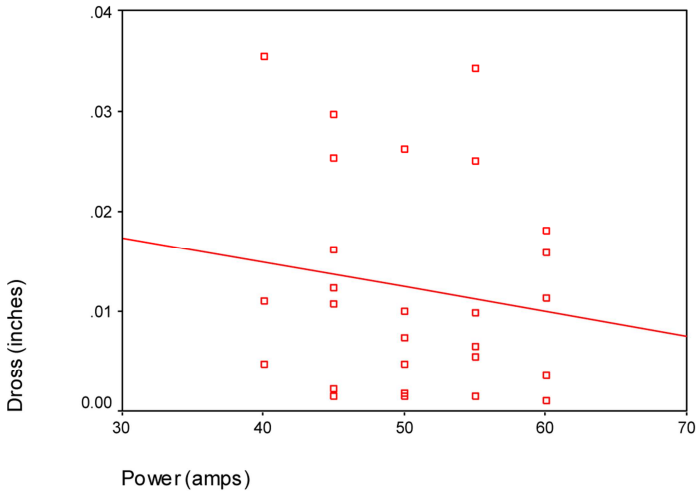

Figure C7. Dross vs. power for 14-gauge steel.

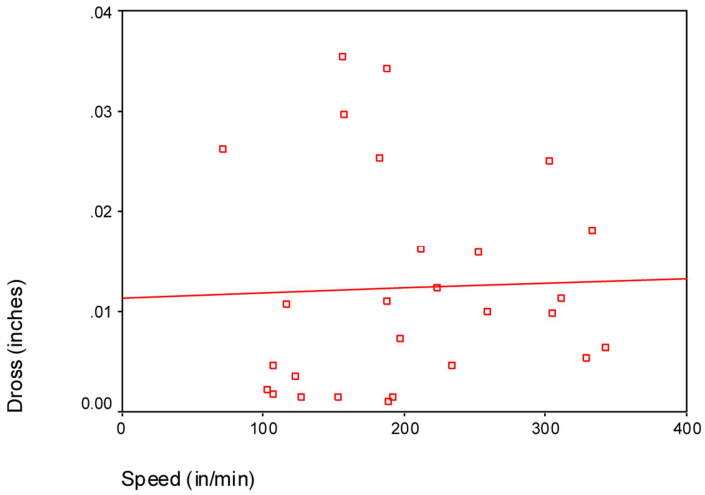

Figure C8. Dross vs. speed for 14-gauge steel.

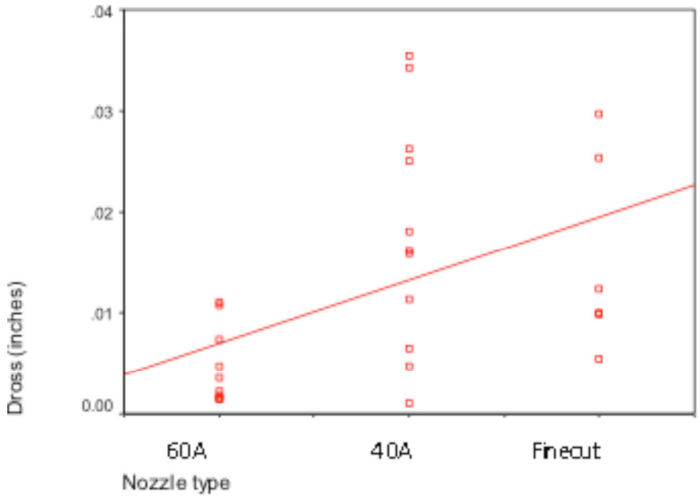

Figure C9. Dross vs. nozzle type for 14-gauge steel.

The P–P plots shown in Figures C10–C13 were examined as indicators of normality, random prediction error, and homoscedasticity. The relationships are all approximately linear which indicates normality and random prediction error, and equal variation about the line on the chart indicates homoscedasticity.

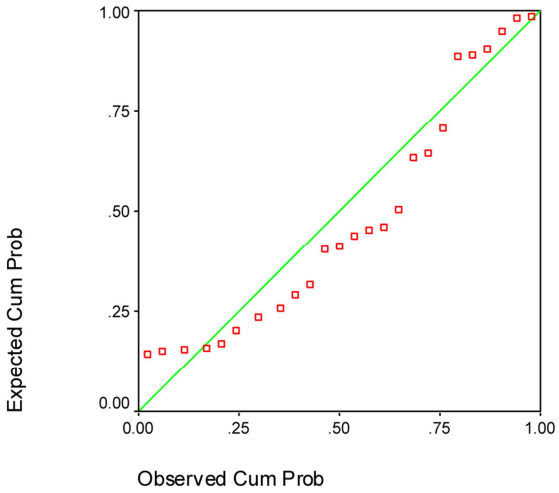

Figure C10. Normal P–P plot of dross for 14-gauge steel.

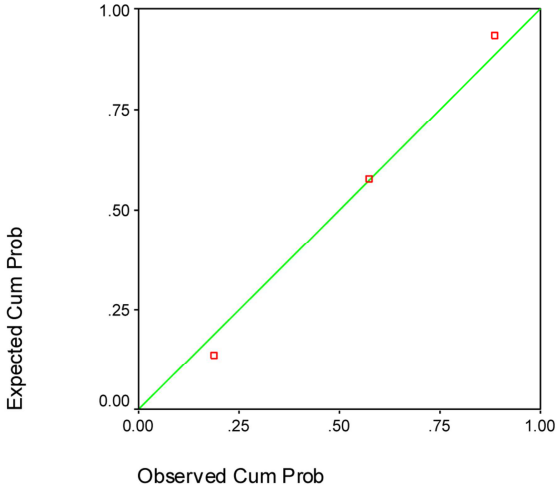

Figure C11. Normal P–P plot of nozzle type for 14-gauge steel.

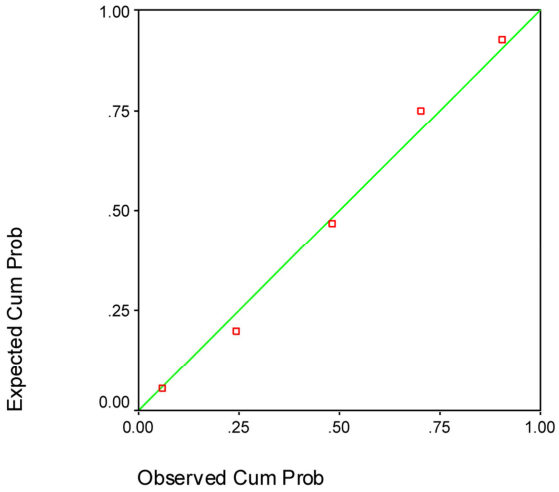

Figure C12. Normal P–P plot of power for 14-gauge steel.

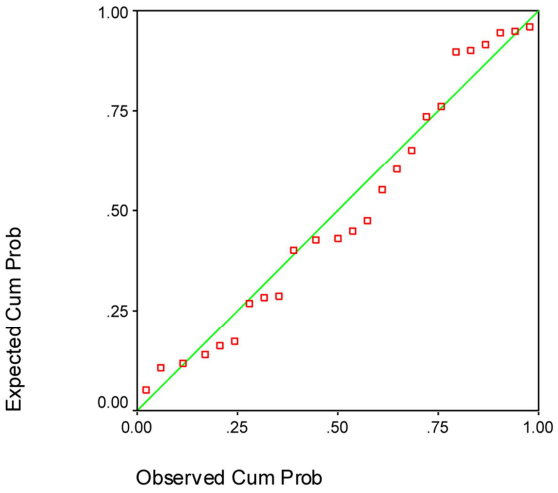

Figure C13. Normal P–P plot of speed for 14-gauge steel.

The VIF values were examined to determine if there is collinearity between the variables. As shown in Table C6, the VIF value of 1.554 for Model 2 indicates no collinearity.

Table C6

Coefficients and VIF Values for 14-Gauge Steel

Coefficients[a]

Model		Unstandardized Coefficients		Standardized Coefficients	t	Sig.	Collinearity Statistics	
		B	Std. Error	Beta			Tolerance	VIF
1	(Constant)	1.689E-02	.002		7.885	.000		
	FINECUT	-1.23E-02	.004	-.574	-3.503	.002	1.000	1.000
2	(Constant)	3.194E-02	.006		5.203	.000		
	FINECUT	-1.84E-02	.004	-.858	-4.654	.000	.643	1.554
	Speed (in/min)	-6.33E-05	.000	-.476	-2.582	.016	.643	1.554

a. Dependent Variable: Dross (inches)

As previously discussed, the analysis of the initial results has shown that multiple regression is an appropriate test for this data. The coefficients that represent the relationship between the independent and dependent variables for 14-gauge steel are also shown in Table C6. The ANOVA shown in Table C7 indicates several important values:

- Comparison of the regression value to the residual value: A high ratio of regression to residual indicates that the model accounts for most of the variation in the dependent variable (.001/.002) = .5. A ratio ~1 or greater is acceptable.
- Examination of the significance value: If the significance value of the *F* statistic is smaller than 0.05, then the independent variables explain the variation in the dependent variable. (For (constant), nozzle finecut, and speed, the sig. = .000)

Table C7

ANOVA Table for 14-Gauge Steel

ANOVA[c]

Model		Sum of Squares	df	Mean Square	F	Sig.
1	Regression	.001	1	.001	12.273	.002[a]
	Residual	.002	25	.000		
	Total	.003	26			
2	Regression	.001	2	.001	10.862	.000[b]
	Residual	.002	24	.000		
	Total	.003	26			

a. Predictors: (Constant), FINECUT

b. Predictors: (Constant), FINECUT, Speed (in/min)

c. Dependent Variable: Dross (inches)

The Durbin–Watson value is used as a test of the autocorrelated residuals. One of the assumptions of regression analysis is that the residuals for consecutive observations are uncorrelated. As indicated in Table C8, the calculated value of 2.145 shows minimal autocorrelation between speed, finecut nozzle, and dross.

Table C8

Durbin–Watson Value for 14-Gauge Steel

Model Summary[c]

Model	R	R Square	Adjusted R Square	Std. Error of the Estimate	Durbin-Watson
1	.574[a]	.329	.302	.0088342	
2	.689[b]	.475	.431	.0079761	2.145

a. Predictors: (Constant), FINECUT

b. Predictors: (Constant), FINECUT, Speed (in/min)

c. Dependent Variable: Dross (inches)

Analysis of 12-Gauge Steel Statistics

The 12-gauge data was analyzed for normality by comparing the mean, median, and skewness. In each case the mean and median values are essentially equal and the skewness value indicates a normal symmetric distribution. The values of mean, median, and skewness are shown in Table C9.

Table C9

Statistics for 12-Gauge Steel

Statistics

		Dross (inches)	Nozzle type	Power (amps)	Speed (in/min)
N	Valid	34	34	34	34
	Missing	0	0	0	0
Mean		.023015	1.68	51.03	100.79
Median		.018100	1.00	52.50	93.00
Skewness		.549	.674	-.318	.452
Std. Error of Skewness		.403	.403	.403	.403
Kurtosis		-.723	-1.111	-1.278	-.574
Std. Error of Kurtosis		.788	.788	.788	.788

Scatterplots were examined to determine the existence of a linear relationship between each independent variable and the dependent variable, dross. The resulting diagrams show that there may be a linear relationship between each of the variables as seen in the scatterplots in Figures C14–C16.

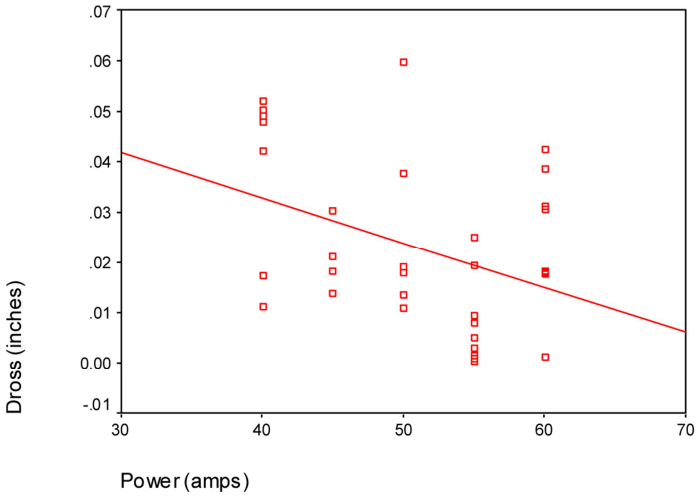

Figure C14. Dross vs. power for 12-gauge steel.

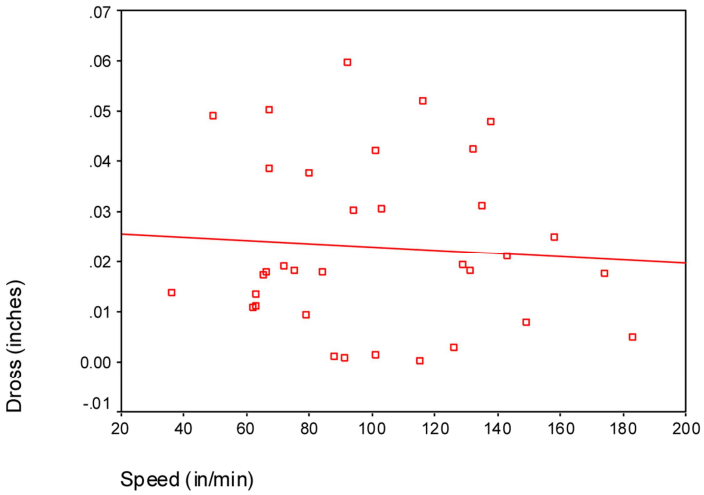

Figure C15. Dross vs. speed for 12-gauge steel.

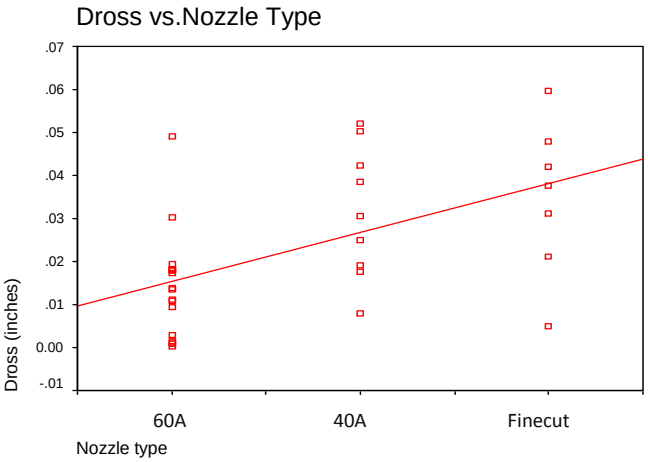

Figure C16. Dross vs. nozzle type for 12-gauge steel.

The P–P plots shown in Figures C17–C20 were examined as indicators of normality, random prediction error, and homoscedasticity. The relationships are all approximately linear which indicates normality and random prediction error, and equal variation about the line on the chart indicates homoscedasticity,

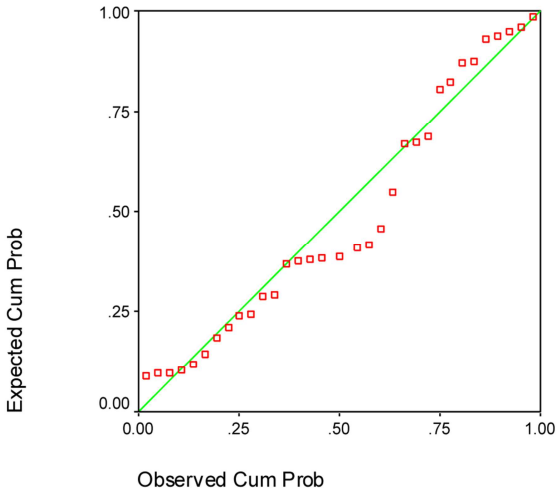

Figure C17. Normal P–P plot of dross for 12-gauge steel.

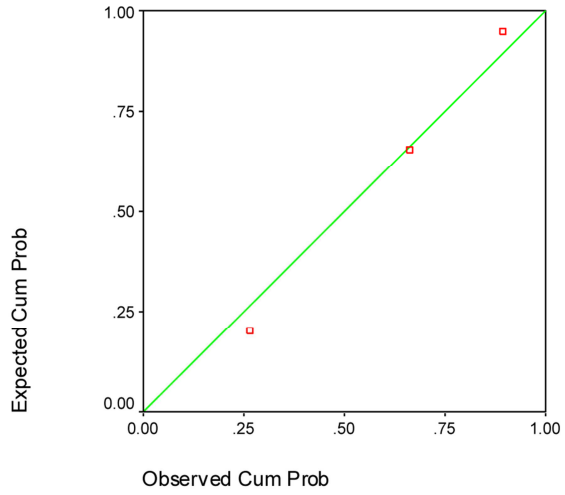

Figure C18. Normal P–P plot of nozzle type for 12-gauge steel.

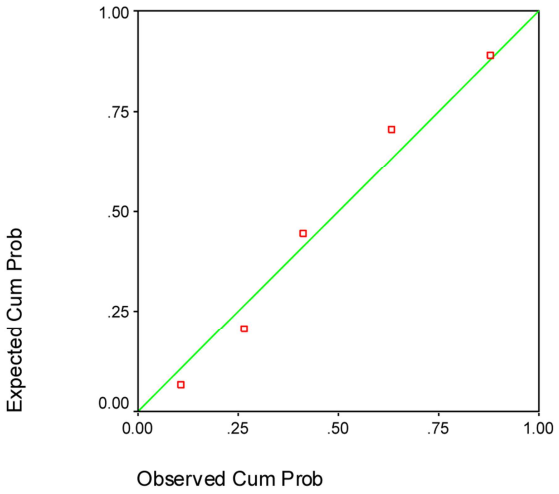

Figure C19. Normal P–P plot of power for 12-gauge steel.

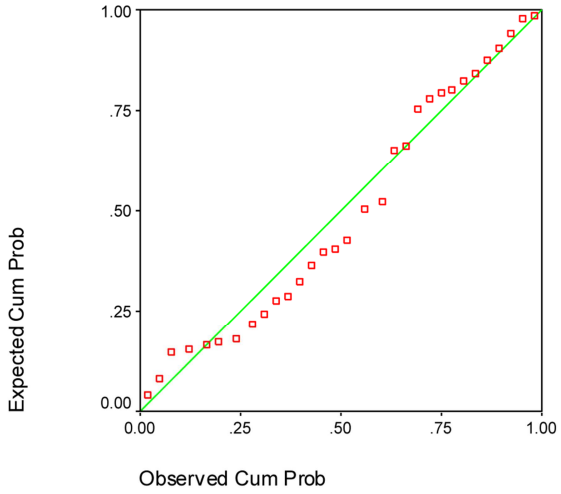

Figure C20. Normal P–P plot of speed for 12-gauge steel.

The VIF values were examined to determine if there is collinearity between the variables. As shown in Table C10, the VIF value of 1.185 for Model 2 indicates no collinearity.

Table C10

Coefficients and VIF Values for 12-Gauge Steel

Coefficients[a]

Model		Unstandardized Coefficients		Standardized Coefficients			Collinearity Statistics	
		B	Std. Error	Beta	t	Sig.	Tolerance	VIF
1	(Constant)	3.299E-02	.004		9.409	.000		
	FINECUT	-1.88E-02	.005	-.569	-3.911	.000	1.000	1.000
2	(Constant)	5.538E-02	.007		8.187	.000		
	FINECUT	-2.53E-02	.004	-.764	-5.696	.000	.844	1.185
	SPEEDPOW	-3.61E-06	.000	-.494	-3.684	.001	.844	1.185

a. Dependent Variable: Dross (inches)

As previously discussed, the analysis of the initial results has shown that multiple regression is an appropriate test for this data. The coefficients that represent the relationship between the independent and dependent variables for 12-gauge steel are also shown in Table C10.

The ANOVA shown in Table C11 indicates several important values:

- Comparison of the regression value to the residual value: A high ratio of regression to residual indicates that the model accounts for most of the variation in the dependent variable (.005/.004) = 1.25. A ratio >1 is acceptable.
- Examination of the significance value: If the significance value of the *F* statistic is smaller than 0.05, then the independent variables explain the variation in the dependent variable. (For (constant), finecut nozzle, and speed x power, the sig. value = .000.)

Table C11

ANOVA Table for 12-Gauge Steel

ANOVA[c]

Model		Sum of Squares	df	Mean Square	F	Sig.
1	Regression	.003	1	.003	15.296	.000[a]
	Residual	.006	32	.000		
	Total	.009	33			
2	Regression	.005	2	.002	17.437	.000[b]
	Residual	.004	31	.000		
	Total	.009	33			

a. Predictors: (Constant), FINECUT

b. Predictors: (Constant), FINECUT, SPEEDPOW

c. Dependent Variable: Dross (inches)

The Durbin–Watson value was used to test for the autocorrelation between residuals. One of the assumptions of regression analysis is that the residuals for consecutive observations are uncorrelated. As indicated in Table C12, the calculated value of 1.743 shows minimal autocorrelation between finecut nozzle, speed x power, and dross.

Table C12

Durbin–Watson Test Value for 12-Gauge Steel

Model Summary[c]

Model	R	R Square	Adjusted R Square	Std. Error of the Estimate	Durbin-Watson
1	.569[a]	.323	.302	.0140269	
2	.728[b]	.529	.499	.0118854	1.743

a. Predictors: (Constant), FINECUT

b. Predictors: (Constant), FINECUT, SPEEDPOW

c. Dependent Variable: Dross (inches)

Analysis of 1/8" Steel Statistics

The 1/8" data was analyzed for normality by comparing the mean, median, and skewness for each variable. In each case the mean and median values are essentially equal, and the skewness values indicate a normal symmetric distribution. The values of mean, median, and skewness are shown in Table C13.

Table C13

Statistics for 1/8" Steel

Statistics

		Dross (inches)	Nozzle type	Power (amps)	Speed (in/min)
N	Valid	28	28	28	28
	Missing	0	0	0	0
Mean		.023661	1.96	50.89	130.89
Median		.020500	2.00	52.50	121.00
Skewness		.475	.066	-.253	1.241
Std. Error of Skewness		.441	.441	.441	.441
Kurtosis		-1.196	-1.374	-1.612	.771
Std. Error of Kurtosis		.858	.858	.858	.858

Scatterplots were examined to determine the existence of a linear relationship between each independent variable and the dependent variable, dross. The resulting diagrams show that there may be a linear relationship between each of the variables as seen in the scatterplots in Figures C21–C23.

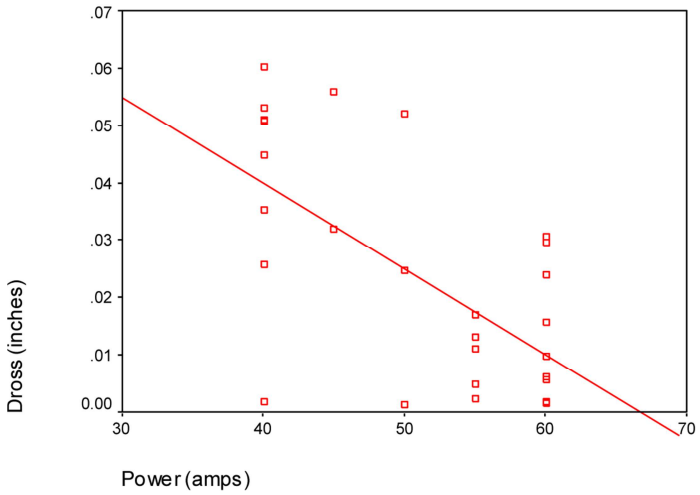

Figure C21. Dross vs. power for 1/8" steel.

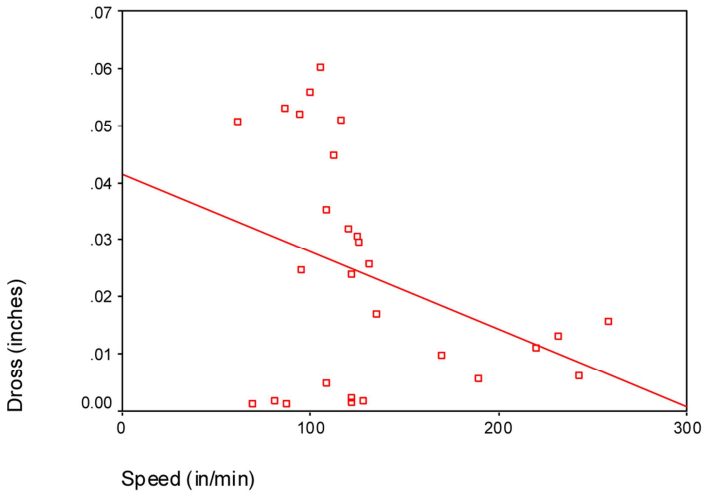

Figure C22. Dross vs. speed for 1/8" steel.

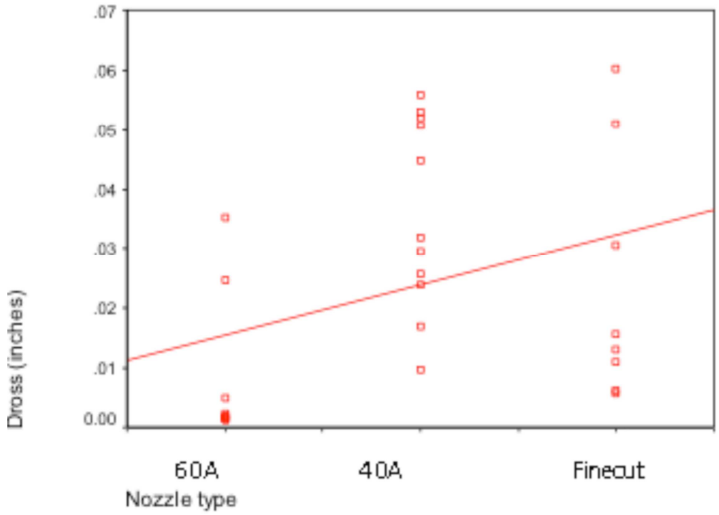

Figure C23. Dross vs. nozzle type for 1/8" steel.

The P–P plots shown in Figures C24–C27 were examined as indicators of normality, random prediction error, and homoscedasticity. The relationships are all approximately linear which indicates normality and random prediction error, and equal variation about the line on the chart indicates homoscedasticity.

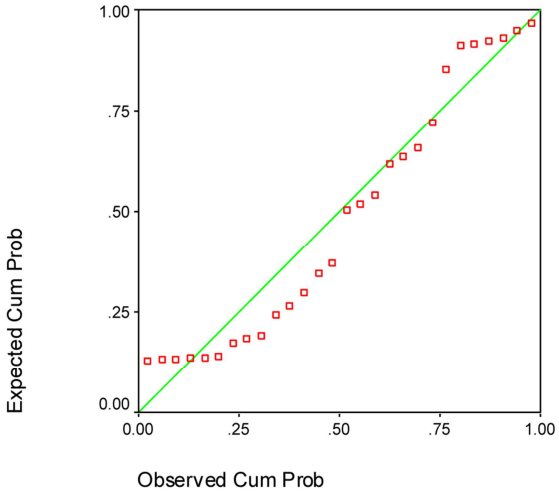

Figure C24. Normal P–P plot of dross for 1/8" steel.

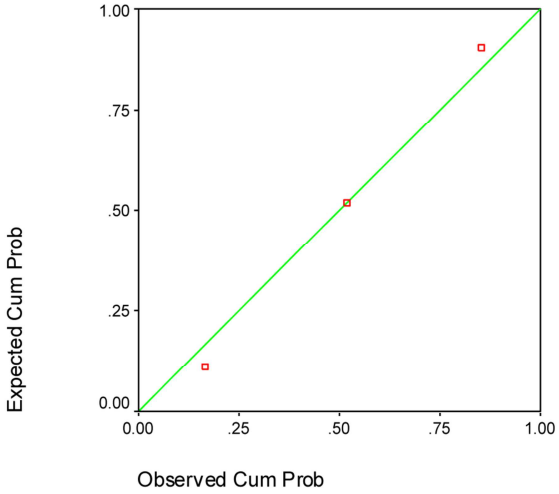

Figure C25. Normal P–P plot of nozzle type for 1/8" steel.

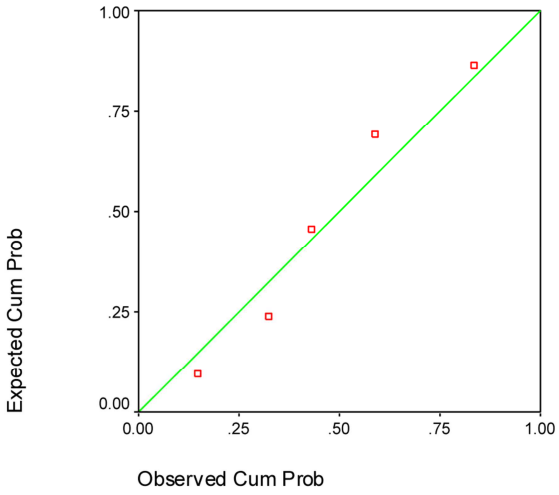

Figure C26. Normal P–P plot of power for 1/8" steel.

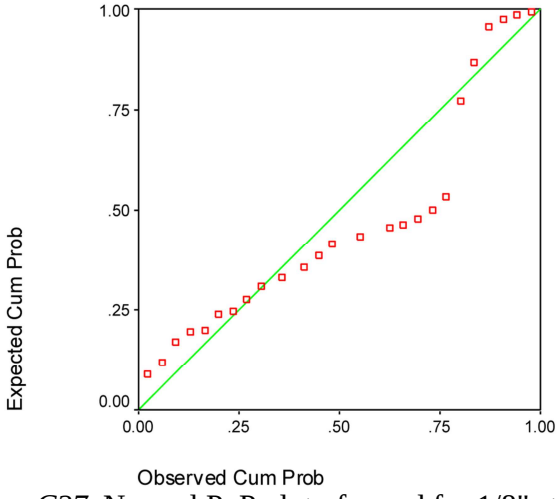

Figure C27. Normal P–P plot of speed for 1/8" steel.

The VIF values were examined to determine if there is collinearity between the variables. As shown in Table C14, the VIF values of 1.613, 1.298, and 1.895 for Model 3 indicate no collinearity.

As previously discussed, the analysis of the initial results has shown that multiple regression is an appropriate test for this data. The coefficients that represent the relationship between the independent and dependent variables for 1/8" steel are also shown in Table C14.

Table C14

Coefficients and VIF Values for 1/8" Steel

Coefficients[a]

Model		Unstandardized Coefficients		Standardized Coefficients	t	Sig.	Collinearity Statistics	
		B	Std. Error	Beta			Tolerance	VIF
1	(Constant)	9.957E-02	.019		5.229	.000		
	Power (amps)	-1.49E-03	.000	-.621	-4.037	.000	1.000	1.000
2	(Constant)	.105	.014		7.327	.000		
	Power (amps)	-1.47E-03	.000	-.611	-5.276	.000	1.000	1.000
	FINECUT	-2.21E-02	.005	-.529	-4.566	.000	1.000	1.000
3	(Constant)	9.972E-02	.013		7.792	.000		
	Power (amps)	-9.13E-04	.000	-.380	-2.942	.007	.620	1.613
	FINECUT	-2.89E-02	.005	-.690	-5.956	.000	.771	1.298
	Speed (in/min)	-1.55E-04	.000	-.406	-2.903	.008	.528	1.895

a. Dependent Variable: Dross (inches)

The ANOVA shown in Table C15 can be used determine several important values:

- Comparison of the regression value to the residual value: A high ratio of regression to residual indicates that the model accounts for most of the variation in the dependent variable (.008/.003) = 2.67, A ratio >1 is acceptable.
- Examination of the significance value: If the significance value of the *F* statistic is smaller than 0.05, then the independent variables explain the variation in the dependent variable. (For (constant), finecut nozzle, power, and speed, the sig. value = .000.)

Table C15

ANOVA Table for 1/8" Steel

ANOVA[d]

Model		Sum of Squares	df	Mean Square	F	Sig.
1	Regression	.004	1	.004	16.298	.000[a]
	Residual	.007	26	.000		
	Total	.011	27			
2	Regression	.007	2	.004	24.795	.000[b]
	Residual	.004	25	.000		
	Total	.011	27			
3	Regression	.008	3	.003	24.251	.000[c]
	Residual	.003	24	.000		
	Total	.011	27			

a. Predictors: (Constant), Power (amps)

b. Predictors: (Constant), Power (amps), FINECUT

c. Predictors: (Constant), Power (amps), FINECUT, Speed (in/min)

d. Dependent Variable: Dross (inches)

The Durbin–Watson value was used to test for the autocorrelation between residuals. One of the assumptions of regression analysis is that the residuals for consecutive observations are uncorrelated. As indicated in Table C16, the calculated value of 2.399 shows minimal autocorrelation between finecut nozzle, speed, power, and dross.

Table C16

Durbin–Watson Values for 1/8" Steel

Model Summary[d]

Model	R	R Square	Adjusted R Square	Std. Error of the Estimate	Durbin-Watson
1	.621[a]	.385	.362	.0159036	
2	.815[b]	.665	.638	.0119761	
3	.867[c]	.752	.721	.0105153	2.399

a. Predictors: (Constant), Power (amps)

b. Predictors: (Constant), Power (amps), FINECUT

c. Predictors: (Constant), Power (amps), FINECUT, Speed (in/min)

d. Dependent Variable: Dross (inches)

Analysis of 3/16" Steel Statistics

The 3/16" data was analyzed for normality by comparing the mean, median, and skewness for each variable. In each case the mean and median values are essentially equal, and the skewness values indicate a normal symmetric distribution. The values of mean, median, and skewness are shown in Table C17.

Table C17

Statistics for 3/16" Steel

Statistics

		Dross (inches)	Nozzle type	Power (amps)	Speed (in/min)
N	Valid	29	29	29	29
	Missing	0	0	0	0
Mean		.032355	2.31	52.24	74.93
Median		.024100	3.00	55.00	78.00
Skewness		1.658	-.645	-.702	.026
Std. Error of Skewness		.434	.434	.434	.434
Kurtosis		2.653	-1.136	-.028	-.615
Std. Error of Kurtosis		.845	.845	.845	.845

Scatterplots were examined to determine the existence of a linear relationship between each independent variable and the dependent variable, dross. The resulting diagrams show that there may be a linear relationship between each of the variables as seen in the scatterplots in Figures C28–C30.

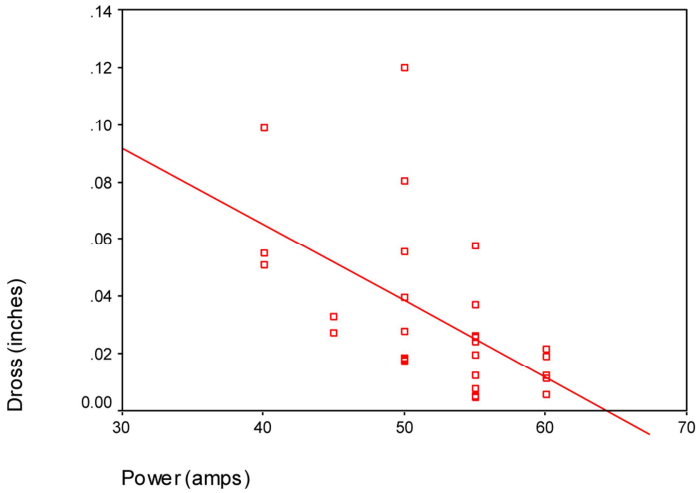

Figure C28. Dross vs. power for 3/16" steel.

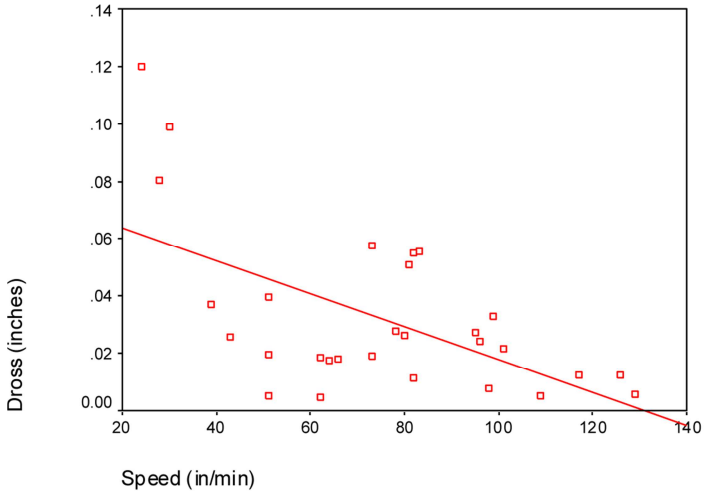

Figure C29. Dross vs. speed for 3/16" steel.

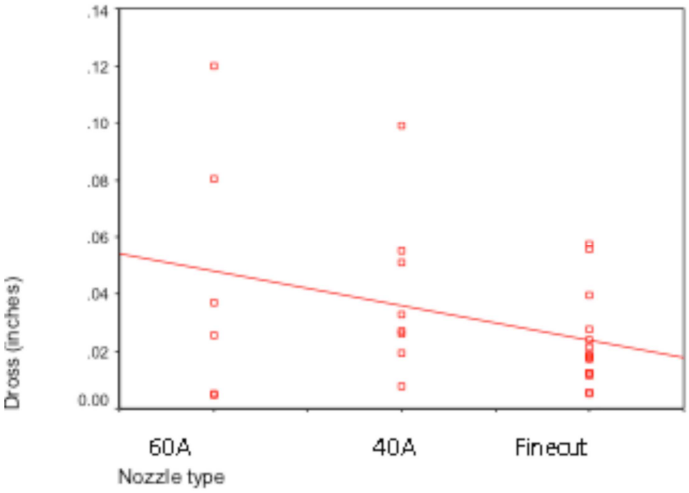

Figure C30. Dross vs. nozzle type for 3/16" steel.

The P–P plots shown in Figures C31–C34 were examined as indicators of normality, random prediction error, and homoscedasticity. The relationships are all approximately linear which indicates normality and random prediction error, and equal variation about the line on the chart indicates homoscedasticity.

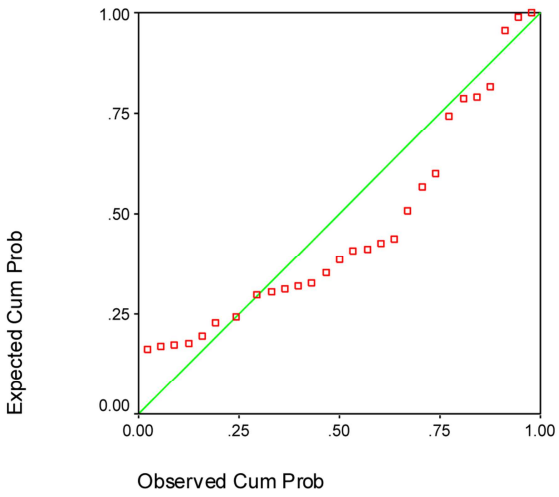

Figure C31. Normal P–P plot of dross for 3/16" steel.

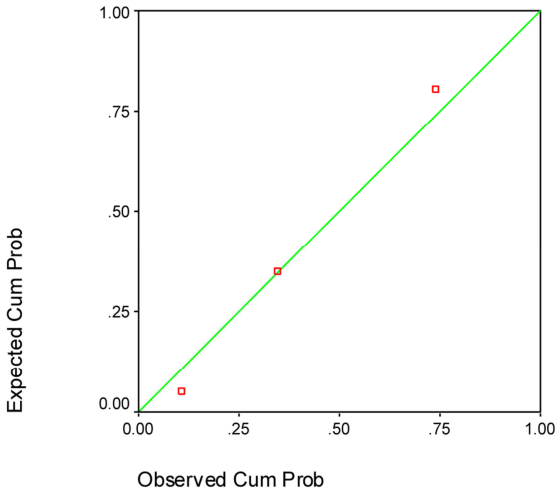

Figure C32. Normal P–P plot of dross for 3/16" steel.

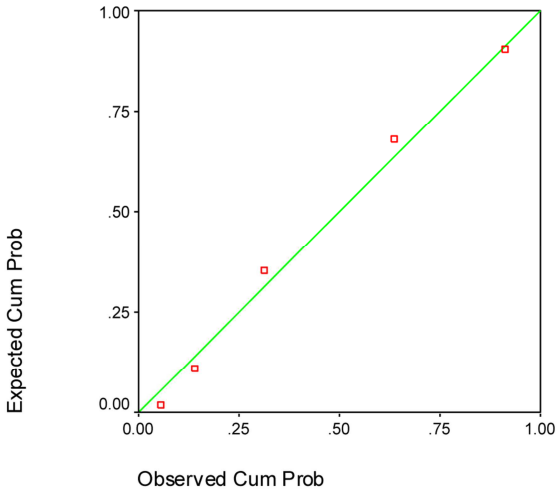

Figure C33. Normal P–P plot of power for 3/16" steel.

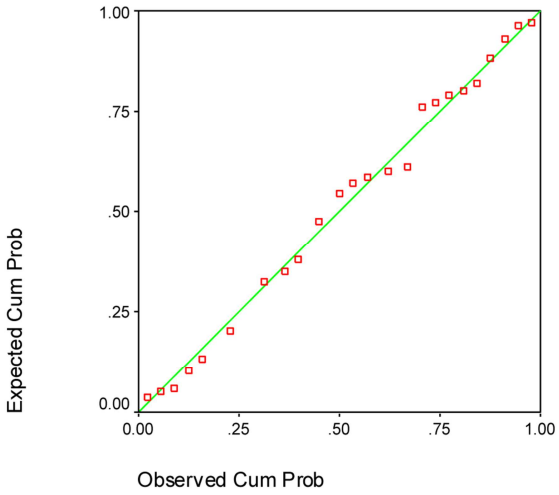

Figure C34. Normal P–P plot of speed for 3/16" steel.

The VIF values were examined to determine if there is collinearity between the variables. As shown in Table C18, the VIF value of 1.095 indicates no collinearity.

Table C18

Coefficients and VIF Values for 3/16" Steel

Coefficients[a]

Model		Unstandardized Coefficients		Standardized Coefficients	t	Sig.	Collinearity Statistics	
		B	Std. Error	Beta			Tolerance	VIF
1	(Constant)	7.560E-02	.013		6.039	.000		
	Speed (in/min)	-5.77E-04	.000	-.579	-3.688	.001	1.000	1.000
2	(Constant)	.172	.035		4.919	.000		
	Speed (in/min)	-4.53E-04	.000	-.454	-3.125	.004	.913	1.095
	Power (amps)	-2.03E-03	.001	-.423	-2.912	.007	.913	1.095

a. Dependent Variable: Dross (inches)

As previously discussed, the analysis of the initial results has shown that multiple regression is an appropriate test for this data. The coefficients that represent the relationship between the independent and dependent variables for 3/16" steel are also shown in Table C18.

The ANOVA shown in Table C19 indicates several important values:

- Comparison of the regression value to the residual value: A high ratio of regression to residual indicates that the model accounts for most of the variation in the dependent variable (.011/.011) = 1.0. A ratio ~1 or greater is acceptable.
- Examination of the significance value: If the significance value of the *F* statistic is smaller than 0.05, then the independent variables explain the variation in the dependent variable. (For (constant), speed, and power, the sig. value = .000.)

Table C19

ANOVA Table for 3/16" Steel

ANOVA[c]

Model		Sum of Squares	df	Mean Square	F	Sig.
1	Regression	.008	1	.008	13.598	.001[a]
	Residual	.015	27	.001		
	Total	.023	28			
2	Regression	.011	2	.006	12.921	.000[b]
	Residual	.011	26	.000		
	Total	.023	28			

a. Predictors: (Constant), Speed (in/min)

b. Predictors: (Constant), Speed (in/min), Power (amps)

c. Dependent Variable: Dross (inches)

The Durbin–Watson value was used to test for the autocorrelation between residuals. One of the assumptions of regression analysis is that the residuals for consecutive observations are uncorrelated. As indicated in Table C20, the calculated value of 1.834 shows minimal autocorrelation between speed, power, and dross.

Table C20

Durbin–Watson Value for 3/16" Steel

Model Summary[c]

Model	R	R Square	Adjusted R Square	Std. Error of the Estimate	Durbin-Watson
1	.579[a]	.335	.310	.0235895	
2	.706[b]	.498	.460	.0208752	1.834

a. Predictors: (Constant), Speed (in/min)

b. Predictors: (Constant), Speed (in/min), Power (amps)

c. Dependent Variable: Dross (inches)

Analysis of 1/4" Steel Statistics

The 1/4" data was analyzed for normality by comparing the mean, median, and skewness for each variable. In each case the mean and median values are essentially equal, and the skewness values indicate a normal symmetric distribution. The values of mean, median, and skewness are shown in Table C21.

Table C21

Statistics for 1/4" Steel

Statistics

		Dross (inches)	Nozzle type	Power (amps)	Speed (in/min)
N	Valid	33	33	33	33
	Missing	0	0	0	0
Mean		.070779	2.09	56.52	44.85
Median		.050100	3.00	55.00	38.00
Skewness		.860	-.191	-.595	.846
Std. Error of Skewness		.409	.409	.409	.409
Kurtosis		-.645	-2.094	-1.033	.543
Std. Error of Kurtosis		.798	.798	.798	.798

Scatterplots were examined to determine the existence of a linear relationship between each independent variable and the dependent variable, dross. The resulting diagrams show that there may be a linear relationship between each of the variables as seen in the scatterplots in Figures C35–C37.

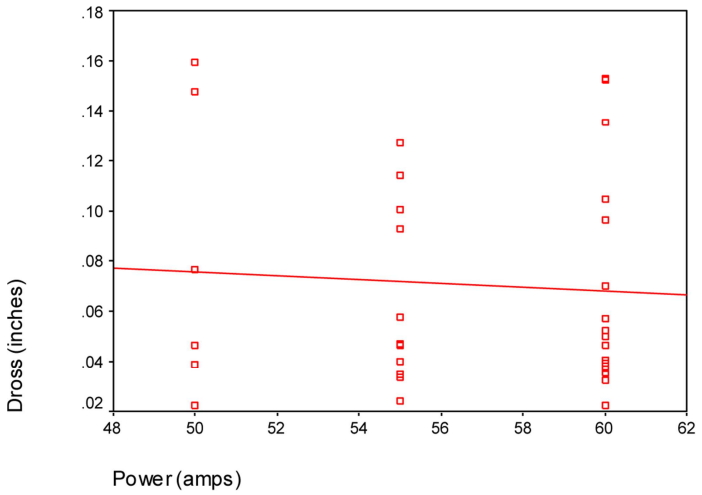

Figure C35. Dross vs. power for 1/4" steel.

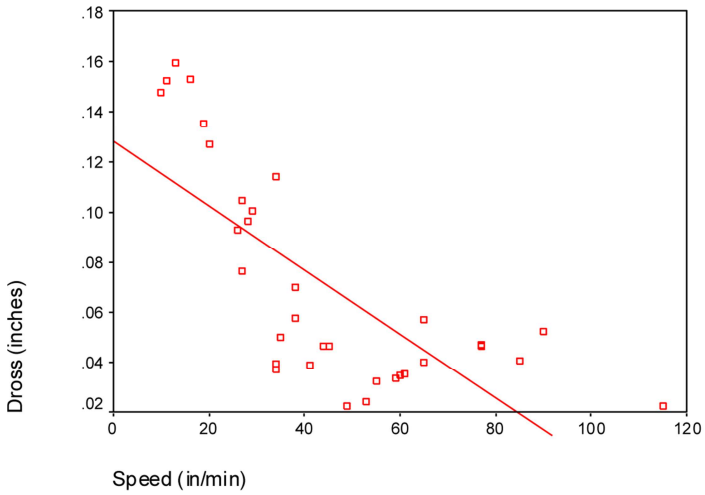

Figure C36. Dross vs. speed for 1/4" steel.

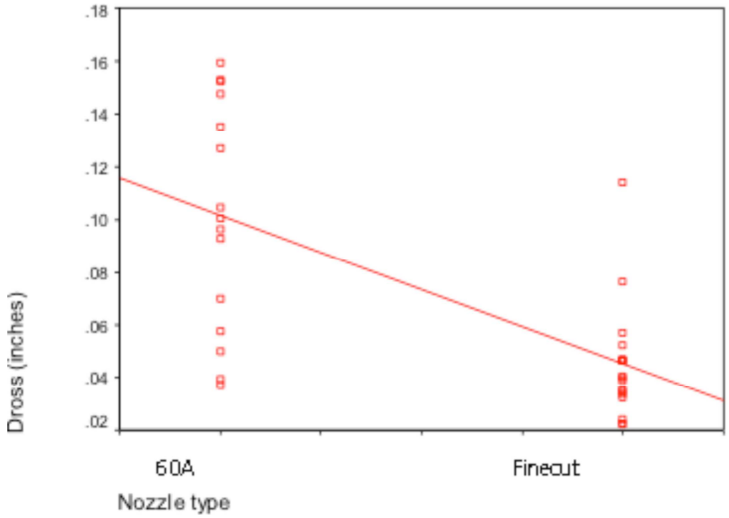

Figure C37. Dross vs. nozzle type for 1/4" steel.

The P–P plots shown in Figures C38–C41 were examined as indicators of normality, random prediction error, and homoscedasticity. The relationships are all approximately linear which indicates normality and random prediction error, and equal variation about the line on the chart indicates homoscedasticity.

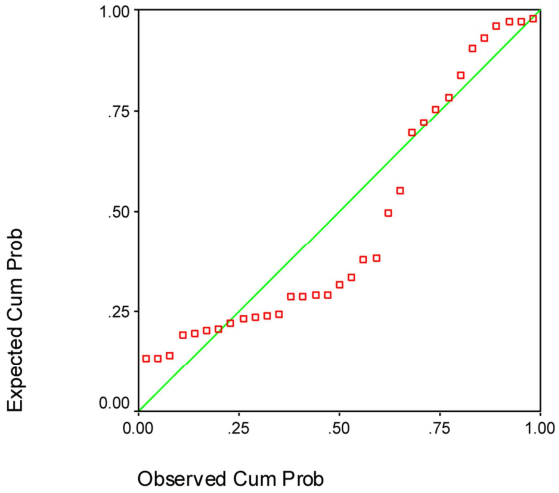

Figure C38. Normal P–P plot of dross for 1/4" steel.

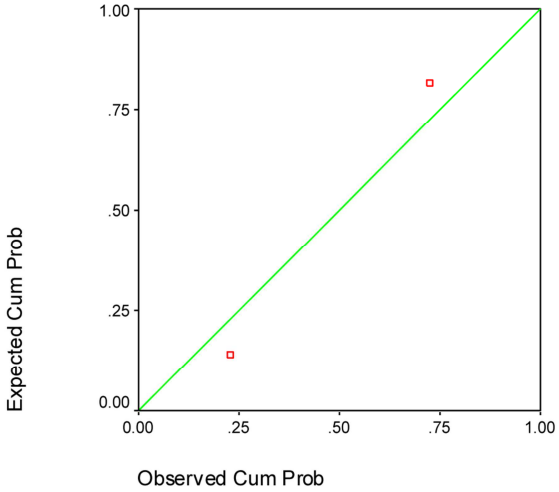

Figure C39. Normal P–P plot of nozzle type for 1/4" steel.

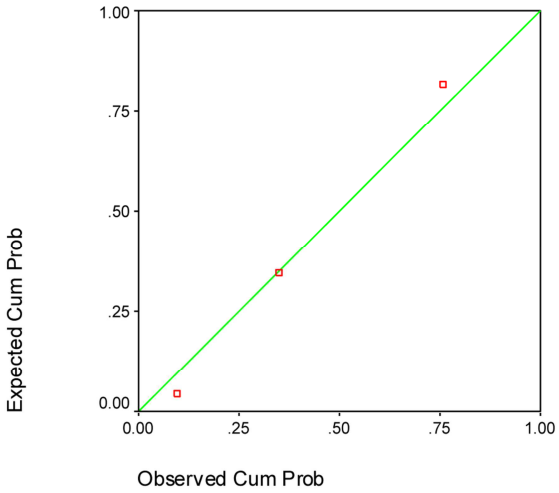

Figure C40. Normal P–P plot of power for 1/4" steel.

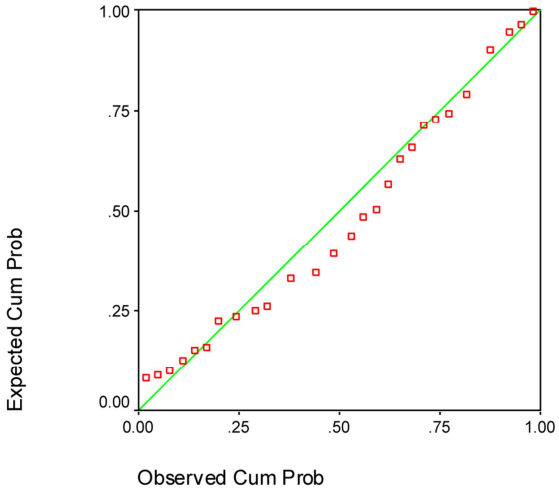

Figure C41. Normal P–P plot of speed for 1/4" steel.

The VIF values were examined to determine if there is collinearity between the variables. As shown in Table C22, the VIF value of 1.000 indicates no collinearity.

Table C22

Coefficients and VIF Values for 1/4" Steel

Coefficients[a]

Model		Unstandardized Coefficients		Standardized Coefficients	t	Sig.	Collinearity Statistics	
		B	Std. Error	Beta			Tolerance	VIF
1	(Constant)	.128	.011		11.890	.000		
	Speed (in/min)	-1.28E-03	.000	-.737	-6.079	.000	1.000	1.000

a. Dependent Variable: Dross (inches)

As previously discussed, the analysis of the initial results has shown that multiple regression is an appropriate test for this data. The coefficients that represent the relationship between the independent and dependent variables for 1/4" steel are also shown in Table C22. The ANOVA shown in Table C23 indicates several important values:

- Comparison of the regression value to the residual value: A high ratio of regression to residual indicates that the model accounts for most of the variation in the dependent variable (.033/.027) = 1.222. A ratio ~1 or greater is acceptable.
- Examination of the significance value: If the significance value of the *F* statistic is smaller than 0.05, then the independent variables explain the variation in the dependent variable. (For (constant), and speed, the sig. value = .000.)

Table C23

ANOVA Table for 1/4" Steel

ANOVA[b]

Model		Sum of Squares	df	Mean Square	F	Sig.
1	Regression	.033	1	.033	36.953	.000[a]
	Residual	.027	31	.001		
	Total	.060	32			

a. Predictors: (Constant), Speed (in/min)

b. Dependent Variable: Dross (inches)

The Durbin–Watson value was used to test for the autocorrelation between residuals. One of the assumptions of regression analysis is that the residuals for consecutive observations are uncorrelated. As indicated in Table C24, the calculated value of 2.308 shows minimal autocorrelation between speed and dross.

Table C24

Durbin–Watson Value for 1/4" Steel

Model Summary[b]

Model	R	R Square	Adjusted R Square	Std. Error of the Estimate	Durbin-Watson
1	.737[a]	.544	.529	.0297796	2.308

a. Predictors: (Constant), Speed (in/min)

b. Dependent Variable: Dross (inches)

Analysis of 3/8" Steel Statistics

The 3/8" data was analyzed for normality by comparing the mean, median, and skewness for each variable. In each case the mean and median values are essentially equal, and the skewness values indicate a normal symmetric distribution. The values of mean, median, and skewness are shown in Table C25.

Table C25

Statistics for 3/8" Steel

Statistics

		Dross (inches)	Nozzle type	power (amps)	speed (in/min)
N	Valid	31	31	31	31
	Missing	62	62	62	62
Mean		.052671	2.35	55.97	53.42
Median		.042900	3.00	55.00	49.00
Skewness		1.304	-.798	-.370	1.161
Std. Error of Skewness		.421	.421	.421	.421
Kurtosis		1.323	-1.462	-1.289	1.771
Std. Error of Kurtosis		.821	.821	.821	.821

Scatterplots were examined to determine the existence of a linear relationship between each independent variable and the dependent variable, dross. The resulting diagrams show that there may be a linear relationship between each of the variables as seen in the scatterplots in Figures C42–C44.

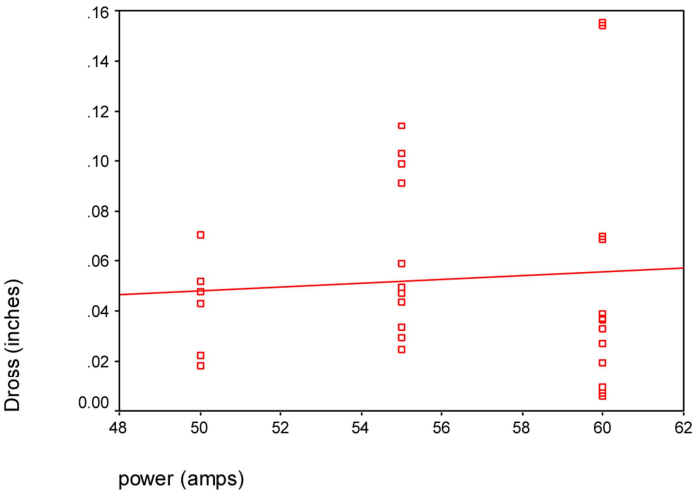

Figure C42. Dross vs. power for 3/8" steel.

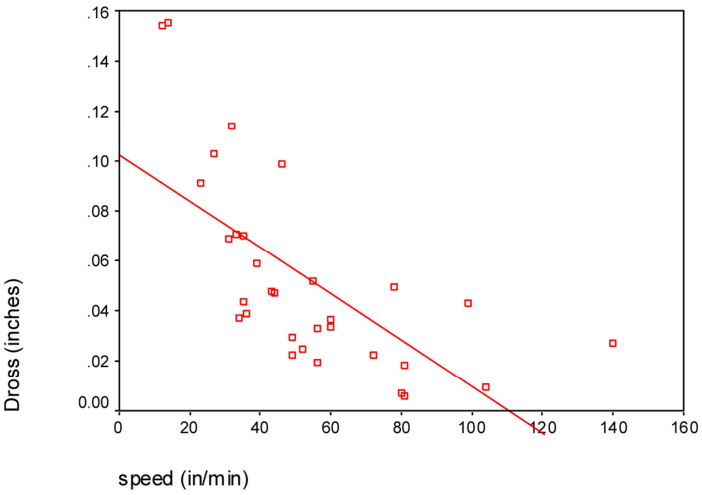

Figure C43. Dross vs. speed for 3/8" steel.

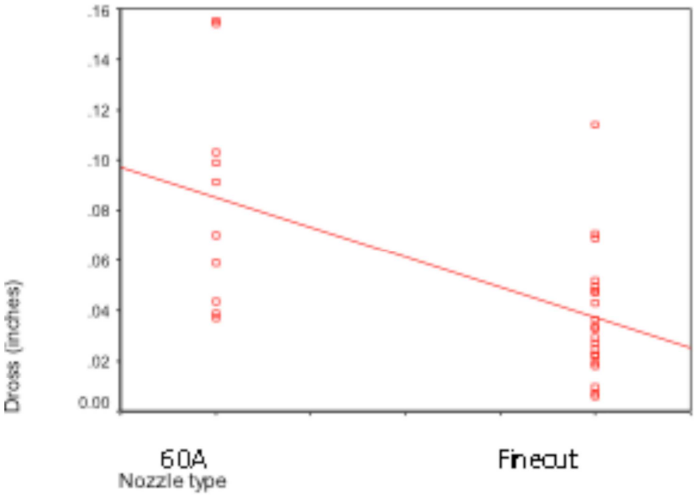

Figure C44. Dross vs. nozzle type for 3/8" steel.

The P–P plots shown in Figures C45–C48 were examined as indicators of normality, random prediction error, and homoscedasticity. The relationships are all approximately linear which indicates normality and random prediction error, and equal variation about the line on the chart indicates homoscedasticity.

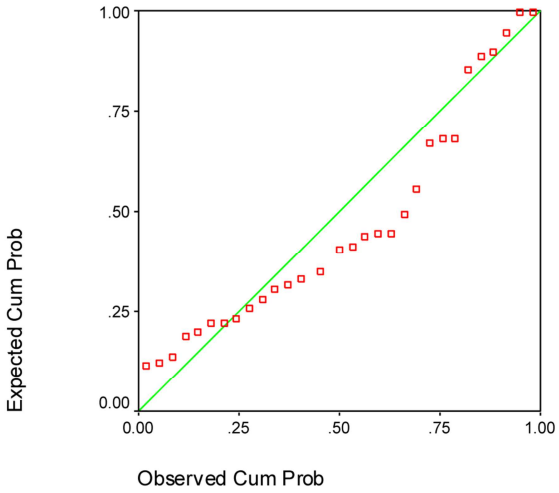

Figure C45. Normal P–P plot of dross for 3/8" steel.

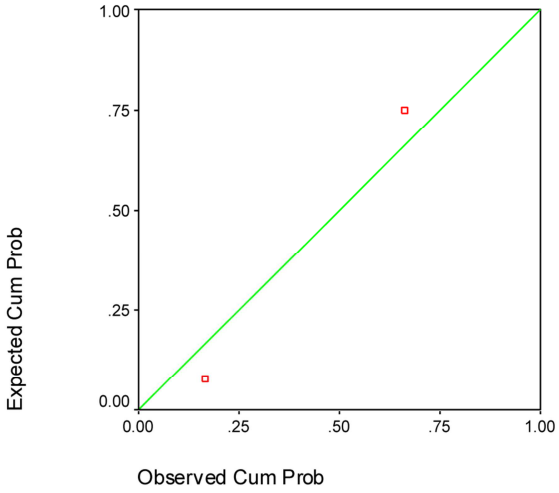

Figure C46. Normal P–P plot of nozzle type for 3/8" steel.

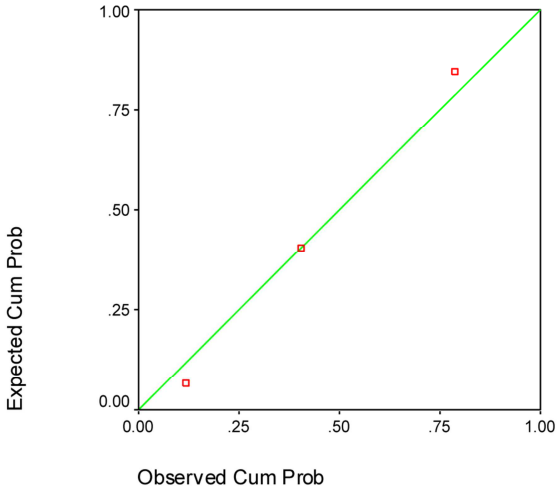

Figure C47. Normal P–P plot of power for 3/8" steel.

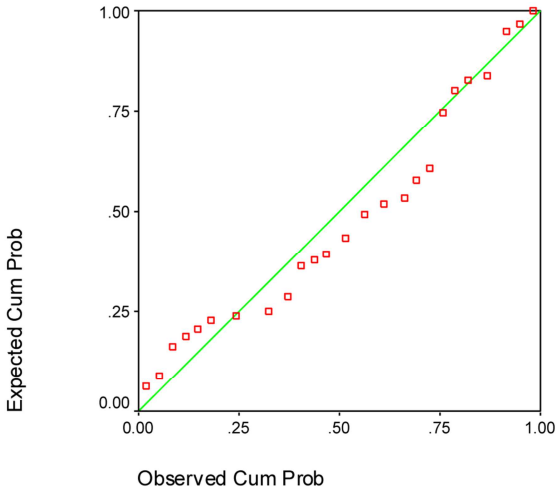

Figure C48. Normal P–P plot of speed for 3/8" steel.

The VIF values were examined to determine if there is collinearity between the variables. As shown in Table C26, the VIF value of 1.000 indicates no collinearity.

Table C26

Coefficients and VIF Values for 3/8" Steel

Coefficients[a]

Model		Unstandardized Coefficients		Standardized Coefficients	t	Sig.	Collinearity Statistics	
		B	Std. Error	Beta			Tolerance	VIF
1	(Constant)	.102	.012		8.798	.000		
	speed (in/min)	-9.26E-04	.000	-.665	-4.794	.000	1.000	1.000

a. Dependent Variable: Dross (inches)

As previously discussed, the analysis of the initial results has shown that multiple regression is an appropriate test for this data. The coefficients that represent the relationship between the independent and dependent variables for 3/8" steel are also shown in Table C26. The ANOVA shown in Table C27 indicates several important values:

- Comparison of the regression value to the residual value: A high ratio of regression to residual indicates that the model accounts for most of the variation in the dependent variable (.020/.025) = .8. A ratio ~1 or greater is acceptable.

- Examination of the significance value: If the significance value of the *F* statistic is smaller than 0.05, then the independent variables explain the variation in the dependent variable. (For (constant), and speed, the sig. value = .000.)

Table C27

ANOVA Table for 3/8" Steel

ANOVA[b]

Model		Sum of Squares	df	Mean Square	F	Sig.
1	Regression	.020	1	.020	22.979	.000[a]
	Residual	.025	29	.001		
	Total	.046	30			

a. Predictors: (Constant), speed (in/min)

b. Dependent Variable: Dross (inches)

The Durbin–Watson value was used to test for the autocorrelation between residuals. One of the assumptions of regression analysis is that the residuals for consecutive observations are uncorrelated. As indicated in Table C28, the calculated value of 1.915 shows minimal autocorrelation between speed and dross.

Table C28

Durbin–Watson Value for 3/8" Steel

Model Summary[b]

Model	R	R Square	Adjusted R Square	Std. Error of the Estimate	Durbin-Watson
1	.665[a]	.442	.423	.0296304	1.915

a. Predictors: (Constant), speed (in/min)

b. Dependent Variable: Dross (inches)